

From the Department of Neurology
(Director: Prof. Dr. T. Münte)
with the Section of Clinical and Molecular Neurogenetics
(Director: Prof. Dr. C. Klein)
of the University of Lübeck

**Molecular studies of two genetic movement disorders:
PRKRA-linked dystonia
and *PINK1*-linked Parkinson disease**

Dissertation
for fulfillment of requirements
for the doctoral degree
of the University of Lübeck

- From the Section of Natural Sciences -

Submitted by
Philip Seibler
from Bremen

Lübeck, 2011

1. Berichterstatterin: Prof. Dr. med. C. Klein

2. Berichterstatter: Prof. Dr. rer. nat. J. Rohwedel

Tag der mündlichen Prüfung: 18.10.2011

Zum Druck genehmigt. Lübeck, den 07.06.2012

LIST OF CONTENT

1. INTRODUCTION	1
1.1. Movement disorders: Dystonia and Parkinson disease.....	1
1.2. Dystonia	2
1.2.1. Genetic causes of dystonia	3
1.2.2. <i>PRKRA</i> -linked dystonia	4
1.3. Parkinson disease.....	5
1.3.1. Genetic causes of Parkinson disease	5
1.3.2. <i>PINK1</i> -linked Parkinson disease	6
1.3.3. <i>PINK1</i> , Parkin and mitochondrial dysfunction in Parkinson disease	7
1.4. Human neuronal disease modeling by using induced pluripotent stem cells	8
1.4.1. Induced pluripotent stem cells	9
1.4.2. Neurons derived from patient-specific induced pluripotent stem cells	12
1.5. Hypotheses	14
2. PATIENTS, MATERIAL and METHODS	15
2.1. Study subjects.....	15
2.1.1. Dystonia patients and healthy control individuals.....	15
2.1.2. PD patients with mutations in <i>PINK1</i> and healthy control individuals	16
2.2. Material.....	17
2.2.1. Chemicals.....	17
2.2.2. Kits	18
2.2.3. Cells	19
2.2.4. Recombinant proteins	19
2.2.5. Antibodies.....	19
2.2.6. Cell culture media.....	20
2.2.7. Equipment	20
2.3. Methods.....	21
2.3.1. Extraction of nucleic acids.....	21
2.3.2. Polymerase chain reaction	21
2.3.2.1. Standard PCR	21
2.3.2.2. Quantitative RT-PCR.....	22
2.3.3. Sequencing	23
2.3.4. Gel electrophoresis	24
2.3.4.1. Agarose gel electrophoresis.....	24

2.3.4.2. Denaturing polyacrylamide gel electrophoresis.....	24
2.3.5. Denaturing high-performance liquid chromatography	25
2.3.6. Restriction digest.....	25
2.3.7. DNA cloning	26
2.3.7.1. Retroviral vectors	26
2.3.7.2. Lentiviral vectors	26
2.3.7.3. Amplification of DNA plasmids	27
2.3.8. Viral vectors.....	27
2.3.8.1. Production of viral vectors	28
2.3.8.2. Titering of viral vectors	28
2.3.9. Flow cytometry	29
2.3.10. Cell culture	30
2.3.10.1. Fibroblast culture.....	30
2.3.10.2. 293FT cell line culture	30
2.3.10.3. IPS cell culture	30
2.3.11. Reprogramming.....	31
2.3.12. Karyotype analysis	32
2.3.13. Spontaneous <i>in vitro</i> differentiation	32
2.3.14. Neuronal <i>in vitro</i> differentiation.....	33
2.3.15. Immunofluorescence and cell counts.....	34
2.3.16. Confocal microscopy	35
2.3.17. Western blotting	35
3. RESULTS	36
3.1. Dystonia: Exploring the role of mutations in <i>PRKRA</i>.....	36
3.1.1. Patients	36
3.1.2. Mutational screen	36
3.2. Parkinson disease: Establishing a human neuronal model using iPS cells	38
3.2.1. Generation of iPS cells from PD patients and controls	38
3.2.1.1. Patient-derived fibroblasts.....	38
3.2.1.2. Reprogramming of fibroblasts into iPS cells.....	38
3.2.2. Generation of human dopaminergic neurons from PD patients and controls.....	45
3.2.3. Mitochondrial Parkin recruitment is impaired in mutant <i>PINK1</i> human neurons ...	49
3.2.4. Change of mitochondrial copy number and PGC-1 α levels in mutant <i>PINK1</i> human neurons	52
4. DISCUSSION.....	54
4.1. The role of mutations in <i>PRKRA</i>.....	54
4.1.1. Frequency and type of <i>PRKRA</i> mutations.....	54

4.1.2. Consequences of <i>PRKRA</i> mutations for molecular pathways in dystonia	55
4.2. Human neuronal models for Parkinson disease research	57
4.2.1. Non-patient specific cell culture models	58
4.2.2. Patient-specific cell culture models	60
4.3. The effect of <i>PINK1</i> mutations on human neurons	62
4.4. Conclusions	64
5. PERSPECTIVES	66
6. SUMMARY	67
7. ZUSAMMENFASSUNG	69
8. REFERENCES	72
9. APPENDIX	84
9.1. List of abbreviations	84
9.2. Supplementary material	87
9.3. Publications	89
9.4. Acknowledgements	91
9.5. Declaration	92

LIST OF FIGURES

Figure 1	<i>Organization of the basal ganglia.</i>	2
Figure 2	<i>The generation of cellular disease models or transplants using iPS cells.</i>	9
Figure 3	<i>Pedigree of Family W.</i>	16
Figure 4	<i>Vector maps of pER4-Parkin and pER4-PINK1-V5.</i>	27
Figure 5	<i>iPS colonies grown on matrigel.</i>	31
Figure 6	<i>Selection of CNS neural precursors on day 11 of differentiation.</i>	34
Figure 7	<i>Changes detected in PRKRA.</i>	37
Figure 8	<i>Infection efficiency of retroviral vectors.</i>	39
Figure 9	<i>Reprogramming of fibroblasts into iPS cells.</i>	40
Figure 10	<i>Generation of iPS cells from PD patients harboring a PINK1 mutation and healthy control individuals.</i>	41
Figure 11	<i>RT-PCR analysis of iPS cells from PD patients harboring a PINK1 mutation and healthy control individuals.</i>	42
Figure 12	<i>Spontaneous in vitro differentiation of iPS cells.</i>	43
Figure 13	<i>Fingerprinting of iPS cell lines.</i>	43
Figure 14	<i>Karyotype analysis of iPS cell lines.</i>	44
Figure 15	<i>Differentiation of iPS cells into dopaminergic neurons.</i>	46
Figure 16	<i>Generation of human dopaminergic neurons from wild-type and mutant PINK1 iPS cells.</i>	47
Figure 17	<i>Validation of lentiviral Parkin and PINK1-V5 infection of iPS cell-derived neurons by immunostaining.</i>	50
Figure 18	<i>Stress-induced mitochondrial translocation of Parkin is impaired in mutant PINK1 iPS cell-derived human dopaminergic neurons.</i>	51
Figure 19	<i>Abnormalities in mtDNA copy number and PGC-1α expression in mutant PINK1 iPS neurons.</i>	53
Figure 20	<i>Schematic of PRKRA protein.</i>	56
Figure S1	<i>Stress-induced mitochondrial translocation of Parkin is impaired in all three mutant PINK1 iPS cell lines.</i>	88

1. INTRODUCTION

The present thesis investigates two neurological monogenetic forms of movement disorders: *Protein kinase, interferon-inducible double-stranded RNA-dependent activator (PRKRA)*-linked dystonia and *PTEN-induced putative kinase 1 (PINK1)*-linked Parkinson disease (PD). In the following both diseases are described regarding their physiological features (1.1.). Further, the current state of knowledge concerning their genetic causes and molecular basis is given (1.2. and 1.3.). The approach of using induced pluripotent stem (iPS) cells for neuronal disease modeling is presented in the last section (1.4.).

1.1. Movement disorders: Dystonia and Parkinson disease

Movement disorders (dystonic disorders, gait disorders, Huntington disease, myoclonus, parkinsonism, spasticity, tardive dyskinesia, tics and tremor) are a heterogeneous group of neurological conditions characterized by the common features of impaired planning, control or execution of movement (Klein, 2005).

Dystonias are classified as hyperkinetic syndromes whereas PD belongs to the class of hypokinetic movement disorders. Interestingly, both diseases are caused by alterations within the same neuronal circuit of the brain, the basal ganglia (Brotchie and Obeso, 2010). The organization of the basal ganglia comprises the striatum, globus pallidus, substantia nigra, and subthalamic nucleus (STN) (Fig. 1). The globus pallidus is divided into an external segment (GPe) and an internal segment (GPi); the substantia nigra is composed of a pigmented region, the substantia nigra pars compacta (SNc) and an unpigmented region, substantia nigra pars reticulata (SNr). The principal region that receives inputs is the striatum. GPi and SNr are the output regions projecting beyond the basal ganglia. Input and output sections are connected by either a direct or an indirect pathway. Direct inhibitory projections arise in the striatum and end in the output regions of the basal ganglia (GPi/SNr). The indirect pathway includes SNc, GPe and STN in a more circuitous way. Inhibitory neurons project from the striatum to the SNc and the GPe. The latter has in turn inhibitory function on the output regions and the STN. The exceptions to the predominant inhibitory connections of the basal ganglia are excitatory neurons of the STN that project to the GPi/SNr and excitatory neurons of the SNc that project back onto the striatum. In dystonias, the classical model proposes a reduced activity in the STN-GPi projection or a dysfunction of striatal neurons leading to a decreased firing in the basal ganglia output. In PD, the degeneration of dopamine (DA)-producing neurons in the SNc leads to a striatal DA depletion. This reduces the inhibition of indirect pathway neurons leading to increased

excitation of GPi/SNr by the STN. At the same time the firing of direct pathway neurons is decreased, which contributes to excessive neuronal activity in basal ganglia output neurons. This classic model of basal ganglia function is supported by a large number of observations. However, there is evidence for additional mechanisms such as direct DA projections to the STN, GPe, and GPi or the thalamus (García-Cabezas *et al.*, 2007).

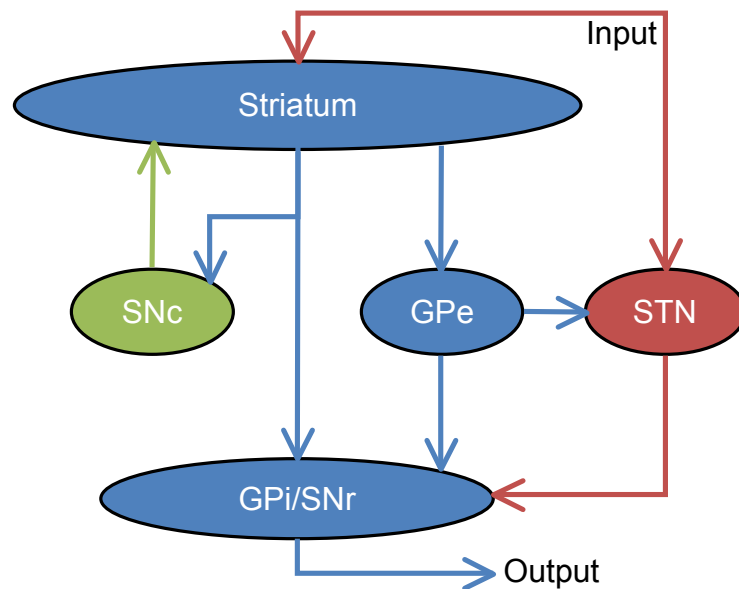


Figure 1 *Organization of the basal ganglia.* This circuit represents the main components of the basal ganglia and the interconnecting pathways. The major input from outside is the striatum, which projects in the direct pathway towards the output regions globus pallidus internal (GPi) and substantia nigra pars reticulata (SNr). The indirect pathway projects from the striatum via globus pallidus external (GPe) to GPi/SNr. The GPe influences in addition the STN, which then innervates the output regions. The substantia nigra pars compacta (SNc) projects back to the striatum. Inhibitory regions and pathways use γ -aminobutyric acid as principal transmitter and are colored in blue. Excitatory regions and pathways that use glutamate, are colored in red. The SNc uses dopamine, and is colored in green. Scheme modified from Brotchie and Obeso (2010).

1.2. Dystonia

The term dystonia can be traced back to a report of Hermann Oppenheim in 1911. The German neurologist described four young patients with a generalized abnormality of tone with coexistent hypo- and hypertonia (Oppenheim, 1911).

To date, dystonias comprise a group of disorders characterized by sustained muscle contractions that cause twisting and involuntary movements or abnormal postures affecting many different parts of the body. The prevalence is estimated to be at least 1/10,000 individuals in different populations (Butler *et al.*, 2004; Matsumoto *et al.*, 2003). Dystonias can be distinguished based on somatic distribution of symptoms (focal, segmental, or

generalized), age of disease onset (early or late), and etiology (primary or secondary). In primary forms, dystonia (with the exception of tremor) is the only symptom of the disease and the cases have no connection to disease or injury. In the secondary form, dystonia is usually one of several clinical features and the cause is identifiable (e.g. lesion, drugs/toxins, metabolic disorders) (Klein, 2005).

1.2.1. Genetic causes of dystonia

During the last two decades, several monogenetic forms of primary dystonia have been identified (Tab. 1). Presently, 18 distinct gene loci (DYT1-8, 10-13, 15-18, 21) have been recognized. Twelve forms are inherited as autosomal dominant, four as autosomal recessive and one represents as an X-linked recessive form. Two additional autosomal dominant forms (DYT19 and DYT20) might exist based on linkage mapping to regions apparently different from, yet in close proximity to or overlapping with the known loci DYT10 and DYT8 (Müller, 2009).

Table 1 Genetic causes of dystonia

Acronym	Inheritance	Locus	Gene	Mutations	Exemplary references
DYT1	AD	9q34	<i>DYT1</i>	GAG deletion, 18bp deletion in a single family	Ozelius <i>et al.</i> , 1997 Leung <i>et al.</i> , 2001
DYT2	AR	Unknown	Unknown		
DYT3	XR	Xq13	<i>TAF1</i>	DSC3 prevailing in affected	Evidente <i>et al.</i> , 2004 Makino <i>et al.</i> , 2007
DYT4	AD	Unknown	Unknown		
DYT5a*/	AD	14q22	<i>GCH1</i>	>100 small mutations	Ichinose <i>et al.</i> , 1994
DYT5b	AR	11p	<i>TH</i>	<20 small mutations	Swaans <i>et al.</i> , 2000
DYT6	AD	8p	<i>THAP1</i>	>20 small mutations	Fuchs <i>et al.</i> , 2009
DYT7	AD	18p	Unknown		
DYT8	AD	2q33-q35	<i>MR-1</i>	2 missense mutations	Lee <i>et al.</i> , 2004
DYT10	AD	16p11-q12	Unknown		
DYT11	AD	7q21	<i>SGCE</i>	>60 small mutations	Zimprich <i>et al.</i> , 2001
DYT12	AD	19q12-q13	<i>ATP1A3</i>	6 missense mutations	De Carvalho Aguiar <i>et al.</i> , 2004
DYT13	AD	1p36-p35	Unknown		
DYT15	AD	18p	Unknown		
DYT16	AR	2q31	<i>PRKRA</i>	1 missense mutation	Camargos <i>et al.</i>, 2008
DYT17	AR	20p11-q13	Unknown		
DYT18*	AD	1p	<i>SLC2A1</i>	3 mutations	Weber <i>et al.</i> , 2008
DYT19	AD	16q13-q22	Unknown		
DYT20	AD	2q31	Unknown		
DYT21	AD	2q14.3-q21.3	Unknown		

Note: AD – autosomal dominant, AR – autosomal recessive, *ATP1A3* – *ATPase alpha 3*, *DSC3* – disease-specific sequence changes, DYT16 is investigated in the present thesis and highlighted in bold print, *GCH1* – *GTP cyclohydrolase 1*, *MR-1* – *myofibrillogenesis regulator 1*, *PRKRA* – *protein kinase, interferon-inducible double-stranded RNA-dependent activator*, *SGCE* – *epsilon-sarcoglycane*, *SLC2A1* – *solute carrier family 2, facilitated glucose transporter member 1*, *TAF1* – *TAF1 RNA polymerase II*, *TH* – *tyrosine hydroxylase*, XR – X-chromosomal recessive, *DYT9 and 14 shown to be identical with DYT18 and 5A, respectively

At ten of these loci (DYT1, 3, 5a/5b, 6, 8, 11, 12, 16, 18), genes have been identified to carry mutations that are linked to the disease. All these mutations appear to disturb the normal function of striatal neurons. However, the gene products involved do not appear to be part of one interdependent pathway. This makes development of therapies more difficult and treatment of patients is still mainly symptomatic. The only exceptions are dystonias 5a and 5b with mutations in genes involved in the biopterin/DA pathway. They respond in an excellent way to levodopa substitution (Müller, 2009).

The present study focused on the recently reported *PRKRA*-linked dystonia (Camargos *et al.*, 2008). The current knowledge about this disorder is described in the following.

1.2.2. *PRKRA*-linked dystonia

PRKRA-linked dystonia was identified in two unrelated Brazilian families including six affected members and in one single patient from Brazil (Camargos *et al.*, 2008). All patients presented with primary generalized dystonia, which was diagnosed as slight in one, moderate in three and severe in three. Onset of symptoms was during childhood in six (2-12 years) and during adolescence (18 years) in one patient. The disease started in the lower extremities in four, in the upper limbs in two, and initially presented with dysphonia in one. Interestingly, concurrent parkinsonism was diagnosed in four patients (Müller, 2009). Magnetic resonance imaging (MRI) scans appeared to be normal in the patients tested. Levodopa/carbidopa treatment had a moderate positive effect on bradykinesia, which might suggest a dysfunction in the DA pathway.

The mode of inheritance is autosomal recessive. Autozygosity mapping with a high-density *Genomewide Single Nucleotide Polymorphism* analysis revealed a large disease-segregating region. Sequence analysis revealed a single disease-segregating mutation, c.665C>T (P222L), in exon 7 of *PRKRA* (NM_003690). *PRKRA* is transcribed as a 1,826bp mRNA and translated into a protein of 313 amino acids. It is composed of eight exons and occurs in three splice variants. The protein consists of three DRBM (double-stranded RNA binding motif) domains through which it is able to interact with dsRNA. The p.P222L mutation in the Brazilian patients occurred at a position that is evolutionarily conserved in mammals and is located between the second and third DRBMs. The role and frequency of *PRKRA* mutations in other populations is unknown (Camargos *et al.*, 2008; Müller, 2009).

1.3. Parkinson disease

Several early sources describe symptoms resembling those of Parkinson disease (PD), including an Egyptian papyrus, the Bible, or Galen's writings (García Ruiz, 2004). In 1817, the English doctor James Parkinson published the first study of the disease "An Essay on the Shaking Palsy".

To date, PD is the most frequent form of parkinsonism (about 75%), a term used to describe movement disorders with parkinsonian features independent of their (unknown) etiology. Parkinsonism has been suggested for the symptom triad of bradykinesia, rigidity, and rest tremor (not all features are mandatory). The symptoms result from the loss of the neurotransmitter DA due to the degeneration of DA neurons in the SNc. The most widely used treatment is levodopa, which is the precursor of DA. The prevalence is estimated to be more than 1% of the population over the age of 65 years. Although the etiology of PD is still uncertain, about 2 to 3% of the "idiopathic" cases can currently be identified as PD syndroms caused by a single genetic event (Klein and Schlossmacher, 2007).

1.3.1. Genetic causes of Parkinson disease

During the last 15 years, 18 gene loci (PARK1-18) have been identified that are associated with PD, including four autosomal dominantly (PARK1/4, 3, 5, 8, 11, 13) and six autosomal recessively (PARK2, 6-7, 9, 14-15) inherited syndromes. In addition, five chromosomal regions have been suggested as risk factors (PARK10, 12, 16-18). For six of these loci, genes have been identified carrying mutations that are linked to the clinically typical disease with conclusive evidence (*alpha-synuclein (SNCA)*, *Parkin*, *PINK1*, *DJ-1*, and *Leucin-rich repeat kinase 2 (LRRK2)*). Molecular studies of these genes have provided unique opportunities to investigate the mechanisms of neuronal degeneration in pathogenetic models of PD. The studies demonstrated the significance of oxidative stress, mitochondrial dysfunction, and impaired protein turnover (Klein and Schlossmacher, 2007). However, the detailed functions of most of the proteins involved in monogenic PD remain unknown.

Parkin (PARK2) and *PINK1* (PARK6) gene mutations are the most prevalent genetic factor in early-onset PD (age of onset <40 years) accounting for up to 50% of familial cases and for about 10-20% of all early-onset cases. Interestingly, both proteins have been shown to function, at least in part, in the same pathway (Clark *et al.*, 2006). This interaction is of particular interest for the present thesis and is reviewed in the following with a focus on *PINK1* function.

Table 2 Genetic causes of PD

Acronym	Inheritance	Locus	Gene	Mutations	Exemplary references
PARK1/ PARK4	AD	4q21-q23	<i>SNCA</i>	Whole gene duplications/ triplications in <10 families, 3 missense mutations	Polymeropoulos <i>et al.</i> , 1997 Singleton <i>et al.</i> , 2003
PARK2	AR	6q25-q27	<i>Parkin</i>	>150 gene dosage alterations and small mutations	Kitada <i>et al.</i>, 1998 Hedrich <i>et al.</i>, 2004
PARK3	AD	2p13	Unknown		
PARK5	AD	4p14	<i>UCH-L1</i>	1 mutation in a single family	Leroy <i>et al.</i> , 1998
PARK6	AR	1p36-p35	<i>PINK1</i>	>40 small mutations, rarely large deletions	Valente <i>et al.</i>, 2004 Marongiu <i>et al.</i>, 2007
PARK7	AR	1p36	<i>DJ-1</i>	15 mutations	Bonifati <i>et al.</i> , 2003
PARK8	AD	12p11-q13	<i>LRRK2</i>	>40 variants, only 6 of them pathogenic	Zimprich <i>et al.</i> , 2004 Paisan-Ruiz <i>et al.</i> , 2004
PARK9	AR	1p36	<i>ATP13A2</i>	>10 small mutations	Ramirez <i>et al.</i> , 2006
PARK10	Risk factor	1p32	Unknown		
PARK11	AD	2q36-q37	Unknown		
PARK12	Risk factor	Xq21-q25	Unknown		
PARK13	AD	2p12	<i>Omi/HtrA2</i>	1 mutation in 4 families	Strauss <i>et al.</i> , 2005
PARK14	AR	22q13	<i>PLA2G6</i>	2 mutations in 2 families	Paisan-Ruiz <i>et al.</i> , 2009
PARK15	AR	22q12-q13	<i>FBXO7</i>	3 mutations in 3 families	Shojaee <i>et al.</i> , 2008
PARK16	Risk factor	1q32	Unknown		
PARK17	Risk factor	4p16	<i>GAK</i>		Hamza <i>et al.</i> , 2010
PARK18	Risk factor	6p21	<i>HLA-DRA</i>		Hamza <i>et al.</i> , 2010

Note: AD – autosomal dominant, AR – autosomal recessive, *ATP13A2* – *ATPase type 13A2*, *FBXO7* – *F-box protein 7*, *GAK* - *cyclin G associated kinase*, *HLA-DRA* – *major histocompatibility complex, class II, DR alpha*, *LRRK2* – *Leucin-rich repeat kinase 2*, *Omi/HtrA2* – *HtrA serine peptidase 2*, *PINK1* – *PTEN-induced putative kinase 1*, *PLA2G6* – *phospholipase A2, group VI*, *SNCA* – *alpha-synuclein*, *UCH-L1* – *ubiquitin C-terminal hydrolase-L1*. Genes investigated in the present thesis are highlighted in bold print.

1.3.2. *PINK1*-linked Parkinson disease

The PARK6 locus was first mapped to chromosome 1p36 as a disease-segregating region in eight families from four different European countries (Valente *et al.*, 2002). Two years later, Valente and colleagues reported two homozygous mutations that were identified in the *PINK1* gene (NM_032409) in three consanguineous PARK6 families (Valente *et al.*, 2004). The mode of inheritance is autosomal recessive and the affected are presented with a clinical syndrome closely resembling idiopathic PD with the exception of an overall earlier age of onset and slower disease progression. So far more than 60 different mutations have been found in a wide range of populations with the majority of investigated cases harboring a missense mutation (72%). Nonsense mutations cause the disease in 17% of all *PINK1*-linked PD patients and about 12% of the patients carry deletions or insertions. For 80% of the cases, the mutation was localized near or within the functional kinase domain of *PINK1* (Grünewald, 2008). The coding sequence has a length of 1,746bp and comprises eight exons. It is translated into a 581 amino acid polypeptide with a predicted N-terminal

mitochondrial targeting signal (MTS) and a serine/threonine kinase domain which is similar to that in the Ca²⁺/calmodulin kinase family (Deas *et al.*, 2009). Full-length PINK1 (~66 kDa) is proteolytically processed upon entry into mitochondria to its cleaved ~55 kDa form (Weihofen *et al.*, 2008). Overexpression of this cytosolic isoform of cleaved PINK1 was reported to protect neurons against the mitochondrial toxin 1-methyl-4-phenyl-1,2,3,6-tetrahydropyridine (MPTP) *in vitro* and *in vivo* (Haque *et al.*, 2008). Endogenous cleaved PINK1 appears to become rapidly degraded via the proteosomal pathway, possibly a regulatory step (Lin and Kang, 2008).

Putative PINK1 substrates have been identified, including tumor necrosis factor receptor-associated protein 1 (TRAP1) and the serine protease high temperature requirement A2 (HtrA2/Omi). Both proteins are localized in the mitochondrial intermembrane space, suggesting a functional role of PINK1 in the mitochondria as well.

In order to study loss of PINK1 function, animal models have been generated. The first model was *PINK1*-mutant *Drosophila* exhibiting loss of DA neurons, mobility abnormalities, reduced life span, and mitochondrial defects (Clark *et al.*, 2006). In contrast, *PINK1* knockout mice were characterized with a normal population of DA neurons. However, mitochondrial functional defects were observed in the striatum of the mice, spreading to areas of the cortex with age or following application of cellular stress (Gautier *et al.*, 2008).

1.3.3. PINK1, Parkin and mitochondrial dysfunction in Parkinson disease

The reason for the selective loss of DA neurons is still unclear. Involvement of mitochondria in this process has been postulated for many years and a growing body of evidence implicates mitochondrial dysfunction as the primary event sufficient to cause PD. First evidence emerged since various “parkinsonian toxins”, such as rotenone and MPTP were found to inhibit mitochondrial complex I. This finding was further supported by the detection of a complex I deficiency in the SNc of PD patients (Schapira *et al.*, 1989). More recently, levels of mitochondrial DNA (mtDNA) deletions were investigated in SNc neurons. The extent of the mtDNA damage was increased with age (Bender *et al.*, 2006) and more pronounced in PD patients than in healthy age-matched controls (Schapira, 2008). Since neurons in the SNc are postmitotic, any mitochondrial damage they acquire could accumulate over an organism’s lifetime and therefore lead to progressive mitochondrial dysfunction. The accumulation of damaged mitochondria might cause increased oxidative stress, decreased calcium buffering capacity, loss of adenosine triphosphate (ATP), and, eventually, cell death. Recent studies have linked Parkin and PINK1 in a pathway critical for the mitochondrial quality control. Parkin is an E3 ubiquitin-protein ligase functioning in the ubiquitin proteasome system, a cellular system for removal of toxic, incompletely formed or redundant proteins.

Parkin is localized in both the Golgi complex and cytosol (Shimura *et al.*, 1999). In 2008, Narendra and colleagues reported that Parkin is selectively recruited to dysfunctional mitochondria with low membrane potential and subsequently promotes their autophagic degradation (mitophagy). According to these findings, Parkin limits mitochondrial damage by acting in a pathway that identifies and eliminates damaged mitochondria from the mitochondrial network. Two years later, it was shown that Parkin recruitment was dependent on the accumulation of full-length PINK1 on depolarized mitochondria (Vives-Bauza *et al.*, 2010; Narendra *et al.*, 2010). We further expanded these findings by using patient-derived fibroblast cultures harboring *PINK1* mutations demonstrating that these disease-causing mutations disrupted Parkin translocation (Rakovic *et al.*, 2010).

1.4. Human neuronal disease modeling by using induced pluripotent stem cells

Human cells explanted *in vitro* have provided important insights into both normal and pathologic cellular processes for many decades. However, there is a lack for appropriate neuronal human-derived cell models. Most of the human cell lines that are in use carry genetic and epigenetic changes due to long-term tissue culturing and with the intention of having immortalized cells, they were derived either from malignant tissue or have been genetically modified for this purpose (Grimm, 2004). In terms of primary human cells, the major constraint has been the inaccessibility of living neuronal cells from patients and healthy control individuals and the reliance on *postmortem* samples. Besides, primary cells derived from *postmortem* brain samples have only a short live span in culture; except for some tissue preparations from human brain that provided progenitor cell populations (Palmer *et al.*, 2001; Walton *et al.*, 2006). To overcome this barrier, human pluripotent cells could be used. Pluripotency is the term used to describe embryonic cells that theoretically can give rise to any cell type within a mature organism. There are several types of pluripotent cells, including embryonic stem (ES) cells, which are derived from the inner cell mass of mammalian blastocysts. ES cells have the additional feature of self-renewal, which allows them to grow indefinitely while maintaining pluripotency. Human ES cells could eventually be used not only to model but to treat a host of diseases, such as PD, spinal cord injury, and diabetes. However, the “production” and utilization of human embryos is highly questionable, as well as the problem of tissue rejection following transplantation in patients. These issues may be avoided by a new type of pluripotent cells known as induced pluripotent stem (iPS) cells. These cells share the pluripotent characteristics of ES cells but are instead generated via

direct reprogramming of the patients' own somatic cells through the expression of key transcription factors (Takahashi *et al.*, 2007).

1.4.1. Induced pluripotent stem cells

In the first report of iPS cell generation, mouse skin fibroblasts were successfully reprogrammed to a pluripotent state through the integration of four selected factors (POU class 5 homeobox 1 (OCT4), SRY-box 2 (SOX2), Krüppel-like factor 4 (KLF4) and cMYC) into the fibroblast genome (Takahashi and Yamanaka, 2006). Shortly thereafter, human skin fibroblast reprogramming was achieved concurrently by four groups using slightly different combinations of genes (Takahashi *et al.*, 2007; Yu *et al.*, 2007; Lowry *et al.*, 2008; Park *et al.*, 2008c). There are a number of possible uses of patient-specific derived iPS cells, ranging from disease modeling to cell and tissue regenerative therapy (Fig. 2).

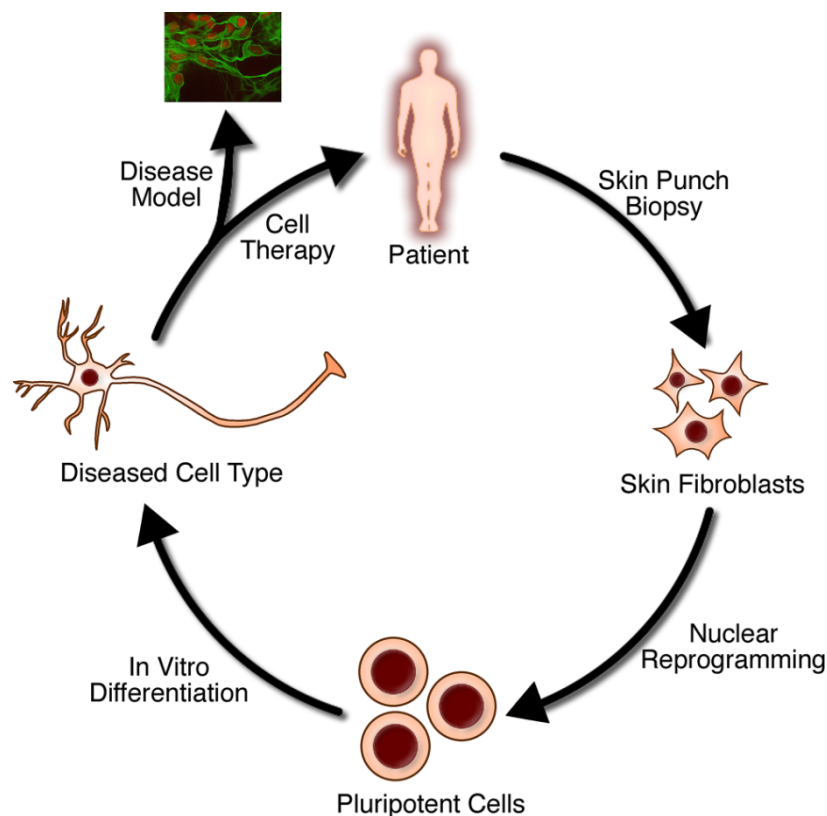


Figure 2 The generation of cellular disease models or transplants using iPS cells. i) Isolation and culture of somatic cells from a patient. ii) Reprogramming of these cells into a pluripotent state. iii) Directed differentiation of those patient-specific pluripotent cells into the cell type relevant to their disease, which can be used for *in vitro* disease modeling or transplantation into the patient (www.stembook.org).

Over the last years, an increasing number of different approaches have been established to create human iPS cell lines. So far, the most important variables are the beginning cell type, and the choice of the reprogramming cocktail. The addition of various small molecules in addition to the transgenes was shown to substantially improve the efficiency of reprogramming (Huangfu *et al.*, 2008). However, the best method to use ultimately depends on the intended application of the resulting cells. The initial protocols relied on the use of retroviral vectors to deliver the reprogramming factors into the fibroblasts. Expression of the reprogramming transgenes in these cells is silenced once the cells reach a pluripotent state, an effect that is specific to retroviral expression in stem cells (Yao *et al.*, 2004). However, it is possible that residual transgene expression can eventually misdirect the subsequent differentiation of the cells, or could also give rise to tumors, thus limiting their clinical potential. In order to counteract this problem new methods have used excision or transposon approaches in order to remove the transgenes following successful reprogramming (Soldner *et al.*, 2009; Kaji *et al.*, 2009). Another approach uses non-integrating episomal vectors for reprogramming which can later be removed through the removal of drug selection (Yu *et al.*, 2009). Still, despite the potential issues with residual transgene expression lenti- and retroviral transduction remained the fastest and most efficient method for iPS cell reprogramming. The exact functional role of the reprogramming factors is still an active area of research. During the process of reprogramming, the gene expression profiles that define the characteristics of the host cell types are set back to their initial, pluripotent state.

Several studies shed light on some mechanisms of this fascinating phenomenon. The following gives an overview of the current state of knowledge according to a recent review (Plath and Lowry, 2011). The key question is how the somatic program is erased and the pluripotency network established. This is particularly interesting as, despite the development of several methods to generate iPS cells, only a small percentage of cells give rise to the pluripotent state. According to the present model, expression of the pluripotency factors *per se* is not sufficient to induce the transition to pluripotency (Hanna *et al.*, 2009). It is suggested that the reprogramming consists of key intermediate steps and at each step fewer and fewer cells advance the next stage (Stadtfeld *et al.*, 2008; Smith *et al.*, 2010). Most of these studies have been performed in mouse embryonic fibroblasts and stages were set as early, middle and late phases of reprogramming. By using a high-resolution time-lapse imaging approach retroactive tracking of these steps showed that the first changes at the early phase are an increase in proliferation rate and a decrease in cell size (Smith *et al.*, 2010). These changes are accompanied by the upregulation of proliferation genes and downregulation of the somatic program, indicating transcriptional changes and chromatin events. Tightly packed clusters of rounded, epithelial cells occur during the middle phase of reprogramming. This suggests that fibroblasts transduced with the reprogramming factors undergo a

mesenchymal-to-epithelial (MET) transition reversing the epithelial-to-mesenchymal transition that took place during the differentiation of fibroblasts *in vivo* (Li *et al.*, 2010). In accordance with this idea, reprogramming efficiency is affected by signaling pathways that are known to interfere with the MET. The inhibition of transforming growth factor- β (TGF β) has been demonstrated to improve reprogramming, because TGF β prevents MET by repressing the upregulation of epithelial genes and downregulation of the mesenchymal transcriptional repressor zinc finger gene SNAI1 (Li *et al.*, 2010). Further, reprogramming factors OCT4 and SOX2 were found to suppress SNAI1, whereas KLF4 binds directly and activates epithelial markers. The fourth factor, cMYC, reduces TGF β signaling at the same time. During the final phase of reprogramming, genes necessary to develop and form the pluripotency network are upregulated. OCT4, SOX2 and KLF4 are implicated in mediating the transcription of these pluripotency genes. The promoters of these genes are not accessible to the reprogramming factors during the middle phase of reprogramming. It seems that repressive chromatin and enhancers interfere with the binding. One model suggests that the pluripotency transcription factor Nanog homeobox (NANOG) may promote their binding and recruit the co-activator histone acetyltransferase p300 (Chen *et al.*, 2008; Theunissen *et al.*, 2011). But how the reprogramming factors induce directly or indirectly a chromatin remodeling that is crucial for efficient reprogramming is not known.

After about one month of the reprogramming period, iPS cell colonies are isolated. The picked colonies can be subsequently expanded and characterized regarding their expression of endogenous pluripotency factors. The steps to faithfully reprogrammed iPS cells require continuous expression of the reprogramming factors but maintenance of iPS cells is independent of their overexpression, indicating a stable conversion of cell fate (Stadtfield *et al.*, 2008). Although very similar, studies have described minor differences between iPS and ES cells (Chin *et al.*, 2009; Marchetto *et al.*, 2009). They can be distinguished by their RNA expression profile showing a residual expression of somatic genes in iPS cells known as the “epigenetic memory”. Interestingly, it has been reported that iPS cells derived through retroviral genomic integration exhibit a unique gene profile that gradually becomes more similar to that of ES cells with extended *in vitro* culturing (Chin *et al.*, 2009). In general, iPS cell lines are more variable at the molecular level than ES cell lines. Whether the observed differences in gene expression will have functional implications for certain iPS cell lines is currently not clear.

1.4.2. Neurons derived from patient-specific induced pluripotent stem cells

Recent reports have demonstrated that iPS cells can be generated from patients and subsequently differentiated into the disease relevant cell types (Dimos *et al.*, 2008; Park *et al.*, 2008b; Ebert *et al.*, 2009; Soldner *et al.*, 2009). For neurological disorders, neurons have been successfully differentiated from iPS cells of patients with amyotrophic lateral sclerosis (ALS) (Dimos *et al.*, 2008), spinal muscular atrophy (SMA) (Ebert *et al.*, 2009), familial dysautonomia (FD) (Lee *et al.*, 2009), and sporadic PD (Soldner *et al.*, 2009). Neurons were derived from iPS cells by using protocols developed for mouse and human ES cells. Differentiation is induced traditionally by the formation of multicellular aggregates called embryoid bodies (EBs), which contain cell types representing all three germ layers. Neural direction is achieved by sequential addition of exogenous differentiation factors. Others have developed protocols to improve differentiation efficiency by co-culturing ES cells with mouse PA-6 or MS5 cells. These stromal cells induce the activity of unknown signaling factors that promote a neuronal phenotype in ES cells (Kawasaki *et al.*, 2000; Perrier *et al.*, 2004). A midbrain dopaminergic phenotype was achieved by using a combination of stromal feeder and subsequently the addition of different concentrations of recombinant growth and signaling factors to the culture media, such as sonic hedgehog (SHH), fibroblast growth factor 8 (FGF8), brain-derived neurotrophic factor (BDNF), glial cell line-derived neurotrophic factor (GDNF), TGF- β 3, cyclic adenosine monophosphate (cAMP) and ascorbic acid (Perrier *et al.*, 2004). Retinoic acid and SHH are the main factors required for the induction of motor neurons (Li *et al.*, 2005). Most recently, a protocol has been developed to avoid co-culture and eliminate the use of undefined factors while reaching high efficiencies of neural differentiation (Chambers *et al.*, 2009). Neural induction was achieved by inhibiting SMAD (Mothers against decapentaplegic homolog 1) signaling, which has been shown to play a crucial role during differentiation processes.

In the first report of disease-related iPS cells, fibroblasts were reprogrammed from a patient diagnosed with a familial form of ALS. Subsequently, these cells were successfully differentiated into motor neurons by using a protocol that was based on the formation of EBs followed by the addition of retinoic acid and SHH to the culture medium (Dimos *et al.*, 2008). While for these neurons no phenotype was reported, motor neurons derived from an SMA patient showed selective deficits compared to those generated from a healthy control individual (Ebert *et al.*, 2009). The rare genetic disorder leads to the loss of lower motor neurons, which causes infant mortality. Traditional EB formation was found to be very inefficient for neural differentiation from iPS cell cultures in this study and an alternative protocol was established, in which iPS cell colonies were placed directly into a human neural progenitor growth medium. The SMA disease phenotype was observed during neural differentiation when the production of motor neurons seemed to be selectively hindered.

Another explanation for this decrease of motor neuronal population is increased motor neuron degeneration at later time points during the differentiation process. This type of effect can be observed only during the differentiation of stem cells towards motor neurons, which highlights the importance of patient-specific iPS cell-based disease models. For neural induction of iPS cells derived from one FD patient, cells were co-cultured with MS5 stromal cells (Lee *et al.*, 2009). Several growth factors were added to the differentiation medium in order to reach a high population of neural crest lineages, the primary tissue affected in FD, which is a genetically caused rare peripheral neuropathy. Gene expression analysis in FD-derived lineages demonstrated tissues specific mis-splicing of the mutated gene *in vitro*. In addition, defects were observed in neurogenesis and migration of mutated neural crest precursors. Although derivation of iPS cell lines from sporadic PD patients has been reported (Park *et al.*, 2008b; Soldner *et al.*, 2009), a phenotype in DA neurons differentiated from these iPS cells was not described. Neural differentiation of iPS cells was induced by EB formation and additionally by using a second approach based on the combination of MS5 co-culturing and a culture medium supplemented with the SMAD inhibitor Noggin. No obvious differences in the ability to generate DA neurons were observed between PD and non-PD-derived iPS cells and ES cells.

1.5. Hypotheses

The intention of the present thesis was to gain a better understanding of the movement disorders *PRKRA*-linked dystonia and *PINK1*-linked PD, respectively. The recently identified *PRKRA* gene was investigated at the genomic level only. The generation of a human neuronal model was aimed for the examination of the effect of mutations in the well-characterized *PINK1* gene. The following hypotheses were addressed:

***PRKRA*-linked dystonia:**

- *Dystonia-causing mutations in the PRKRA gene are not limited to the Brazilian population.*

***PINK1*-linked PD:**

- *Fibroblasts from genetic PD patients can be reprogrammed into iPS cells.*
- *Mutant PINK1 human iPS cells can be differentiated into dopaminergic neurons.*
- *Parkin recruitment to mitochondria is impaired in mutant PINK1 dopaminergic neurons.*
- *Loss of PINK1 function leads to mitochondria-related phenotypes in human neurons*

2. PATIENTS, MATERIAL and METHODS

Experiments related to dystonia were performed at the Section of Molecular and Clinical Neurogenetics at the University of Lübeck (Professor Christine Klein). The investigations regarding PD were carried out at the MassGeneral Institute for Neurodegenerative Disease at the Massachusetts General Hospital in Boston (Professor Dimitri Krainc). A number of methods described in this chapter have been newly established during the study. However, the main technical part of this thesis was to establish optimized protocols for the previously reported reprogramming method (Park *et al.*, 2008a; 2.3.11.) and the neuronal *in vitro* differentiation method (Chambers *et al.*, 2009; 2.3.14.).

2.1. Study subjects

In this study patients with two different movement disorders (Dystonia and PD) were investigated. The diagnosis was made on the basis of published criteria by movement disorders' specialists (Dystonia: Klein, 2003; PD: Gibb and Lees, 1988). All patients and healthy control individuals gave informed consent and the Ethics Committee at the University of Lübeck approved the study (Ethic approval 05-030).

2.1.1. Dystonia patients and healthy control individuals

Based on the finding of DYT16 dystonia (Camargos *et al.*, 2008), patients displaying the described clinical features were selected for genetic testing of *PRKRA* as a part of the present thesis. The investigations included two cohorts of German affected individuals (Cohort A and B) that were compared with one cohort of healthy individuals from Germany (Cohort C).

Cohort A: 52 unrelated patients with dystonia (age of onset: <25 years, mean age: 13.7 [SD 7.4] years), of whom 22 were presented with generalized dystonia, 11 with segmental dystonia, 15 with musician's dystonia, and four with writer's cramp. Nine of them had a positive family history.

Cohort B: 75 patients with dystonia (age of onset: >25 years, mean age: 31.6 [SD 6.4] years), of whom 15 had a positive family history of dystonia.

Cohort C: 189 neurologically healthy controls (mean age: 57.7 [SD 11.6] years) were available for subsequent validation experiments.

2.1.2. PD patients with mutations in *PINK1* and healthy control individuals

The experiments regarding PD were performed on dermal skin fibroblasts taken from affected and healthy members of a German family (Family W) and a single affected individual from Germany.

The pedigree of Family W consists of three generations (Fig. 3). There are four patients with a homozygous c.1366C>T, p.Q456X nonsense mutation in *PINK1*, two of whom were included into the study (both female, mean age: 70 [SD 5.7] years, mean age at onset: 57 [SD 5.7] years). Two male healthy relatives were included as controls (mean age: 55 [SD 13.4] years). Eleven family members were tested heterozygous for the mutation and were excluded from this study (Hedrich *et al.*, 2006).

The single female (age: 77 years, age at onset: 31 years) affected individual that was additionally studied carried a homozygous *PINK1* missense mutation c.509T>G, p.V170G (Moro *et al.*, 2008).

All patients exhibited clinical signs, characterized as bradykinesia, rigidity, postural instability, and good response to levodopa treatment.

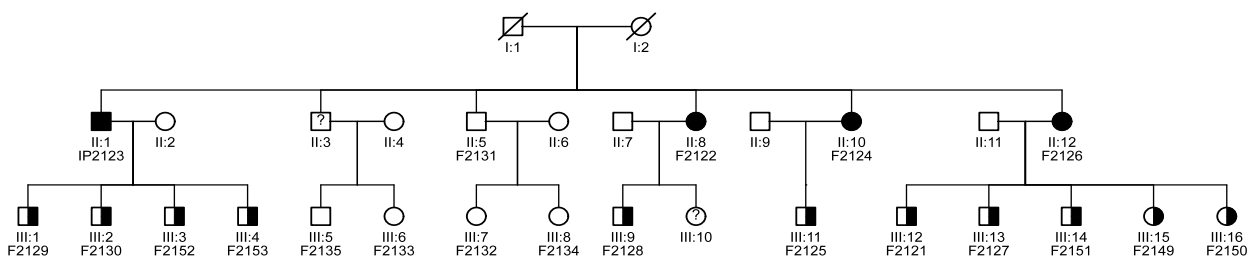


Figure 3 Pedigree of Family W. Circles represent female individuals; squares represent male individuals; deceased individuals are slashed; the individual pedigree number is below each symbol. A code number denotes family members included in the molecular studies. Filled symbols indicate members with a homozygous *PINK1* c.1366C>T mutation. Half-filled symbols indicate heterozygous mutation carriers.

2.2. Material

Materials used in this study are listed below with manufacture's name.

2.2.1. Chemicals

Accutase	Innovative CT
Agarose	Biozym Scientific
Ascorbic Acid	Sigma-Aldrich
Bovine serum albumin (BSA)	Sigma-Aldrich
Collagenase IV	Invitrogen
DAPI Fluoromount G	Southern Biotech
Dibutyl cAMP	Sigma-Aldrich
Dimethyl sulfoxide (DMSO)	Sigma-Aldrich
Desoxyribonucleotides (dNTPs)	Invitrogen
Dulbeccos Modified Eagle Serum (DMEM)	Invitrogen
DMEM/F12 (solution)	StemCell Technologies
DMEM/F12 (powder)	Invitrogen
Ethidium bromide	Sigma-Aldrich
Ethylenediaminetetraacetic acid (EDTA)	Merck
ExoSAP-IT	Usb
Fetal Bovine Serum (FBS)	HyClone
Formamide	Fluka
Fugene 6	RocheDiagnostics
Gelatin	Sigma-Aldrich
Glucose	Sigma-Aldrich
Glycerol	Sigma-Aldrich
Hydrochloric acid	Merck
Insulin	Sigma-Aldrich
Knockout Serum Replacement	Invitrogen
Knockout DMEM	Invitrogen
Laminin	RocheDiagnostics
L-Glutamine	Invitrogen
Matrigel Basement Membrane Matrix	BD Biosciences
MEM non-essential amino acids	Invitrogen
2-Mercaptoethanol	Invitrogen
Methanol	Sigma-Aldrich
mTeSR1 Basal medium with supplement	StemCell Technologies

Nitric acid	Merck
Odyssey Blocking Buffer	LI-COR
Oligonucleotides	Invitrogen
Penicillin/Streptomycin (P/S)	Invitrogen
Phosphate buffered saline (PBS)	Invitrogen
Poly-D-lysine	Sigma-Aldrich
Progesterone	Sigma-Aldrich
Protamine sulfate	Sigma-Aldrich
Putrescine	Sigma-Aldrich
Restriction enzymes	New England Biolabs
Sodium bicarbonate	Sigma-Aldrich
Sodium chloride (NaCl)	Sigma-Aldrich
Sodium selenite	Sigma-Aldrich
Taq-DNA-Polymerase and buffer	Qbiogene / Invitrogen
TGF-beta inhibitor (SB 431542)	Tocris Bioscience
Transferrin (human)	Millipore
Tris-Borate-EDTA buffer (TBE)	Lonza
Tris-Buffered-Saline (TBS)	Boston BioProducts
Tris/Glycine (protein transfer) buffer	Boston BioProducts
Tris/Glycine/SDS (protein running) buffer	Invitrogen
Triton-X100	Sigma-Aldrich
Tween	Merck
TrypLE (Trypsin)	Invitrogen
Valinomycin	Sigma-Aldrich
Y-27632 dihydrochloride	Calbiochem

2.2.2. Kits

BCA Protein Assay Kit	Pierce
DHPLC (WAVE) reagents	Transgenomic
HIV-1 p24 Antigen ELISA	Zeptomatrix
Mycoplasma Detection Kit	Sigma-Aldrich
DNA/RNA Extraction Kits	Qiagen
Sequencing reagents	Applied Biosystems
SuperScript III First-Strand Synthesis	Invitrogen
SYBR Green ER qPCR SuperMix	Invitrogen

2.2.3. Cells

BJ, foreskin fibroblast cell line	ATCC
293FT cell line	Invitrogen
Mouse embryonic fibroblasts (MEFs) (gamma-irradiated CF-1, P3)	GlobalStem

2.2.4. Recombinant proteins

Brain-derived neurotrophic factor (BDNF; human, full length)	R&D Systems
Fibroblast growth factor Basic (FGF-Basic; human, full length)	Invitrogen
Fibroblast growth factor 8a (FGF-8a; human, full length)	R&D Systems
Glial cell-derived neurotrophic factor (GDNF; human, full length)	R&D Systems
Noggin (mouse, full length)	R&D Systems
Sonic Hedgehog (SHH; mouse, N-terminus)	R&D Systems
TGF-beta 3 (human, full length)	R&D Systems

2.2.5. Antibodies

Mouse anti-alpha-Tubulin (1:6000 WB)	Sigma-Aldrich
Mouse anti-SSEA4 (1:200)	Millipore
Mouse anti-Tra-1-60 (1:400)	Millipore
Mouse anti-TUJ1 (1:1000)	Covance
Rabbit anti-NSE (1:2000 WB)	Polysciences
Rabbit anti-NANOG (1:100)	Stemgent
Rabbit anti-Nestin (1:500)	Abcam
Rabbit anti-OCT4 (1:400)	Abcam
Rabbit anti-Tyrosine hydroxylase (1:400, 1:1000 WB)	Calbiochem
Sheep anti-Tyrosine hydroxylase (1:100)	Novus Biologicals
Donkey anti-mouse, Alexa 488 (1:400)	Invitrogen
Donkey anti-rabbit, Alexa 647 (1:400)	Invitrogen
Donkey anti-sheep, Alexa 568 (1:400)	Invitrogen
Goat anti-mouse, Alexa 488 (1:400)	Invitrogen
Goat anti-rabbit, Alexa 568 (1:400)	Invitrogen
Goat anti-mouse, IRDye 680LT (1:10000)	LI-COR
Goat anti-rabbit, IRDye 800CW (1:10000)	LI-COR

2.2.6. Cell culture media

Fibroblast medium:	Dulbeccos Modified Eagle Serum (DMEM), 10% fetal bovine serum (FBS), 2mM L-glutamine, 1mM sodium pyruvate, 0.1mM nonessential amino acid solution (MEM-NEAA) and 1% penicillin/streptomycin (P/S).
IPS medium:	DMEM/F12, 20% knockout serum replacement, 2mM L-glutamine, 0.1mM MEM-NEAA, 0.1mM β -mercaptoethanol, 10ng/ml Fibroblast Growth Factor (FGF) and 1% P/S.
EB differentiation medium:	Knockout-DMEM, 20% FBS (not heat-inactivated), 1mM L-glutamine, 0.1mM β -mercaptoethanol, and 0.1mM MEM-NEAA.
Neural differentiation medium:	Knockout-DMEM, 15% knockout serum replacement, 2mM L-glutamine, 0.1mM MEM-NEAA, 10 μ M SB431542, 500ng/ml Noggin and 1% P/S.
N2 medium:	DMEM/F12, 25 μ g/mL Insulin, 0.1mg/mL Human Transferrin, 5.2ng/mL Sodium Selenite, 16.1 μ g/mL Putrescine, 6.3ng/mL Progesterone (Bottenstein 1985; Johe <i>et al.</i> , 1996).

2.2.7. Equipment

Automatic sequencer Long Read IR2-DNA	LI-COR
Bench-top laminar flow hood	The Baker Company
Capillary Sequencer 3130	Applied Biosystems
CO ₂ Incubator	SANYO
Confocal microscope TCS SL	Leica
DHPLC (WAVE)	Transgenomic
Flow Cytometer LSRII	BD Bioscience
Inverted microscope	Olympus
Microscope	Olympus
NanoDrop Spectrophotometer	NanoDrop
Odyssey Imager	LI-COR
Thermocycler - Mastercycler	Eppendorf
- iCycler	BioRad
Ultra centrifuge (Rotor SW27)	Beckman

2.3. Methods

2.3.1. Extraction of nucleic acids

Genomic DNA was isolated from cells using the DNeasy kit (Qiagen). Cell pellets were processed according to the manufacturer's instructions. Total RNA from cells was prepared by using the RNeasy kit (Qiagen) according to the manufacturer's instructions.

2.3.2. Polymerase chain reaction

The polymerase chain reaction (PCR) is a method for enzymatic amplification of DNA *in vitro* (Saiki *et al.*, 1985). Two primers (short DNA sequences) enable specificity by binding complementarily to a certain target sequence. The thermal stable DNA polymerase elongates the region between the primer pair. Exponential amplification of the target sequence relies on thermal cycling which is divided in three repeating steps: denaturing of DNA, annealing of primers, extension through DNA polymerase.

2.3.2.1. Standard PCR

Standard PCR was performed as follows:

Substance	Stock concentration	Volume	Final concentration
dH ₂ O		ad 15.00µl	
Buffer	10x	1.50µl	1x
dNTPs	1mM	3.00µl	0.2mM
Primer F	10µM	0.60µl	0.4µM
Primer R	10µM	0.60µl	0.4µM
Taq polymerase	5U/µl	0.07µl	0.23U/µl
DNA	~ 5ng/µl	5.00µl	~ 1.67ng/µl

Cycling conditions:

95°C 5min // 35 cycles: 95°C 30s; 52-68°C 30s; 72°C 30s-2min 72°C 10min // 4°C ∞

Annealing temperature and extension time are dependent on the sequence composition of the primers and the product size, respectively.

For the *PRKRA* study (3.1.), the eight exons of the *PRKRA* gene were amplified as described above. Primer sequences are listed in table S1.

2.3.2.2. Quantitative RT-PCR

To investigate gene expression, mRNA was extracted and reverse-transcribed into cDNA with the SuperScript III First-Strand Synthesis System (Invitrogen). Quantitative RT-PCR was performed with SYBR GreenER (Invitrogen) on the iCycler system (BioRad). SYBR Green is a dye that fluoresces upon intercalation with double-stranded DNA. It is used to detect the threshold cycle (Ct) during PCR when the level of fluorescence gives a signal over the background and is in the linear portion of the amplified curve. The Ct value is responsible for the accurate quantification of the PCR.

The PCR amplification mixture was prepared as follows:

Substance	Stock concentration	Volume	Final concentration
dH ₂ O		ad 20.0µl	
SYBR GreenER	2x	10.0µl	1x
Primer F	10µM	0.5µl	0.25µM
Primer R	10µM	0.5µl	0.25µM
cDNA	12.5ng/µl	2.0µl	1.25ng/µl

Cycling conditions: 50°C 2min; 95°C 8.5min // 50 cycles: 95°C 15s; 60°C 1min

Melting curve analysis: 95°C 1min; 55°C 1min // 80 cycles: 55°C + 0.5°C/cycle 10s

To determine a fold change of gene expression levels between sample A and B, the delta-delta-Ct ($\Delta\Delta Ct$) method was used. The Ct value of the target gene is normalized with the Ct value of a reference gene (housekeeping gene of the cell) in the following equation:

$$\text{Fold change} \approx 2^{\Delta\Delta Ct} = 2^{\exp(\Delta Ct_{\text{sample A (target-reference)}} - \Delta Ct_{\text{sample B (target-reference)})}}$$

This method was used to detect expression levels of pluripotency markers *NANOG*, *GDF3*, *OCT4* and *SOX2* in fibroblasts and iPS cell lines relative to *β-actin* (reference gene). Further, residual expression levels were examined of the transgenes *OCT4*, *SOX2*, *cMYC* and *KLF4* (relative to *β-actin*). In these assays, primers were used specific for the endogenous gene loci and the viral transgenes respectively.

IPS cell-derived neurons were examined for relative gene expression levels of *PINK1*. For mitochondrial DNA copy number and *PGC-1α* expression, a fold change, normalized to *β-actin* was calculated. All reactions were performed in triplicates and results were analyzed with an unpaired t-test for statistical significance. Primers used in this study can be found in table S2.

2.3.3. Sequencing

DNA sequencing reactions were performed based on the principle of the chain termination method (Sanger *et al.*, 1977) and subsequent nucleotide sequence determination by using a capillary sequencer. During the sequencing reaction, a DNA polymerase synthesizes complementary DNA strands by incorporating not only dNTPs but dideoxy nucleotides (ddNTPs). Whereas the assembly of dNTPs results in normal elongation of new DNA strands, a ddNTP molecule leads to chain termination. The detection of the synthesized DNA fragments of different lengths is performed through a base (A, T, G, C)-specific fluorescence labeling of the ddNTP molecules that is recognized by the capillary sequencer.

First, the target DNA was amplified in a standard PCR. In a second step, the PCR products were purified using ExoSap (Usb) according to manufacturer's protocol. The actual sequencing reaction was prepared as follows:

Substance	Stock concentration	Volume	Final concentration
PCR product	5-10ng	1.0 μ l	5-10ng
Buffer	5x	1.5 μ l	0.75x
Primer	10 μ M	0.5 μ l	0.5 μ M
Terminator mix 1.1.		0.5 μ l	
dH ₂ O		6.5 μ l	
Σ		10.0 μ l	

Cycling conditions: 96°C 1min // 25 cycles: 96°C 10s; 60°C 5s; 60°C 1min // 4°C ∞

The last step was a sodium acetate precipitation to purify the newly formed DNA fragments from any other substances:

Substance	Volume
Product	10 μ l
dH ₂ O	10 μ l
Sodium acetate, 3M	2 μ l
Ethanol, 100%	50 μ l

Samples were incubated for 20min and centrifuged 1h at 3000rpm. The supernatant was discarded, DNA samples were washed with 50 μ l 70% ethanol and centrifuged again for 1h at 3000rpm. After complete evaporation of ethanol, 12 μ l HiDi-Formamide (Applied Biosystems) was added to each sample and incubated for 12-24h at 4°C.

The samples were analyzed automatically using the capillary sequencer *ABI 3130 Genetic Analyzer* in combination with the separation matrix *POP-7* (Applied Biosystems). Sequencing

results were evaluated with the corresponding software *Sequence Analysis Software v2.5* (Applied Biosystems).

In the *PRKRA* study (3.1.), exons 1, 3 and 6 of the *PRKRA* gene were sequenced as described above. For the remaining exons (2, 4, 5, 7 and 8), PCR products were purified and sent for sequencing to MWG Biotech. Sequencing results of viral constructs and iPS cells were obtained from the MGH DNA Core Facility.

2.3.4. Gel electrophoresis

2.3.4.1. Agarose gel electrophoresis

Agarose gel electrophoresis is a method used to separate DNA fragments by length. Agarose powder is mixed with TBE buffer to the desired concentration and heated until completely melted. To enable visualization of DNA, ethidium bromide is added at this point to the gel (final concentration 0.5µg/ml) and the solution is poured into a casting tray containing a sample comb. DNA samples are mixed with formamide dye and loaded into the solidified gel. In addition, a corresponding molecular weight standard (100bp or 1000bp ladder) is loaded to estimate the size of the DNA fragments. The electrophoresis is run at 120V for 20-60min in TBE buffer.

2.3.4.2. Denaturing polyacrylamide gel electrophoresis

Denaturing polyacrylamide gel electrophoresis separates linear monomer DNA fragments according to their size at high resolution (up to single bp). It uses SDS for denaturing of the samples, which renders their charge proportional to their length so that migration is a function of size. The samples are amplified with a standard PCR supplemented with infrared-labeled oligonucleotides as probes. An automated sequencer (LI-COR) is employed to run the gel and to detect the samples with infrared lasers.

The gel is composed as follows:

Substance	Volume
30% Acrylamid	6ml
10x TBE	3ml
Urea	3g
dH ₂ O	ad 30ml
10% APS	180µl
TEMED	25µl

Conditions: electrophoresis in TBE as running buffer for 3h at 45°C, 25W and 40mA

This method was used in the *PRKRA* study to screen the healthy controls (Cohort C) for the genetic change c.266_267delAT.

2.3.5. Denaturing high-performance liquid chromatography

The WAVE System instrument (Transgenomic) uses the Denaturing high-performance liquid chromatography (DHPLC) technique to detect genetic mutations and single nucleotide polymorphisms (SNPs). The technique is based on DNA heteroduplex formation and separation of heteroduplex from homoduplex molecular species. Heteroduplexes with mismatched base pairs are formed when a PCR product that contains a heterozygous mutation is denatured and subsequently cooled. To detect homozygous mutations, PCR products have to be mixed with each other in order to form heteroduplexes. Samples were amplified by standard PCR, injected into the DHPLC system and analyzed according to manufacturer's instructions.

This method was used to screen healthy control individuals (Cohort C) in the *PRKRA* study for the genetic change c.126C/T in *PRKRA*.

2.3.6. Restriction digest

This enzymatic technique is used for cleaving DNA molecules at specific sites by a class of DNA-cleaving enzymes called restriction endonucleases. They allow to precisely cut DNA in a predictable and reproducible manner. A standard DNA digest was composed as follows:

Substance	Concentration	Volume	Final concentration
dH ₂ O		ad 20.0µl	
DNA	~2µg/µl	0.5µl	0.05µg/µl
Buffer	10x	2.0µl	1x
Enzyme	20,000units/ml	0.5µl	0.5units/µl

Incubation: 3h at 37°C

In the *PRKRA* study this method was used to investigate healthy control individuals (Cohort C) regarding two genetic changes: c.795C/T in exon 8 with the enzyme HhaI and c.665C>T in exon 7 with the enzyme BstNI.

2.3.7. DNA cloning

In this study viral vectors were used to deliver genetic material into human cells. As a starting material, DNA plasmids were prepared containing the gene of interest. Plasmids used in genetic engineering are designed to contain cloning sites of a series of restriction recognition sequences for a variety of restriction endonucleases. Cutting with a restriction enzyme opens up the circular plasmid DNA and allows to an insert DNA to be spliced in. These vectors can be introduced directly into a mammalian cell by transfection to express their genes. When combined with viral genes, transfected cells may produce virus particles (2.3.8.).

2.3.7.1. *Retroviral vectors*

Retroviral pMIG vectors containing the four human genes OCT4, SOX2, cMYC and KLF4 were obtained from Professor G.Q. Daley's laboratory (Children's Hospital, Boston, MA). A map of pMIG vectors is not available. Constructs were amplified and sequenced to verify the gene of interest.

2.3.7.2. *Lentiviral vectors*

Human Parkin and PINK1-V5 cDNA were cloned into lentiviral pER4 vectors (obtained from Novartis, Cambridge, USA) with neuron-specific phosphoglycerate kinase (PGK) promoter. Both cDNAs were obtained from pcDNA3 vectors that were available at the Section of Neurogenetics in Lübeck.

The cloning strategy was to isolate Parkin sequence from pcDNA3, to paste it into the entry vector pENTR1A (Invitrogen) and to subclone it into the destination vector pER4 via recombination technology. In brief, Parkin cDNA was cut out of the vector by restriction digest using enzymes BamHI and NotI. Parkin cDNA was isolated and subsequently inserted into pENTR1A. The ligated plasmid was amplified in bacteria and purified from the cell pellets (2.3.7.3.). Insertion of Parkin sequence from pENTR1A into the destination vector pER4 was performed via the Gateway recombination cloning technology (Invitrogen) according to the manufacturer's instructions. This technique is based on a unique sequence cassette of entry and destination vectors which recombines and exchanges the sequences within it using the enzyme clonase.

PINK1-V5 was cloned directly into pER4. First, PINK1-V5 cDNA was PCR-amplified from pcDNA3 vector using nested primer sequences that contained the restriction sites of BamHI and NotI respectively. Second, the pER4-Parkin vector was digested with enzymes to cut out Parkin sequence and PINK1-V5 PCR product was inserted (Fig. 4).

Ligation reactions were performed with the following conditions:

20ng/kb insert, 60ng/kb vector, 1µl T4 ligase, 1µl 10x T4 ligase buffer in a volume of 10µl (ad dH₂O). The reaction mixture was incubated for 1h at RT.

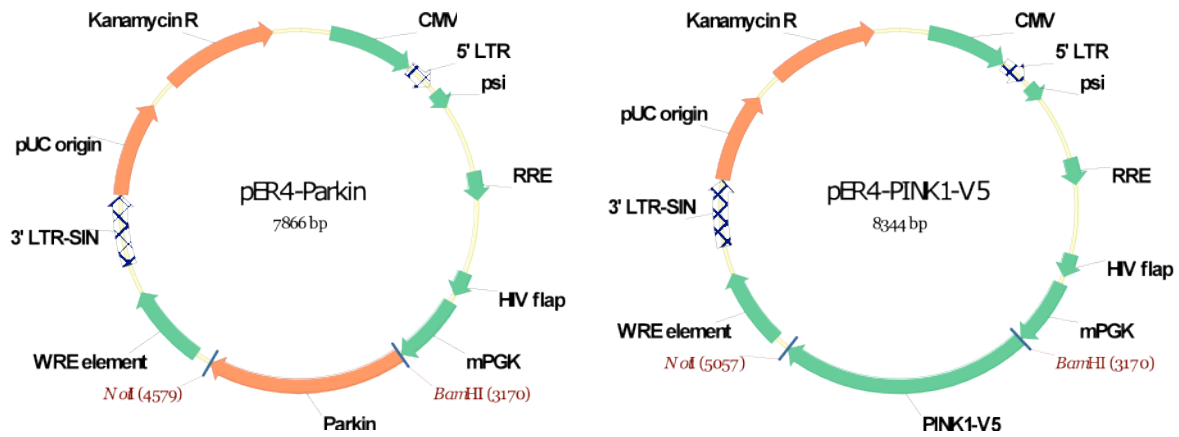


Figure 4 Vector maps of *pER4-Parkin* and *pER4-PINK1-V5*. It contains the coding sequences of Parkin and PINK1-V5, the antibiotic resistance gene Kanamycin and other regulatory sequences such as: Cytomegalovirus (CMV) promoter, 5'LTR (long terminal repeats) and 3'LTR for transcription and integration, viruscapsid sequence (psi), rev responsive element (RRE) for rev nuclear export, HIV flap for nuclear import, mouse phosphoglycerate kinase (PGK) promoter, WRE element for increased protein expression rate.

2.3.7.3. Amplification of DNA plasmids

To amplify plasmids in bacteria, XL10-Gold Ultracompetent Cells (Stratagene) were transformed following the manufacturer's instructions. Because transformation usually produces a mixture of relatively few transformed cells, vectors contain an antibiotic resistance gene. For selection process, the mixture of cells was plated on LB medium agarose dishes containing the antibiotic, thus, only the transformed cells were able to grow. Bacterial clone colonies were picked and further cultured. To amplify the plasmid on a large scale, bacteria culture was added to 150ml LB medium and cultured for 16h at 37°C. For isolation of plasmid DNA, cells were centrifuged and the pellet was processed by using the Maxiprep kit (Qiagen) according to the manufacturer's instructions. Next, plasmid DNA concentration was determined using a spectrophotometer (NanoDrop) and the gene of interest was sequenced in order to exclude any mutations. In addition, the backbone of the plasmid was examined by restriction digest.

2.3.8. Viral vectors

Viral vectors are genetically-engineered viruses carrying modified viral DNA and the gene to be delivered into the target cell. In this study replication-defective vectors were used in which a part of the viral genome critical for viral replication had been deleted. For virus production, three plasmids were transfected into the packaging cell line HEK 293FT: Two packaging plasmids that encode for the viral proteins: pol (reverse transcriptase/integrase), env

(envelope), gag (capsid) and another plasmid that contains the gene of interest to be delivered by the vector. The viral particles are assembled in the packaging cell and released into the cell culture medium. In the present study retroviral and lentiviral vectors were used. Retroviral vectors were originally derived from Moloney murine leukemia virus (MoMLV). They have the ability to integrate into the host genome. The envelope of this virus has been replaced by the G glycoprotein of vesicular stomatitis virus (VSV-G) leading to more stable virus particles that could be concentrated and were used with high infection efficiencies (Burns *et al.*, 1993). As retroviruses can infect only dividing cells, lentiviruses, a subclass of retroviruses, were used in this study to infect neurons.

2.3.8.1. Production of viral vectors

Virus production was conducted with minor modifications according to a standard protocol that was published as part of the iPS cell reprogramming method (Park *et al.*, 2008a). The following steps were accomplished:

- Day 0, Plating: 293FT cells were plated in 10x10cm dishes per virus at a density of 3×10^6 cells/dish and incubated O/N.
- Day 1, Transfection: For each 10cm dish, 20 μ l Fugene 6 was added to 300 μ l DMEM and incubated for 5min at RT. DNA mix of 2.5 μ g viral vector, 0.25 μ g VSV-G and 2.25 μ g Gag-Pol (8.2 Δ R for lentivirus) was added and incubated for 20min at RT. The transfection mix was added to the cells in a drop wise manner.
- Day 2, Medium change: Medium was changed ~18h post-transfection.
- Day 3, Collecting: Virus-containing medium was collected ~48h post-transfection and passed through an 0.45- μ m filter unit. The medium was transferred into 38.5-ml Beckman centrifuge tubes and centrifuged at 70,000g, 4°C for 90min using Beckman ultracentrifuge. Virus pellet was resuspended in DMEM using an appropriate volume (100-300x concentrated) and stored in aliquots at -80°C.

2.3.8.2. Titering of viral vectors

All four retroviral vectors contain a green fluorescence protein (GFP) sequence and the concentrated virus was titered by determining the percentage of infected 293FT cells using flow cytometry (FACS) as reported previously (Tiscornia *et al.*, 2006).

In brief, titering was performed as follows:

- Day 0: 1×10^5 293FT cells were plated per well of a 12-well dish in culture medium supplemented with 5 µg/ml protamine sulfate. Concentrated virus was added directly into the culture medium using volumes 50 µl, 25 µl, 12.5 µl and 6.25 µl.
- Day 2: Medium was aspirated and cells were singled using trypsin and centrifuged. The pellet was resuspended in 100 µl PBS and cells were fixed by adding 4% formaldehyde in 100 µl PBS. Subsequent examination by FACS (2.3.9.) was performed within 3 days.

The titer of lentiviral vectors was determined by using the HIV-1 p24 Antigen ELISA kit (Zeptomatrix) according to the manufacturer's instructions. This method provided as a result the amount of infectious particles per µl (i.p./µl). Infection efficiencies of Parkin virus (4.2×10^5 i.p./µl) and PINK1-V5 (9.4×10^5 i.p./µl) virus were analyzed 5 days post-infection of neuronal cells by immunostaining (2.3.15.). For Parkin a multiplicity of infection (MOI) of 3 and for PINK1-V5 an MOI of 2 was used to infect neuronal cultures.

2.3.9. Flow cytometry

A flow cytometer passes the cells in a stream of fluid by an electronic detection system. There are a number of detectors focused at the point where the stream passes through a light of a singular wavelength beam. The Forward Scatter (FSC), in line with the light beam, the Side Scatter (SSC), orthogonal to it, and one or more fluorescent detectors. The detection of scattered light gives information about the physical structure of the individual cell. FSC is dependent on the cell volume and SSC correlates with the inner complexity of the cell.

In this study the LSRII (BD Biosciences) flow cytometer was used for counting GFP-positive cells in order to determine the infection efficiency of retroviral vectors (2.3.8.). The generated data were analyzed in two-dimensional dot plots with the software FACSDiva (Version 6.1). First, uninfected (GFP-negative) control cells were loaded and voltages were set so that the bulk of cells appeared roughly in the lower left quadrant in FSC/SSC plot. Second, a dot plot GFP/Phycoerythrin (PE) was created as GFP can produce wavelengths which appear in the region of the detector for PE. Regions on these plots can be separated by creating a gate. Therefore, a region, where the GFP-positive cells were expected, was gated. Infected samples were analyzed subsequently and the software calculated percentage of GFP-positive cells. The following voltages were used for 293FT cells: FSC, 293V; SSC, 286V; GFP, 400V; PE, 358V.

2.3.10. Cell culture

In this study human primary fibroblasts, irradiated mouse embryonic fibroblasts (MEFs), 293FT cells and human iPS cells were cultured. All cells were maintained at 37°C in a saturated humidity atmosphere containing 5% CO₂.

2.3.10.1. Fibroblast culture

Human primary fibroblasts and MEFs were cultured in fibroblast medium (2.2.6.). Primary fibroblasts were passaged when 80% confluent: Medium was removed, the cells washed with phosphate buffered saline (PBS), and incubated with 2ml Trypsin for 5min. Cells were singled by pipetting in additional 6ml culture medium and centrifuged for 5min at 1000rpm. To reseed cells, the pellet was resuspended in culture medium and replated in culture dishes (1:2). To freeze cells, the pellet was resuspended in 1ml culture medium supplemented with 10% DMSO and delivered into a cryogenic vial. A freezing container ("Mr. Frosty") filled with isopropyl alcohol provided the critical cooling rate of -1°C/minute when put into a -80°C freezer. For long-term storage, vials were placed in a liquid nitrogen container.

2.3.10.2. 293FT cell line culture

293FT cell line was purchased from invitrogen and used for virus production (2.3.8.1.). Cells were cultured in DMEM (high glucose) supplemented with 10% FBS and passaged at a confluency of 90% using the protocol described for fibroblast culturing (2.3.10.1.). Reseeding of cells was performed at the ratio of 1:6.

2.3.10.3. IPS cell culture

Human iPS cells were maintained on irradiated MEF feeder layers in iPS medium (2.2.6.). Culturing of iPS cells required a medium change every day and a splitting of colonies once a week. IPS cell colonies were passaged enzymatically using Collagenase type IV. Before passaging, any pluripotent colonies that had the appearance of differentiated cells, irregular borders, or transparent centers were removed using the picking hood, stereo microscope and 200µl pipette tips connected to vacuum (Fig. 5). After grooming, medium was aspirated and colonies were incubated in 1mg/ml Collagenase type IV for 15min. Next, collagenase solution was aspirated and colonies were scraped in 1ml DMEM/F12 with a cell lifter and centrifuged for 2min at 100g. Colonies were reseeded on irradiated MEFs (split ratio 1:4-6). The feeder plates had to be prepared 24-48h before iPS cell passaging: MEFs were seeded on gelatin-coated 6-well dishes in fibroblast culturing media at a density of 15,000 cells/cm². In order to separate iPS cells from the MEF feeders and continue growing the iPS cells under feeder-free conditions, colonies were plated during the passaging step on BD Matrigel as a culture matrix. However, it is necessary to culture the iPS cells in mTeSR1 (StemCell

Technologies) medium which includes all the factors needed to maintain pluripotency characteristics of the cells. Passaging under these conditions is performed by using the enzyme dispase (1mg/ml) instead of collagenase.

To freeze iPS cells, the pellet of one confluent 6-well was resuspended in 0.5ml iPS culture medium. A volume of 0.5ml freezing medium containing 80% defined FBS and 20% DMSO was added and the cryogenic vial was placed into a freezing container (2.3.10.1.).

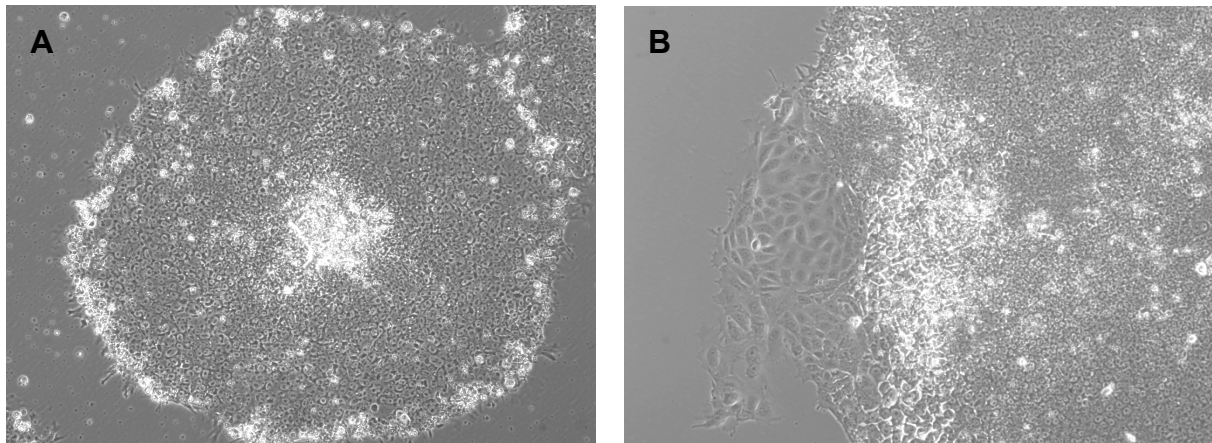


Figure 5 *iPS colonies grown on matrigel.* **(A)** This iPS colony shows the characteristic ES cell-like morphology, round-shaped with a clear-edged border. A beginning differentiation of cells is located at the center, which can be removed easily by using a 200 μ l pipette tip. **(B)** Spontaneous differentiation is observed as an irregular border of the colony. In this case at least half of the colony is removed in order to take out any differentiated part of the colony.

2.3.11. Reprogramming

For the generation of iPS cells, primary human dermal fibroblasts were transduced by retroviral vectors containing the four factors OCT4, SOX2, cMYC and KLF4 (Park *et al.*, 2008a). Viral production was conducted as described (2.3.8.1.). All four vectors contain a GFP sequence and the concentrated virus was titered by determining the percentage of infected 293FT cells using FACS (2.3.8.2.). A histone deacetylase inhibitor, valproic acid, was included in the cocktail to further increase the efficiency of reprogramming (Huangfu *et al.*, 2008). After a month of culturing, iPS cell colonies were picked based on their characteristic ES cell-like morphology and silencing of the retroviral GFP signal. Retroviral expression has been shown previously being suppressed specifically in stem cells through silent chromatin (Yao *et al.*, 2004).

In the following a detailed reprogramming protocol is presented:

- Day 0: 3 x 10⁵ early primary fibroblast cells (< 5 passages) were plated in a 6cm dish in fibroblast medium and incubated O/N.
- Day 1: Infection of fibroblasts: Medium was aspirated and replaced with fresh fibroblast medium containing a virus load to reach 70-80% infection efficiency for OCT4, SOX2 and KLF4 and to reach 40-50% infection efficiency for cMYC. In addition, medium was supplemented with 5µg/ml protamine sulfate. Infection time was 48h.
- Day 3: Reseeding of fibroblasts: Medium was aspirated and cells were washed 2x with PBS, trypsinized and replated onto 2 gelatin-coated 10cm dishes in fibroblast medium.
- Day 4-11: VPA treatment: Fibroblast medium was replaced with iPS medium supplemented with 0.5mM valproic acid (EMD Biosciences) for 1 week. Medium was changed daily.
- Day 12-35: Withdraw VPA: From day 12 on, VPA was withdrawn and fibroblasts were cultured in iPS cell medium that was continuously replaced daily.
- Day 21-35: IPS cell colonies: On day 21 of reprogramming, first iPS cell colonies started appearing on the fibroblast layer. Colonies were picked based on their stem cell-like morphology and the silencing of the retroviral GFP signal using a pipette tip. The picked colonies were subsequently expanded and maintained on MEF feeder layers in iPS medium.

2.3.12. Karyotype analysis

Karyotype analysis of iPS cells was performed at Cell Line Genetics (Madison, WI, USA) using standard protocols for high-resolution G-banding. A confluent T25 flask with iPS cells was sent as live culture for analysis.

2.3.13. Spontaneous *in vitro* differentiation

Spontaneous differentiation was carried out through embryoid body (EB) formation as described before (Xu *et al.*, 2001) in order to show the pluripotent potential of the generated iPS cells. In brief, colonies were detached by collagenase, dissociated into small clumps and cultured in suspension as EBs in EB differentiation medium (2.2.6.) for 4 days. EBs were transferred onto gelatin-coated plates and cultured for an additional 7 days. Differentiated

cells were trypsinized, pelleted and processed for RNA extraction. RT-PCR was performed to analyze expression of markers of the three germ layers.

2.3.14. Neuronal *in vitro* differentiation

Directed differentiation of iPS cells *in vitro* toward DA neurons was conducted as described (Chambers *et al.*, 2009), with minor modifications.

It is important to remove differentiated human cells and MEFs that reduce the efficiency of neural induction. Therefore, iPS cell colonies were groomed as described (2.3.10.3.) and subsequently dissociated into single cells using Accutase. After two washing steps with medium, cells were passed through a cell strainer (0.45 μ m) and replated onto gelatin-coated dishes in iPS medium supplemented with ROCK inhibitor Y-27632 (final concentration 10 μ M). Dishes were incubated at 37°C to let MEFs adhere. After one hour, non-adherent cells were collected and plated onto Matrigel-coated dishes at a density of 35,000 cells/cm² in mTeSR1 medium (StemCell Technologies), supplemented with ROCK inhibitor Y-27632.

Differentiation was started after 3-6 days at a confluence of ~80% by adding neural differentiation medium (2.2.6.), supplemented with SB431542 (10 μ M) and Noggin (500ng/ml). Upon day 5 of differentiation, increasing amounts of N2 medium (2.2.6.) was added (25%, 50%, 75%) to neural differentiation medium every 2 days as reported (Chambers *et al.*, 2009). On day 11 of differentiation, cells were passaged *en bloc* (size of 1-2mm) and plated onto coated glass cover slips (Assistent) in N2 medium. Glass cover slips were incubated in nitric acid for 24h, washed with water and ethanol, incubated overnight in 75 μ g/ml poly-D-lysine, washed with water and incubated overnight in 5 μ g/ml laminin (Roche). The type of glass cover slip and the coating method were critical for monolayer-grown neurons. During these 11 days of differentiation, a large population of the cells turned into CNS neural precursors and a minor population into neural crest cells (Chambers *et al.*, 2009). The desired CNS neural precursors were selected by using a stereomicroscope for this passaging step (Fig. 6).

Patterning of cells into the DA lineage was initiated by adding BDNF (20ng/ml), ascorbic acid (200 μ M), SHH (200ng/ml), and FGF8a (100ng/ml). After 1 week of culture, cells were differentiated in the presence of BDNF (20ng/ml), ascorbic acid (200 μ M), GDNF (20ng/ml), TGF- β 3 (1ng/ml), and cyclic-AMP (500 μ M) as previously reported (Perrier *et al.*, 2004; Chambers *et al.*, 2009).

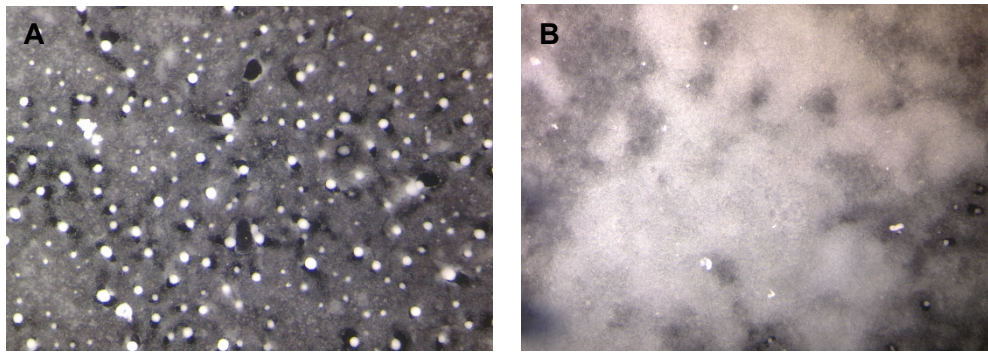


Figure 6 Selection of CNS neural precursors on day 11 of differentiation. The morphology of CNS neural precursors and neural crest cells could be distinguished roughly by using a stereo microscope. **(A)** Example for neural crest cell layer. **(B)** Example for CNS neural precursor cell layer.

2.3.15. Immunofluorescence and cell counts

Immunofluorescence is a technique used for fluorescence microscopy. It takes advantage of the specificity of antibodies to their antigen to target fluorescent dyes to specific targets within a cell and, therefore, allows visualization of the distribution of the target molecule in the investigated cells.

IPS cells and differentiated neurons were grown on glass cover slips, fixed in 4% formaldehyde for 15min, permeabilized and blocked with 0.1% Triton X-100 in 4% appropriate normal serum in PBS for 1h. Immunofluorescence staining was performed in antibody dilution solution (3% BSA, 0.05% NaN_3 in PBS) using primary antibodies with appropriate dilutions (2.2.5.), incubated O/N at 4°C. After 3x PBS washing steps, suitable secondary antibodies connected with a fluorescent dye (2.2.5.) were incubated in antibody dilution solution at RT for 1h. Cover slips were mounted upside down on microscope slides using mounting media. Pictures were taken with a fluorescence microscope and saved as .tif format.

Quantification of immunofluorescence staining was performed on fields of neuronal monolayer cultures acquired at 20x magnification (dimensions: 4080 x 3072). Aggregated clusters of neurons were excluded from counts. Each field was scored first for DAPI (4',6-diamidino-2-phenylindole)-positive nuclei followed by TUJ1 and, subsequently, TH colocalization. The total number of cells analyzed from two independent differentiation experiments exceeded 12,000 cells.

2.3.16. Confocal microscopy

Confocal microscopy was used to increase optical resolution and contrast of immunostained neuronal samples for colocalization imaging. A whole image is obtained pixel-by-pixel and line-by-line with a laser that scans over a plane. The brightness of a resulting image pixel depends on the relative intensity of detected light.

Differentiated neurons were treated with the potassium ionophore valinomycin (1 μ M) for 12h. Colocalization imaging of Parkin translocation was performed on fixed samples using the confocal microscope TCS SL (Leica Microsystems) with the 63x/1.4 oil HCX PL APO objective. Images were acquired in the sequential scan mode, as simultaneous image acquisition of double or triple-stained samples can result in crosstalk, since all dyes will be excited at the same time. Therefore, defining parameters were set specifically for each dye to eliminate this crosstalk.

The quantitative colocalization analysis of Parkin and Tom20 signals was performed with ImageJ and JACoP plug-in (Bolte and Cordelieres, 2006) to determine Manders' coefficient (Manders *et al.*, 1992) from 0 to 1 (0=non-overlapping images and 1=colocalized images). The coefficient displays the ratio of the summed intensities of pixels from the Parkin image for which the intensity in the Tom20 image is above zero to the total intensity in the Parkin image. Therefore, Manders' coefficient is a good indicator of the proportion of the Parkin signal coincident with a signal of Tom20 over its total intensity.

2.3.17. Western blotting

Western blotting is an analytical technique used to detect specific proteins in a biological sample. It uses gel electrophoresis to separate proteins by length (under denaturing conditions). Proteins are transferred subsequently to a membrane, where they are detected using antibodies specific to the target protein.

Proteins from cell pellets were extracted using a 2% SDS buffer. Standard protocols were used for Western blotting. Protein concentration was determined by using the Micro BCA Protein Assay Kit (Pierce) according to manufacturer's instructions. 30 μ g of samples were loaded on a gel (4-12% Tris/Glycine; invitrogen) and electrophoresed for 2h at 125V. The proteins were transferred to a PVDF membrane for 2h at 310mA. Antibodies used for Western blotting were anti-TH, anti-NSE and anti-alpha-Tubulin. Detection was done using the Odyssey infrared imaging system (LI-COR Biosciences) according to the manufacturer's instructions.

3. RESULTS

The present thesis is concerned with two neurological movement disorders: Dystonia and PD. First, a genetic study was performed on *PRKRA*-linked dystonia by screening a large group of patients to explore the role of mutations in *PRKRA* (3.1.). Second, investigations in monogenetic *PINK1*-linked PD were performed on the cellular level by establishing a human neuronal model for PD using iPS cells. This model was further examined for the cellular effect of endogenous *PINK1* mutations (3.2.).

3.1. Dystonia: Exploring the role of mutations in *PRKRA*

This study aimed at the identification of new dystonia-causing mutations in *PRKRA*. A group of patients was selected for the mutation screen based on specific clinical features of examined patients (3.1.1.). The screening was performed in this group by direct sequencing of the coding exons and exon-intron boundaries (3.1.2.).

3.1.1. Patients

The phenotypic spectrum associated with mutations in *PRKRA* was largely unknown, since it had been described in a single study only (Camargos *et al.*, 2008). On the basis of early onset (<25 years) 52 unrelated patients with dystonia were identified as a first patient cohort (Cohort A). The second patient cohort (Cohort B) consisted of an additional 75 dystonia patients with an age of onset >25 years. For any identified genetic changes, a group of 189 neurologically healthy controls (Cohort C) was available to validate the results (2.1.1.).

3.1.2. Mutational screen

By using published primer sequences (Camargos *et al.*, 2008), all coding exons and flanking intronic sequences of *PRKRA* were sequenced in patient cohort A. A novel heterozygous mutation (c.266_267delAT; p.H89fsX20) in exon 3 of *PRKRA* (Fig. 7) was identified in a male patient (Seibler *et al.*, 2008). This mutation was not included in dbSNP (<http://www.ncbi.nlm.nih.gov/SNP>) and was absent in cohort B and cohort C. No other *PRKRA* mutation was detected in this patient. Clinically, he presented with early-childhood-onset leg dystonia that spread gradually over the course of a few years. His family history

was unremarkable for any movement disorder and secondary causes of dystonia were excluded. MRI of the brain was normal. At his last examination, the patient, who is now aged 12 years, had generalized dystonia that spared only the cranial and facial muscles, his walking was severely impaired, but his cognition was normal. The identified heterozygous deletion might have had a pathogenic effect in its own right. It is a predicted frameshift mutation, which causes premature truncation of the protein resulting in a dysfunctional protein (Seibler *et al.*, 2008).

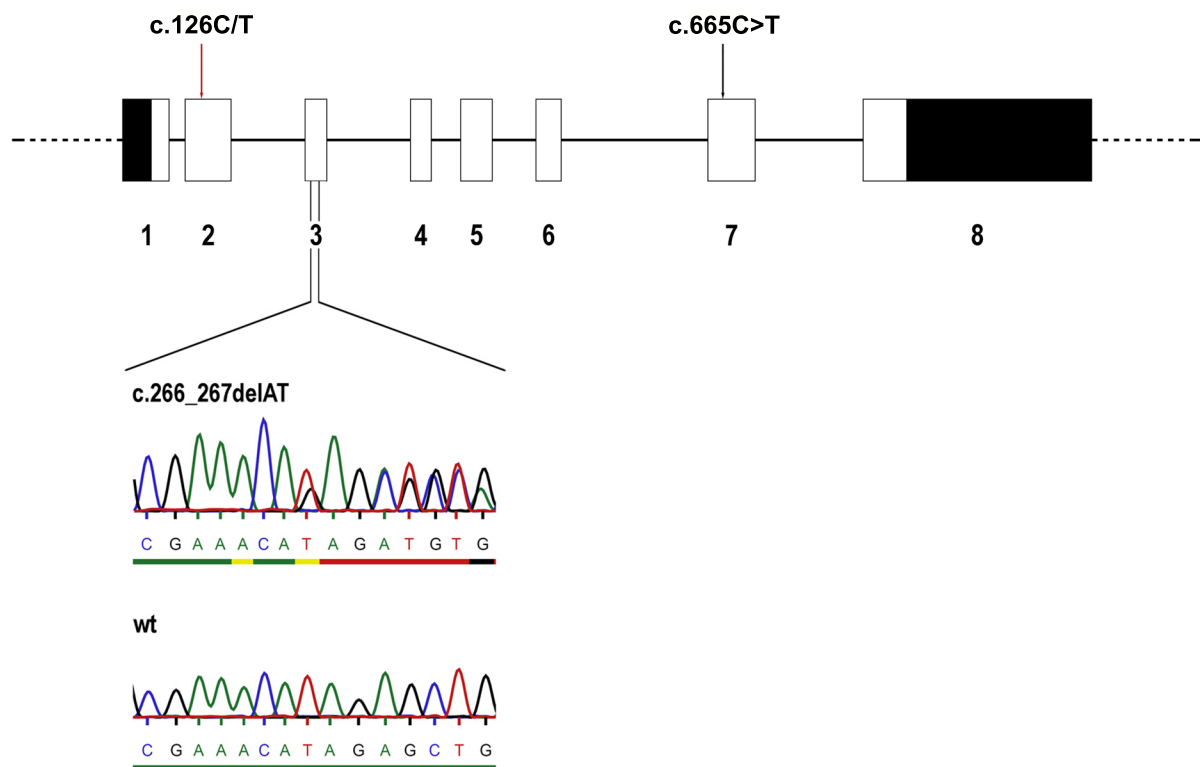


Figure 7 Changes detected in *PRKRA*. Coding and non-coding regions of the exons are shown as white and black boxes, respectively. The positions of the previously reported mutation (c.665C>T) and a novel silent change (c.126C/T) that was absent in 189 screened controls are indicated by the arrows. The exact position and electropherograms of the 2-nucleotide deletion seen in one of the patients and the corresponding wild-type (wt) sequence are shown below.

In addition to this mutation, two new heterozygous silent changes in *PRKRA* were found in other patients. A base pair exchange in exon 2 (c.126C/T; fig. 7) was identified in one patient and was absent in all healthy control individuals, examined by means of a mutation detection system based on denaturing high-performance liquid chromatography (2.3.5.). In three of the patients a base pair exchange in exon 8 (c.795C/T) was found. It was present in five of the controls, as well. The previously identified missense mutation (c.665C>T; fig. 7) in *PRKRA*

(Camargos *et al.*, 2008) and the frequent GAG deletion in *DYT1* dystonia (Ozelius *et al.*, 1997) were excluded in all 127 patients.

RNA samples were unavailable to test for any possible effects of the two silent changes on splicing. Therefore, software was used as an approach to predict possible splice sites (http://www.fruitfly.org/seq_tools/splice.html; Reese *et al.*, 1997). A change of donor and acceptor sites caused by the c.126C/T base pair exchange could be excluded. The c.795C/T base pair exchange caused a minor score change for the acceptor site. However, this silent mutation has been identified in the controls, as well.

3.2. Parkinson disease: Establishing a human neuronal model using iPS cells

This study deals with the generation of PD patient-derived iPS cells carrying *PINK1* mutations (3.2.1.), their subsequent differentiation into DA neurons (3.2.2.) and the validation of the established model by performing a key experiment (3.2.3.) to further investigate the function of endogenous mutations (3.2.4.).

3.2.1. Generation of iPS cells from PD patients and controls

3.2.1.1. Patient-derived fibroblasts

For the production of iPS cell lines, three human fibroblast cultures harboring wild-type *PINK1* and three harboring mutant *PINK1* were used. Two of the mutation carriers were recruited from a German family (Hedrich *et al.*, 2006). The identified homozygous *PINK1* nonsense mutation, c.1366C>T (p.Q456X) leads to a premature stop codon. Two of the control fibroblast cultures were established from healthy family members of these PD patients without the *PINK1* mutation. In addition, a third mutant *PINK1* fibroblast line was derived from a single affected individual from Germany harboring a missense mutation in the *PINK1* gene (c.509T>G; p.V170G). The established human foreskin BJ fibroblasts (ATCC) were used as an independent control.

3.2.1.2. Reprogramming of fibroblasts into iPS cells

The scope of this study was to establish the previously reported iPS cell technology (Park *et al.*, 2008a) in the laboratory of Professor D. Krainc at the Massachusetts General Hospital, Boston, USA. Subsequently this technique was launched at the laboratory of Professor C. Klein at the University of Lübeck. Therefore, the following part will describe the set-up of this method. The reprogramming was initiated by transduction of the four factors OCT4, SOX2,

KLF4 and cMYC via retrovirus into the genome of the fibroblasts (2.3.11.) (Seibler *et al.*, 2011). Production of retrovirus was performed according to standard protocols. However, it was found to be critical for a successful reprogramming to titer the four viruses by using an exact method in order to infect the fibroblasts with certain efficiencies. As each of the constructs contain a GFP sequence, flow cytometry was used to determine the percentages of infected cells (Fig. 8). Fibroblasts were transduced with 70-80% efficiency for OCT4, SOX2 and KLF4 and with 40-50% efficiency for cMYC as recommended by Dr. L. Daheron (Harvard Stem Cell Institute, Boston, USA). Higher concentrations of the cMYC virus result in more non-iPS cell colonies that may overgrow the culture. A histone deacetylase inhibitor, valproic acid, was included in the cocktail to further increase the effectiveness of reprogramming (Huangfu *et al.*, 2008).

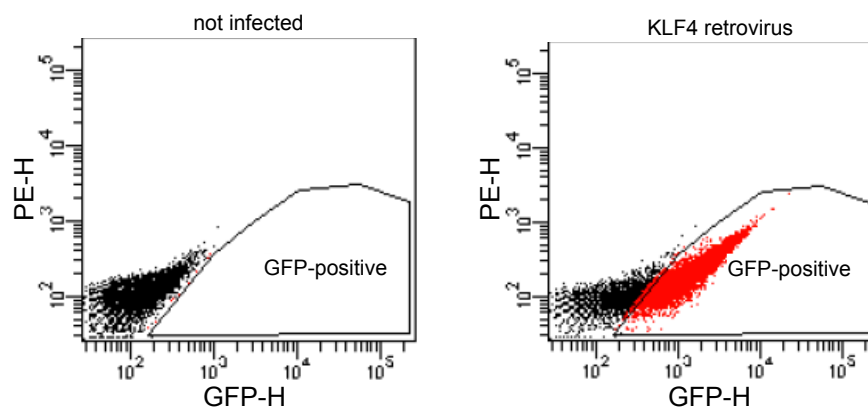


Figure 8 Infection efficiency of retroviral vectors. 293FT cells were infected with GFP-containing retroviruses and analyzed by flow cytometry to count the exact percentage of GFP-positive cells. These two-dimensional dot plots display Phycoerythrin (PE) / GFP signal as GFP can produce wavelengths which appear in the region of the detector for PE. The left dot plot shows not-infected cells. A region, where GFP-positive cells were expected, is gated. The cells in the right dot plot were infected with KLF4-containing virus and the infected cells (74%) appeared in the gated region. Cells were infected with various volumes of concentrated virus in order to generate a curve that allows identifying the volume required to reach certain infection efficiencies.

After a month of culturing, iPS cell colonies were picked based on their characteristic ES cell-like morphology and silencing of the retroviral GFP signal (Fig. 9). Retroviral expression has been shown previously to be suppressed specifically in stem cells through silent chromatin (Yao *et al.*, 2004). This silencing is therefore a powerful tool to distinguish between iPS cell colonies and the numerous iPS cell-like colonies that did not turn into a pluripotent state. The reprogramming efficiency was about 0.001% and two to four colonies per fibroblast culture gave rise to stable iPS cell lines (Tab. 3) that were further expanded on irradiated mouse embryonic fibroblasts (MEFs).

Table 3 Summary of iPS cells derived from human fibroblasts

Parental cell culture	Donor	Mutation in <i>PINK1</i>	Age at onset	Age at biopsy	Number of iPS cell clones established	ID of selected iPS cell clone*
L2124	PD patient	c.1366C>T	53	61	3	iPS-PINK1
L2122	PD patient	c.1366C>T	61	69	4	iPS-PINK1-2
L1703	PD patient	c.509T>G	31	73	2	iPS-PINK1-3
L2135	Control			40	2	iPS-WT
L2131	Control			59	4	iPS-WT-2
BJ line	Control			newborn	2	iPS-WT-3

*One of the established iPS cell clones from each parental cell line was selected for further characterization

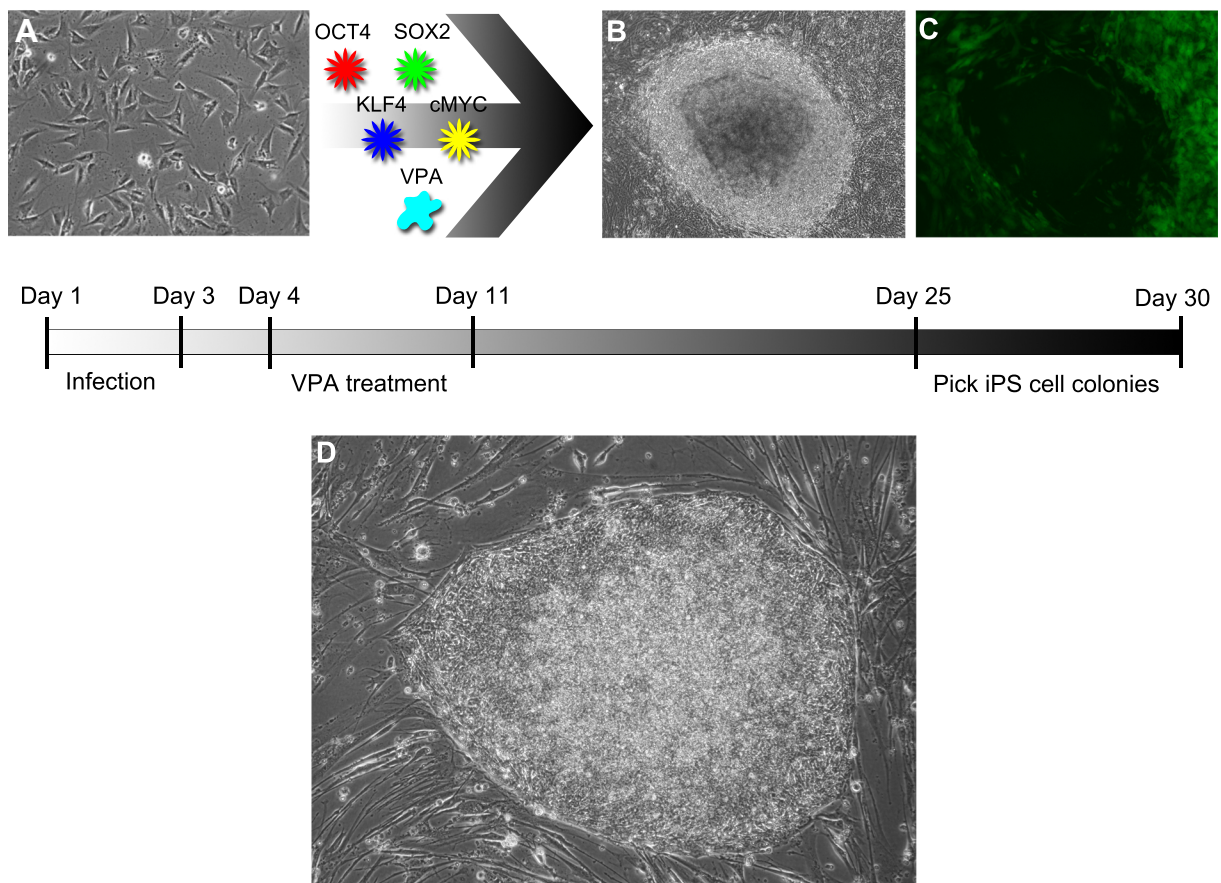


Figure 9 Reprogramming of fibroblasts into iPS cells. **(A)** Fibroblasts were infected with the four retroviruses OCT4, SOX2, KLF4 and cMYC. The retroviruses co-expressed GFP as a marker. A timeline is shown below indicating infection time of 2d, valproic acid (VPA) treatment for 7d to increase reprogramming efficiency and colony picking from day 25-30. **(B)** A round shaped colony that appeared one month post-infection on the fibroblast layer. **(C)** GFP signal channel is shown for the colony (B), indicating a silencing of the retroviral expression of this colony. An effect that is specific for stem cells (Yao *et al.*, 2004). **(D)** IPS cells were further expanded on MEFs where they showed the characteristic round clear-edged morphology of iPS cell colonies combined with a dense colony center and a cobblestone-like morphology of the cells.

One iPS cell clone from each fibroblast culture was selected (Tab. 3) and characterized in more detail for pluripotency features. Immunofluorescence staining showed high expression of pluripotency markers OCT4, NANOG, Tra-1-60, and SSEA-4 (Fig. 10).

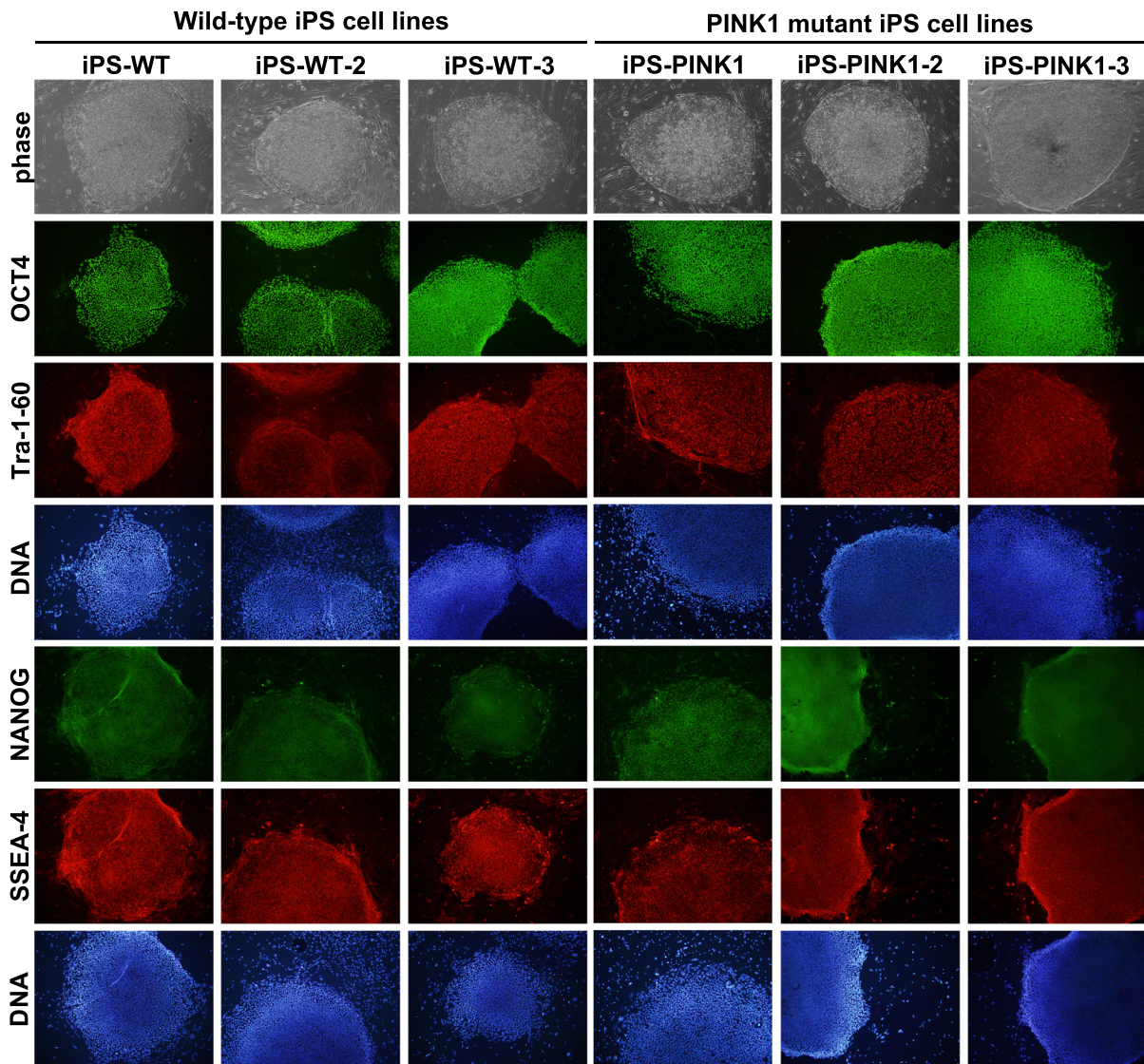


Figure 10 Generation of iPS cells from PD patients harboring a PINK1 mutation and healthy control individuals. Immunofluorescence analysis of iPS cell colonies shows presence of pluripotency markers OCT4, NANOG, and stem cell-specific antigens Tra-1-60 and SSEA-4. IPS cells were cultured on MEFs, visible in the nuclear DAPI staining (blue).

Quantitative RT-PCR analysis confirmed a dramatic increase of pluripotency marker genes NANOG, GDF3, OCT4 and SOX2 in iPS cell lines compared with the parental fibroblast cells (Fig. 11A). Expression of the viral transgenes OCT4, SOX2, KLF4 and cMYC was efficiently silenced as determined by quantitative RT-PCR compared with fibroblasts that were isolated one week post-infection (Fig. 11B). In these assays, the used primers were specific for the endogenous genes and the viral transgenes, respectively.

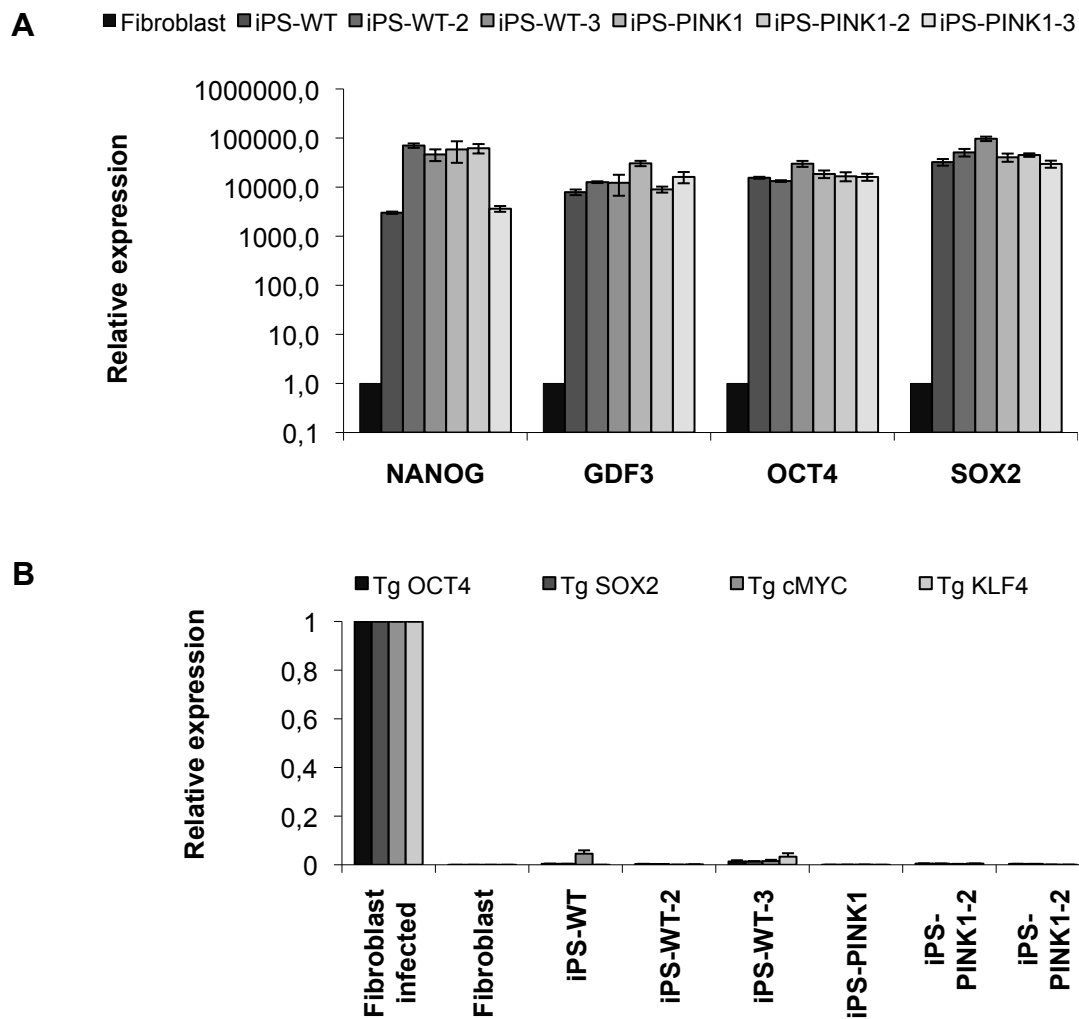


Figure 11 RT-PCR analysis of iPS cells from PD patients harboring a PINK1 mutation and healthy control individuals. **(A)** Expression levels of pluripotency markers NANOG, growth differentiation factor 3 (GDF3), OCT4 and SOX2 in fibroblasts and iPS cell lines relative to β -actin (a loading control) as assessed by quantitative RT-PCR. The values from parental fibroblasts were set to 1. **(B)** Residual expression levels of transgenes OCT4, SOX2, cMYC and KLF4 (relative to β -actin) were examined by quantitative RT-PCR. The values from the infected fibroblasts (isolated 7d post-infection) were set to 1. Uninfected fibroblasts were used as negative controls. The error bars indicate SD.

Next, the *in vitro* differentiation capacity of iPS cells was examined through the formation of embryoid bodies (EBs). Spontaneous differentiation into derivatives of the three embryonic germ layers (endoderm: GATA4, AFP; mesoderm: RUNX1, BRACHYURY; ectoderm: PAX6, NCAM) was confirmed by quantitative RT-PCR after 11 days of culture (Fig. 12). RNA expression of marker genes in the undifferentiated cells is most likely due to spontaneous differentiation in the iPS cell culture. A substantial increase in the expression could be demonstrated after 11 days for most of the markers investigated.

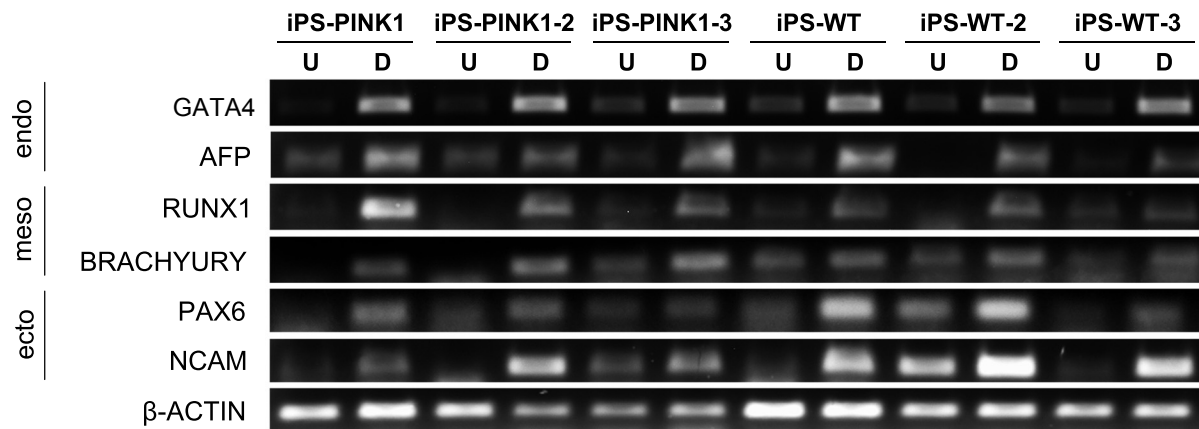


Figure 12 Spontaneous *in vitro* differentiation of iPS cells. RT-PCR analyses of various differentiation markers for the three germ layers (endoderm: GATA binding protein 4 (GATA4), alpha-fetoprotein (AFP); mesoderm: Runt-related transcription factor 1 (RUNX1), BRACHYURY; ectoderm: Paired box 6 (PAX6), Neural cell adhesion molecule 1 (NCAM)) in iPS cells that were undifferentiated (U) and after four days in suspension culture followed by seven days in adherent culture (D). Beta-actin was used as a loading control.

The mutation status was confirmed by direct sequencing of the *PINK1* mutant lines (Fig. 13). In addition to the demonstration of pluripotency, it is crucial to ensure that the resulting iPS cells are free from genetic aberrations. Reprogrammed lines usually have a normal karyotype (Lowry *et al.*, 2008), but it has remained formally possible that subkaryotypic alterations accompany reprogramming (Chin *et al.*, 2009). All six iPS cell lines exhibited a normal karyotype (Fig. 14). Together, these data indicated successful reprogramming of wild-type and mutant *PINK1* fibroblasts to a pluripotent state.

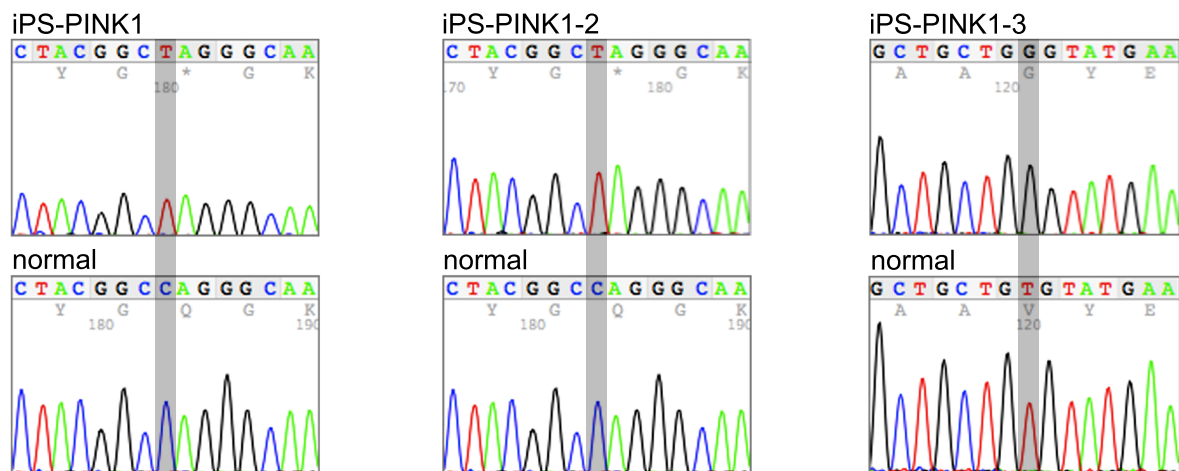
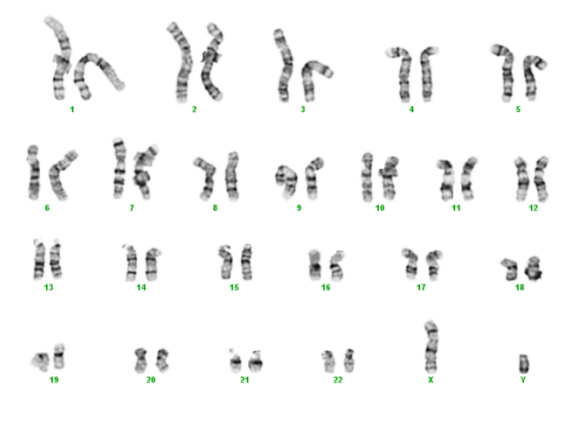
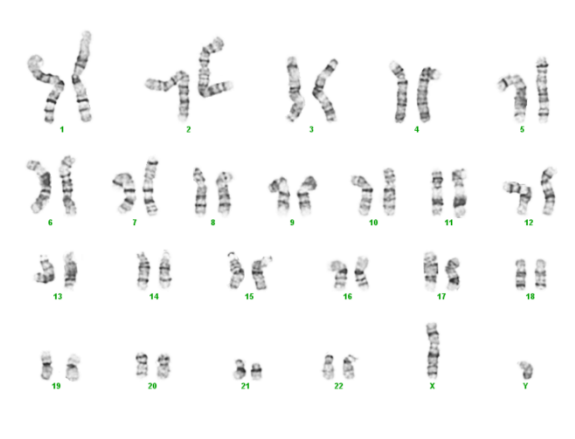


Figure 13 Fingerprinting of iPS cell lines. Direct sequencing of *PINK1* mutant iPS cell lines confirmed the mutations in iPS-PINK1 (c.1366C>T), iPS-PINK1-2 (c.1366C>T) and iPS-PINK1-3 (c.509T>G).

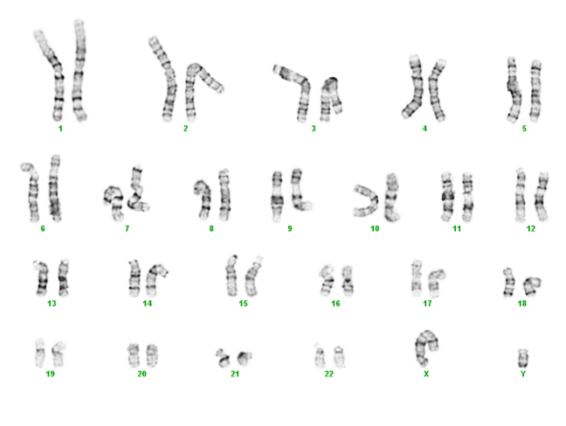
iPS-WT, 46,XY



iPS-WT-2, 46,XY



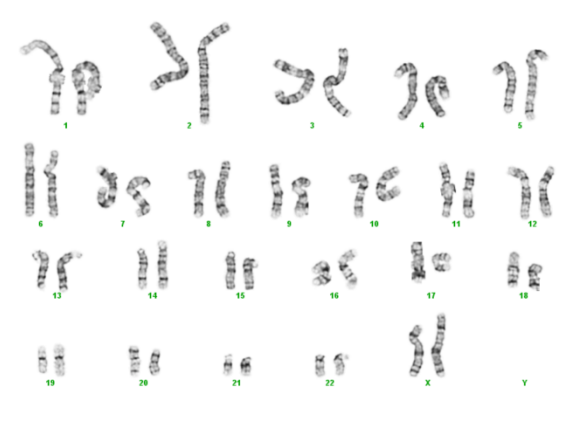
iPS-WT-3, 46,XY



iPS-PINK1, 46,XX



iPS-PINK1-2, 46,XX



iPS-PINK1-3, 46,XX

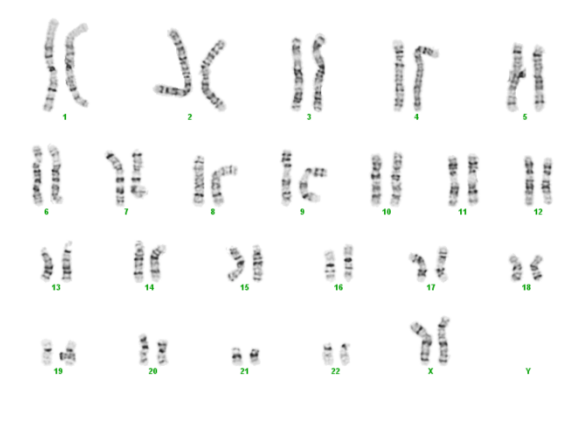


Figure 14 Karyotype analysis of *iPS* cell lines. High-resolution G-banding was performed at Cell Line Genetics (Madison, WI, USA). All *iPS* cell lines, wild-type (WT) and *PINK1* mutants, displayed a normal karyotype after reprogramming. For iPS-PINK1-3, the number of tetraploid cells in the culture was found to be slightly higher than usual.

3.2.2. Generation of human dopaminergic neurons from PD patients and controls

The next step was to differentiate iPS cell lines into DA neurons. Part of the present thesis was to setup and optimize a method of neural differentiation in the laboratory of Professor D. Krainc. A recently published protocol with minor modifications was used that achieves rapid neuronal conversion (25-30 days) on adherent cell culture (Chambers *et al.*, 2009). Traditional EB formation (30-50 days) was found to be inefficient for neural differentiation from iPS cell cultures and stromal feeder cells could contribute undefined factors to the cell culture (Chambers *et al.*, 2009).

In the first step, undifferentiated iPS cell colonies were dissociated into single cells and replated onto Matrigel-coated dishes in mTeSR1 medium, supplemented with a ROCK inhibitor (Y-27632). This factor prevents apoptosis and enhances the survival of dissociated iPS cells. At a cell density of ~80%, differentiation was started by changing the medium to neural differentiation medium containing SMAD inhibitors Noggin and SB431542 (Chambers *et al.*, 2009). SMAD proteins are signal transducers and transcriptional modulators that mediate signaling pathways. The blockade of SMAD signaling has been shown to help destabilize pluripotency, while promoting neuralization of primitive ectoderm (Xu *et al.*, 2008). By day 11 of culture, a dense layer of cells (Fig. 6) was mechanically isolated and passaged *en bloc* (2.3.14.). Several conditions were tested at this point in order to reach a large portion of neurons growing in a monolayer as the cells tend to grow in three-dimensional clusters. The type of glass cover slip and the coating method used during this step was found to be critical (2.3.14.). In order to push the differentiating neural precursor cells toward a DA state, the cells were exposed to a number of sequential factors including Brain-derived neurotrophic factor (BDNF), ascorbic acid, the morphogenic factors Sonic hedgehog (SHH) and FGF8a as reported previously (Perrier *et al.*, 2004; Chambers *et al.*, 2009) and allowed to differentiate for a total of one week. During this period of differentiation, neuronal precursor cells were seen migrating out from the bloc. By day 16 of differentiation the formation of “neural rosette” structures was observed (Fig. 15), indicating the presence of immature CNS cells. Neural rosettes are characterized by radially organized columnar epithelial cells, which have been observed during neural differentiation of hESCs (Zhang *et al.* 2001; Perrier *et al.* 2004). These structures are capable of differentiating into various region-specific neuronal and glial cell types in response to appropriate developmental signals (Elkabetz *et al.*, 2008). Terminal differentiation was induced by replacement of factors SHH and FGF8a with Glial cell-derived neurotrophic factor (GDNF), TGF- β 3 and cyclic-AMP (Perrier *et al.*, 2004; Chambers *et al.*, 2009). Neurogenesis was largely completed by day 30 of differentiation (Fig. 15) (Seibler *et al.*, 2011).

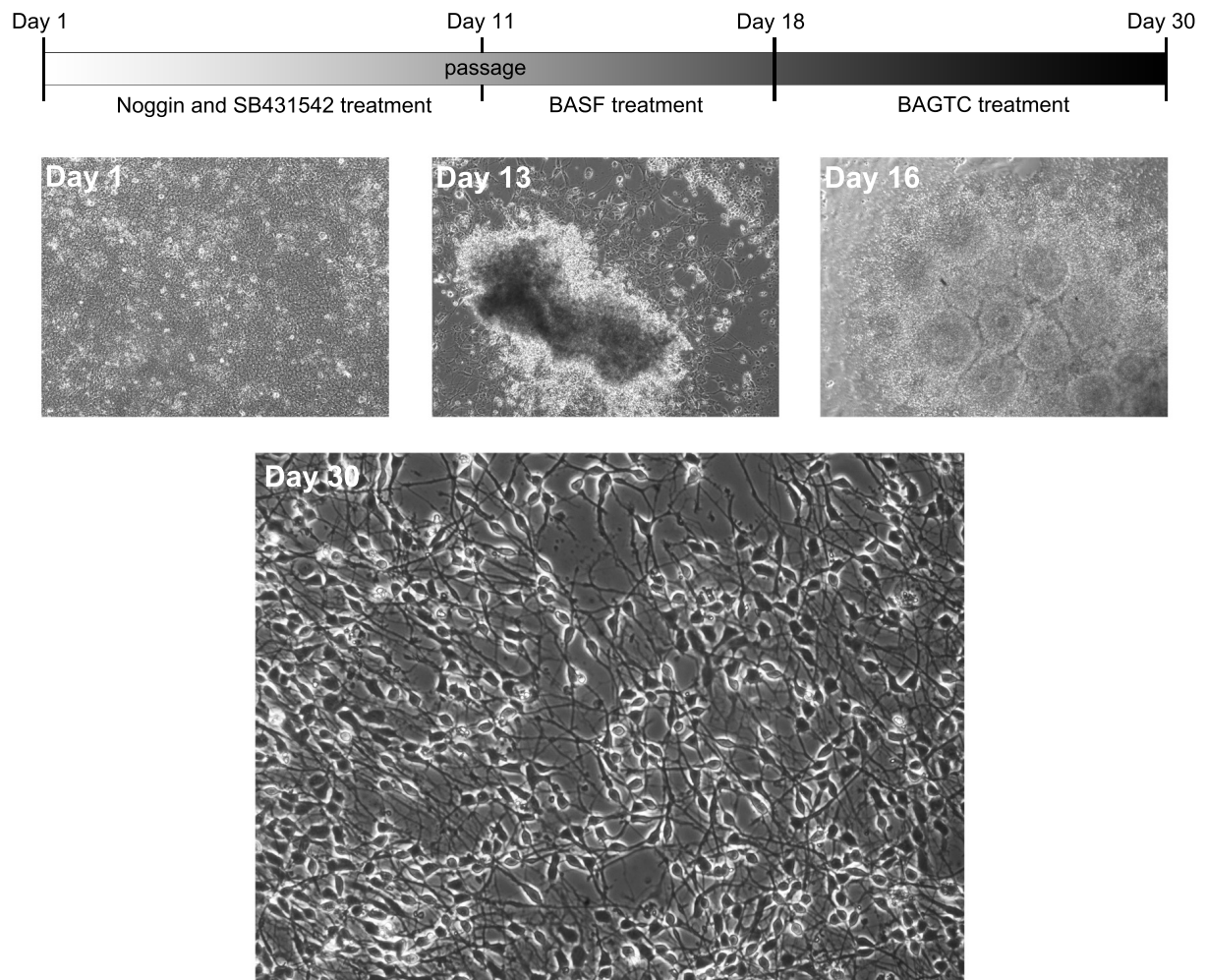
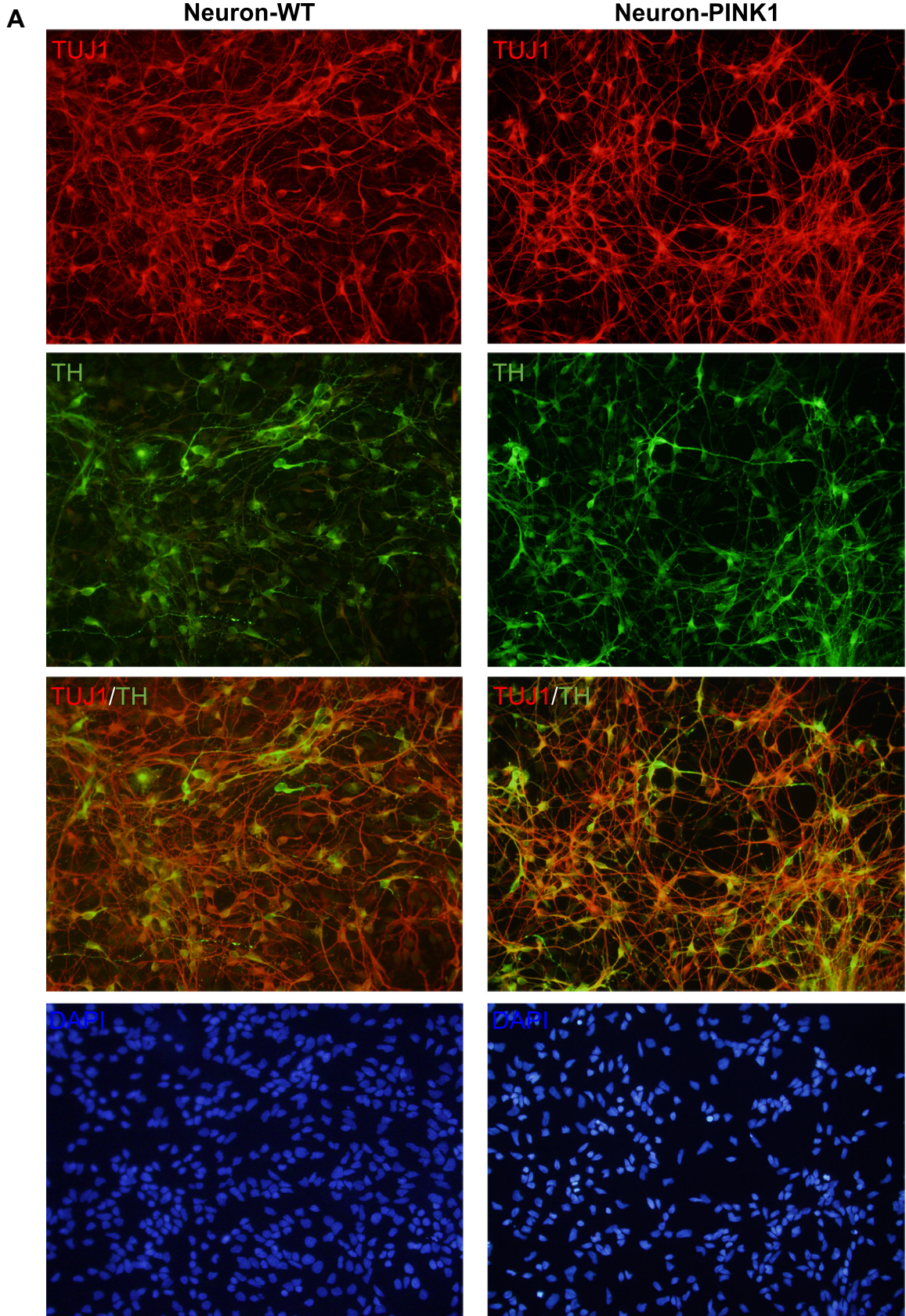


Figure 15 Differentiation of iPS cells into dopaminergic neurons. Differentiation was started by changing the medium to neural differentiation medium containing SMAD inhibitors Noggin and SB431542 (Chambers *et al.*, 2009). By day 11 cells were passaged *en bloc* and cells were cultured in N2 medium supplemented with BDNF, ascorbic acid, and the morphogenic factors SHH and FGF8a (BASF) for one week. During subsequent weeks, the composition of factors was BDNF, ascorbic acid, GDNF, TGF- β 3 and cyclic-AMP (BAGTC). On day 11 of differentiation, cells have formed a dense layer. After passaging *en bloc*, cells were migrating out of the bloc by day 13. Neural rosette structures were seen by day 16, indicating the presence of premature CNS cells. On day 30 of differentiation, neurogenesis was largely completed with a large proportion of neurons growing in a monolayer.

However, neural differentiation capacity was different among the six established iPS cell lines. Repeated attempts resulted in approximately 50% of neuronal population for lines iPS-WT, iPS-PINK1 and iPS-PINK-2. A lower neural differentiation capacity of roughly 10% showed lines iPS-WT-2, iPS-WT-3 and iPS-PINK1-3. This qualitative analysis was performed based on the characteristic morphology of neurons in culture (Fig. 15) in order to select two comparable lines, one wild-type (iPS-WT) and one *PINK1* mutant (iPS-PINK1), for a quantitative neuronal characterization and further studies.

Immunofluorescence staining (Fig. 16A) revealed that approximately 60% of the total cells (Fig. 16B) derived from iPS-WT and iPS-PINK1 expressed the neuron-specific marker

neuronal class III β -Tubulin (TUJ1) (Neuron-WT, $62 \pm 15\%$; Neuron-PINK1, $66 \pm 16\%$). The percentage of neurons coexpressing TUJ1 and tyrosine hydroxylase (TH), the rate-limiting enzyme in the synthesis of DA, was slightly higher in Neuron-PINK1 ($16 \pm 1\%$) compared to Neuron-WT ($11 \pm 3\%$) (Seibler *et al.*, 2011).



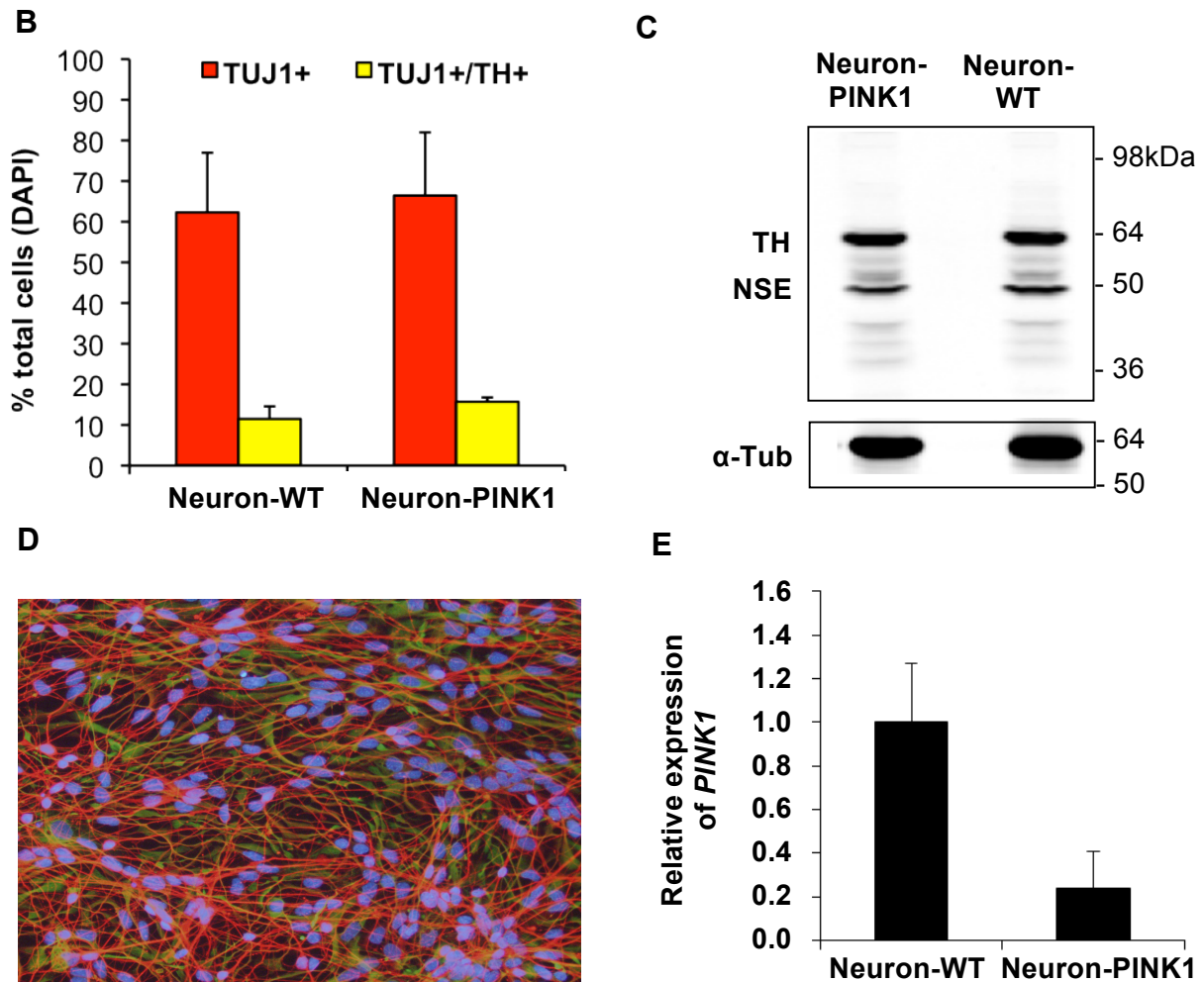


Figure 16 Generation of human dopaminergic neurons from wild-type and mutant *PINK1* iPS cells. **(A)** Immunofluorescence staining of neuronal cultures derived from iPS cell lines iPS-WT (Neuron-WT) and iPS-*PINK1* (Neuron-*PINK1*) for neuron-specific class III β -Tubulin (TUJ1; red) and the DA marker tyrosine hydroxylase (TH; green), nuclear DAPI staining (blue). **(B)** Quantification of TUJ1-positive neurons and TUJ1/TH-coexpressing DA neurons. The graph displays the percentage of cells that stain positive relative to nuclear DAPI staining (total cells). Error bars indicate the SD generated from two independent differentiation experiments. The total number of cells analyzed exceeded 12,000 cells. **(C)** Western blot analysis of neuronal culture lysates from Neuron-WT and Neuron-*PINK1*. The Western blot was probed with TH, neural specific enolase (NSE) and α -Tubulin (as loading control) antibodies. **(D)** Remaining cells were Nestin positive (TUJ1: red, Nestin: green, DAPI: blue). **(E)** RT-PCR revealed 80% reduction in expression of *PINK1* in mutant compared to control neurons (control normalized to 1). Beta-actin was used as control gene. The results were analyzed with an unpaired t-test ($p < 0.001$), with error bars representing SEM, $n = 3$.

Expression of TH and an additional neuronal marker, neural specific enolase (NSE), which is found in mature neurons, were confirmed by Western blotting in both neuronal cultures (Fig. 16C). Most of the remaining cells were positively stained for the neural precursor cell marker Nestin, indicating a subpopulation that did not differentiate into mature neurons (Fig. 16D). Furthermore, neuronal cultures were examined for *PINK1* mRNA levels. We have shown

previously a reduction of *PINK1* expression by 80-90% in the parental fibroblast lines of iPS cells carrying the nonsense mutation, most likely due to nonsense-mediated mRNA decay (Grünewald *et al.*, 2007). As expected, levels of *PINK1* were reduced in mutant neuronal cultures (Fig. 16E).

Taken together, these data demonstrate differentiation of the two lines iPS-WT and iPS-PINK1 into DA neurons at comparable levels.

3.2.3. Mitochondrial Parkin recruitment is impaired in mutant *PINK1* human neurons

While previous studies reported Parkin recruitment to depolarized mitochondria in animal cells, immortalized human cell lines and human PD patient's fibroblasts (Narendra *et al.*, 2010; Vives-Bauza *et al.*, 2010; Rakovic *et al.*, 2010), it remains to be shown whether the Parkin/*PINK1* interaction is impaired in human DA neurons that contain an endogenous *PINK1* mutation. To address this question, neurons derived from iPS-WT and iPS-PINK1 lines were treated with the potassium ionophore valinomycin that triggers loss of mitochondrial membrane potential and induces mitochondrial translocation of Parkin in PD patient fibroblasts (Rakovic *et al.*, 2010). In order to exclude variations due to reprogramming and differentiation, Parkin translocation was examined additionally in Neuron-PINK1-2 and Neuron-PINK1-3.

Since the anti-Parkin antibody was not sensitive enough for immunostaining of endogenous Parkin, wild-type Parkin was cloned into a lentiviral construct (with neuron-specific phosphoglycerate kinase promoter) and iPS cell-derived neurons were transduced with a three-fold multiplicity of infection (MOI 3). Infection efficiency was approximately 70% as determined by immunostaining (Fig. 17A). In order to be able to link any changes observed in *PINK1* mutant neurons to the function of *PINK1*, wild-type PINK1-V5 was cloned into a lentiviral construct so that *PINK1* mutant neurons can be transduced.

As full-length *PINK1* (~66kDa) is proteolytically processed upon entry into mitochondria to its cleaved ~55kDa form (Weihofen *et al.*, 2008) and is rapidly degraded by the proteasome, expression of transduced *PINK1* cannot be detected when using anti-V5 antibody (Fig. 17B). It has been reported recently that full-length *PINK1* accumulates on mitochondria when mitochondrial stressors were applied (Narendra *et al.*, 2010). Upon treatment of our iPS cell-derived neurons with 1 μ M valinomycin for 12h, PINK1-V5 accumulated in its uncleaved full-length form (~66kDa) which permits its detection (Fig. 17C). And high transduction efficiency (~90%) was achieved for the *PINK1* construct (MOI 2), as determined by immunostaining with anti-V5 antibody.

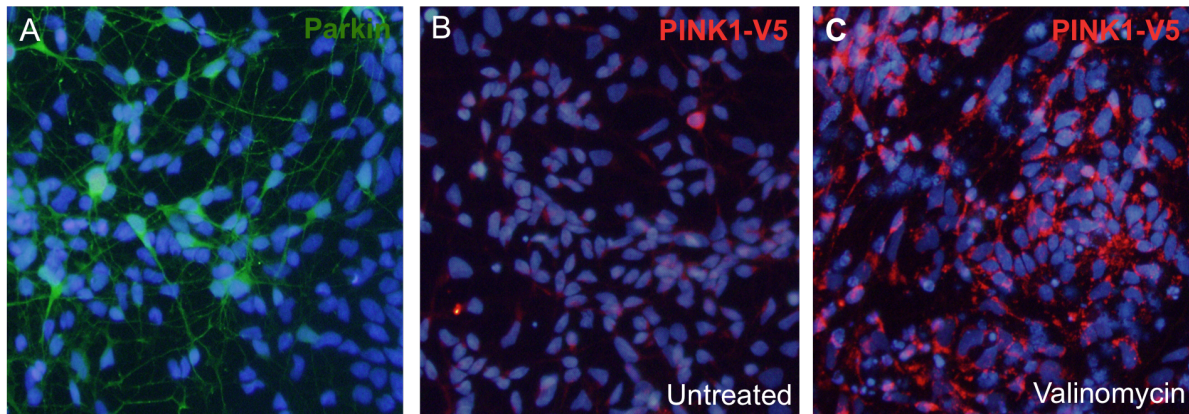
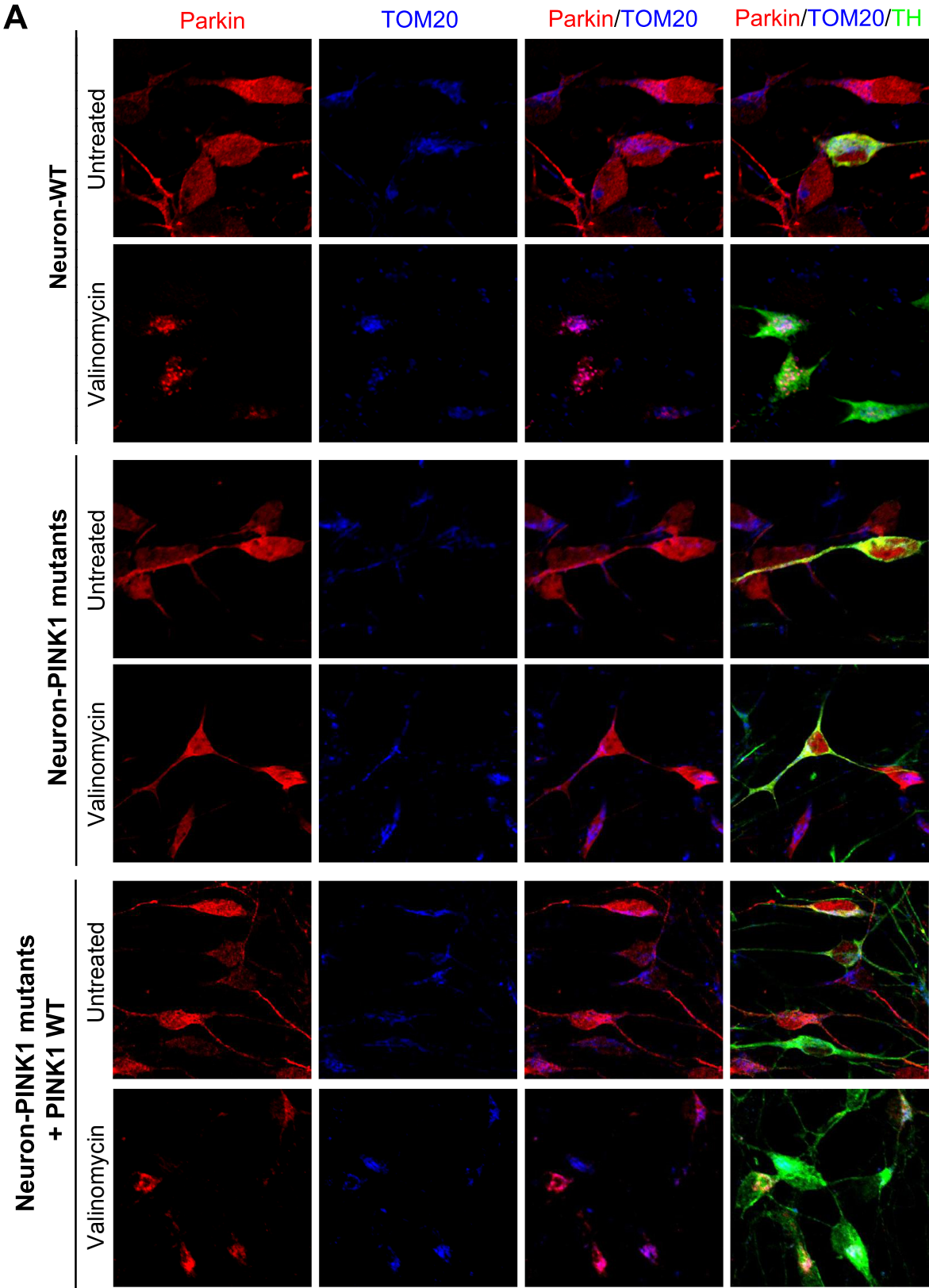


Figure 17 Validation of lentiviral *Parkin* and *PINK1-V5* infection of iPS cell-derived neurons by immunostaining. A neuronal culture (A) was infected with *Parkin* (MOI 3). Cells were fixed 5 days post-infection, co-immunostained with anti-*Parkin* antibody (green) and DAPI (blue) and an infection efficiency of ~70% was observed. Neuronal cultures (B) and (C) were both infected with *PINK1-V5* and co-immunostained with DAPI (blue) and anti-V5 antibody (red). *PINK1* is synthesized as a full-length form (~66 kDa) which is proteolytically processed upon entry into mitochondria to its cleaved ~55 kDa form under basal conditions. (B) Untreated neuronal culture in which *PINK1* is after cleavage rapidly degraded and only a few cells are *PINK1-V5*-positive. (C) Neuronal culture was treated with 1 μ M valinomycin for 12h. *PINK1-V5* accumulated in its uncleaved full-length version (~66 kDa) and the infection efficiency was >90%. Stress-induced accumulation of full-length *PINK1* has been reported previously (Narendra *et al.*, 2010).

Under basal conditions, *Parkin* was localized in the cytosol and the neurites of DA neurons in both control (Fig. 18A; upper panel) and mutant *PINK1* cells (Fig. 18A; middle panel). However, treatment with valinomycin resulted in dramatic mitochondrial translocation of *Parkin* in the control but not in the *PINK1* mutant neurons (Fig. 18A; upper panel, middle panel). These results suggested that in the presence of endogenous *PINK1* mutation, *Parkin* did not translocate to mitochondria even when moderately overexpressed by lentiviral transduction. To determine whether expression of wild-type *PINK1* could rescue this phenotype, *PINK1* mutant neurons were transduced which restored the translocation of *Parkin* to mitochondria (Fig. 18A; lower panel). This effect was observed in neurons derived from all the three *PINK1* mutant iPS lines (Fig. S1). Colocalization images shown in figure 18A were quantified by using ImageJ software (Fig. 18B).

Taken together, these results demonstrate that *PINK1* mediates mitochondrial translocation of *Parkin* in human DA neurons (Seibler *et al.*, 2011).



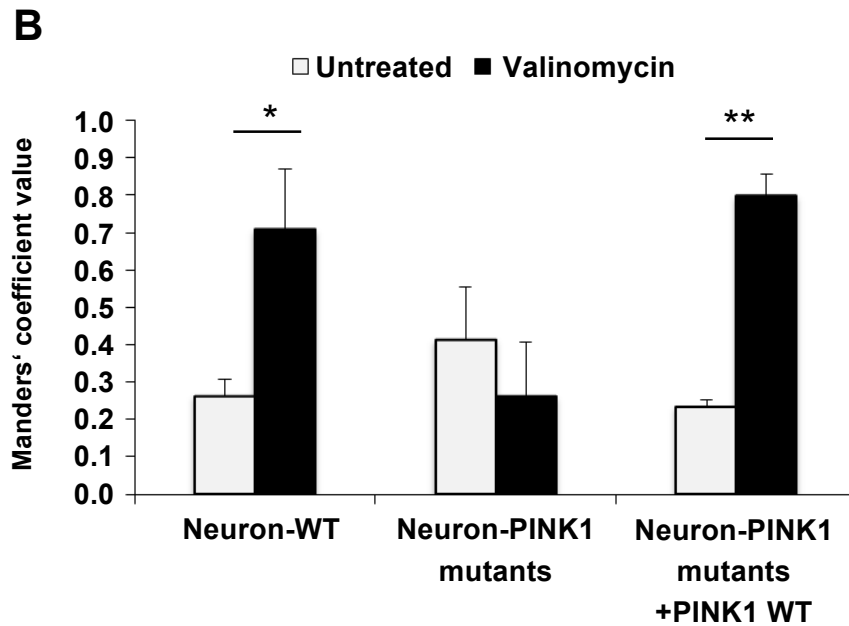


Figure 18 Stress-induced mitochondrial translocation of Parkin is impaired in mutant *PINK1* iPS cell-derived human dopaminergic neurons. **(A)** Neuronal cultures were infected on day 25 of differentiation with wild-type Parkin (MOI 3) and treated with 1 μ M valinomycin 5 days post-infection for 12h. Cells were fixed and immunostained with antibodies against Parkin (red), mitochondrial marker TOM20 (blue) and the DA marker TH (green). Parkin colocalizes with mitochondria in control DA neurons (Neuron-WT, left panel) but not in mutant *PINK1* neurons (Neuron-*PINK1* mutants, middle panel). Lentiviral transduction of mutant *PINK1* neurons with wild-type *PINK1* restored Parkin translocation (right panel). **(B)** The quantitative colocalization analysis of Parkin and Tom20 signals in confocal images was performed with ImageJ and JACoP plug-in (Bolte and Cordelieres, 2006) to determine Manders' coefficient (Manders *et al.*, 1992) from 0 to 1 (0=non-overlapping images and 1=colocalized images). The highest values were found for valinomycin-treated Neuron-WT and *PINK1* wild-type infected Neuron-*PINK1* mutants, suggesting a translocation of Parkin to mitochondria in the presence of a functional *PINK1* protein. The results were analyzed with an unpaired t-test with error bars indicating SD, n=4 (Neuron-WT untreated vs. treated: p=0.002; Neuron-*PINK1* mutants+*PINK1* WT untreated vs. treated: p=0.0003).

3.2.4. Change of mitochondrial copy number and PGC-1 α levels in mutant *PINK1* human neurons

Since previous studies suggested that Parkin translocation to mitochondria participates in autophagic degradation of dysfunctional mitochondria (Narendra *et al.*, 2010; Vives-Bauza *et al.*, 2010; Rakovic *et al.*, 2010), it was investigated in the present study whether *PINK1* deficiency affects mitochondrial DNA (mtDNA) copy number. Using quantitative RT-PCR for mtDNA (Parfait *et al.*, 1998), a reduction in mtDNA copy number in Neuron-WT was observed, but not in the *PINK1* mutant neurons upon mitochondrial depolarization (Fig. 19A). Importantly, overexpression of wild-type *PINK1* in the mutant line resulted in a comparable effect of mitochondrial depolarization on mtDNA as observed in wild-type cells (Fig. 19A).

These results suggested that deficient translocation of Parkin to mitochondria in mutant *PINK1* neurons may lead to accumulation of mitochondria due to their decreased clearance. Since the increase in mtDNA can be also due to increased mitochondrial production, the expression levels of PGC-1 α were investigated, an important inducer of mitochondrial biogenesis (Aquilano *et al.*, 2010; Wu *et al.*, 2006). Interestingly, PGC-1 α levels were significantly increased in mutant *PINK1* but not in wild-type neurons upon mitochondrial depolarization and this effect was abolished by lentiviral wild-type *PINK1* expression in mutant *PINK1* cells (Fig. 19B) (Seibler *et al.*, 2011).

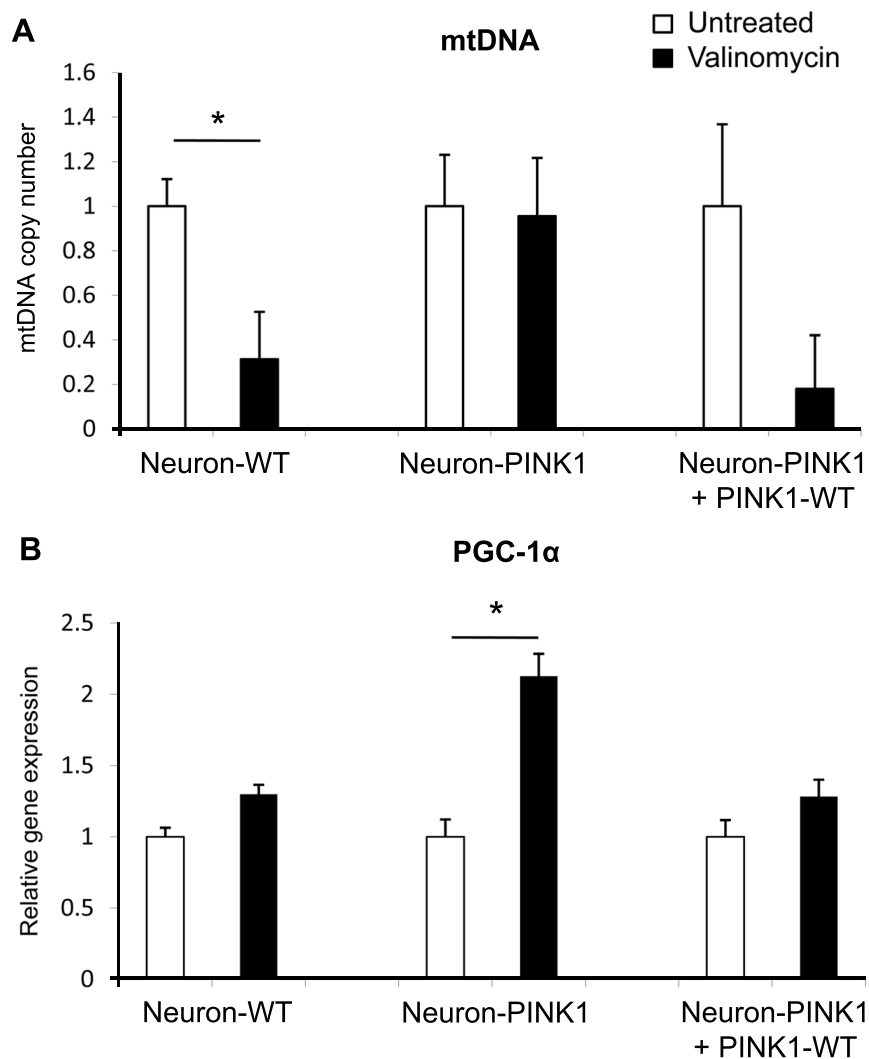


Figure 19 Abnormalities in mtDNA copy number and PGC-1 α expression in mutant *PINK1* iPS neurons. Neurons were either untreated or treated with 1 μ M valinomycin for 12h. **(A)** Upon treatment, there is a significant reduction in mtDNA copy number in the iPS-WT and mutant iPS-*PINK1* neurons transduced with wild-type *PINK1*, but not in the *PINK1* mutant line. **(B)** PGC-1 α gene expression is significantly upregulated after valinomycin treatment in the *PINK1* mutant line but not in the wild-type or lenti-*PINK1*-expressing mutant line. Results are shown as fold change relative to untreated samples and normalized to β -actin. The results were analyzed with an unpaired t-test, with error bars representing SEM (mtDNA untreated vs. treated: $p < 0.005$; PGC-1 α untreated vs. treated: $p = 0.02$; $n = 3$).

4. DISCUSSION

The investigations of the present thesis range from *PRKRA* mutation screening of dystonia patients (4.1.) to studies on human neurons derived from PD patients carrying *PINK1* mutations (4.2. and 4.3.). One novel *PRKRA* mutation was identified and in the following it is discussed which etiological role this gene plays in dystonias (4.1.1.) and how this mutation might lead to a cellular dysfunction causing abnormal neural activity in the basal ganglia circuitry (4.1.2.). Human DA neurons were generated using iPS cells and a *PINK1*-linked effect was found in neurons derived from PD patients. This newly established disease model is evaluated in the context of other neuronal PD models (4.2.1. and 4.2.2.) and it is discussed which consequences for the function of DA neurons of the basal ganglia arise from the observed phenotypes (4.3.).

4.1. The role of mutations in *PRKRA*

As part of the present thesis, 52 unrelated patients with dystonia were screened for mutations in the *PRKRA* gene and a novel frameshift mutation (c.266_267delAT) was identified in one allele of a German patient. In addition to this mutation, two new heterozygous silent changes in *PRKRA* were found in other dystonia patients (c.126C/T and c.795C/T).

4.1.1. Frequency and type of *PRKRA* mutations

In this study, the frequency of *PRKRA* mutations is about 2% (1/52) within a group of early-onset dystonia patients (<25 years), of whom 22 presented with generalized dystonia (Seibler *et al.*, 2008). The original mutation (c.665C>T) was found in six affected members from two Brazilian families diagnosed with an overall generalized dystonia and the beginning of symptoms at <18 years (Camargos *et al.*, 2008). Screening for this mutation in the same study revealed an additional mutation carrier in a group of 12 unrelated early-onset cases with generalized dystonia from Brazil (8.3%). Another study examined 43 patients of Caucasian origin with writer's cramp, including seven early-onset patients, for mutations in *torsinA* (DYT1), *SGCE* (DYT11) and *PRKRA* (Ritz *et al.*, 2009). They identified one patient carrying the previously reported GAG deletion in *torsinA* but no mutation was found in *SGCE* or *PRKRA*. Furthermore, a large group of dystonia patients was screened by us, of whom 17 were diagnosed with generalized dystonia, 53 with segmental dystonia and 234 with focal

dystonia (unpublished data). However, a disease-causing mutation in *PRKRA* was not identified. According to these data, mutations in *PRKRA* are responsible only for a minor subset of dystonia cases. However, the clinical phenotype of the originally reported *PRKRA* mutation is described as generalized dystonia (Camargos *et al.*, 2008). This observation was confirmed by the identification of the new *PRKRA*-linked dystonia patient reported in the present study. Most of the patients examined in the other studies presented with a milder expression of symptoms combined with a later disease onset, thus, more studies are required to define the role of mutations in *PRKRA*. Importantly, the new frameshift mutation was found in a German patient, indicating that the occurrence of mutations in *PRKRA* is not limited to the Brazilian population.

The two heterozygous silent changes that were newly described in the present study are most likely not pathogenic. The c.126C/T base pair exchange was found only in a patient and not in controls but there is no change in the splicing process according to software predictions. The other genetic variation (c.795C/T) was identified in patients and controls and can be therefore excluded as a cause of the disease.

The novel frameshift mutation (c.266_267delAT) was found in one allele of the patient suggesting a dominant mode of inheritance. By contrast, Camargos and colleagues reported that the *PRKRA* mutation is inherited in an autosomal recessive fashion. Interestingly, in one Brazilian family, the mother of a homozygous carrier was also affected but could not be genotyped. This raises the question of whether a heterozygous mutation might act as a susceptibility factor for dystonia. A similar scenario has been discussed for seemingly recessive genes that are linked to parkinsonism (Klein *et al.*, 2007). Alternatively, a heterozygous (truncating) mutation might have had a pathogenic effect in its own right.

Investigations of the relevance of mutations in *PRKRA* stand at the very beginning. Further studies are required to answer the question if and how heterozygous mutations may contribute to the disease. Moreover, with the methods used in this study and previous investigations we cannot rule out gene dosage mutations or sequence changes in a noncoding region. Although relatively little information is available about the function of the *PRKRA* protein, it is of great interest to examine how *PRKRA* may integrate with other dystonia genes in an interacting pathway.

4.1.2. Consequences of *PRKRA* mutations for molecular pathways in dystonia

PRKRA (also known as PACT) has been shown to regulate the activity of the latent protein kinase PKR through its three modular domains (M1-3). Domains M1 and M2 bind the kinase while M3 is required to activate it. Different stresses induce *PRKRA* to activate PKR, which subsequently phosphorylates the eukaryotic initiation factor eIF2 α leading to the inhibition of

protein synthesis (Patel *et al.*, 2000; Peters *et al.*, 2001; Huang *et al.*, 2002). In a similar manner eIF2 α is phosphorylated by the endoplasmic reticulum (ER) stress-related kinase PERK in order to reduce global protein synthesis. This is thought to be a protective function against toxic insults (Raven and Koromilas, 2008). PRKRA responds to cytosolic (Patel *et al.*, 2000) and ER stresses (Lee *et al.*, 2007) but it has not been studied yet which functional effects exist for dystonia-related mutations in PRKRA. A previous study reported that mutations in the domain M3 of PRKRA that disrupt its activation function lead to binding and subsequent inhibition of mutant PRKRA to PKR, thus preventing phosphorylation of eIF2 α by PKR (Huang *et al.*, 2002). The (truncating) frameshift mutation H89fsX20 described in the present thesis is located in the M1 domain and results in a mutated protein missing M3 (Fig. 20). Based on this finding, it was hypothesized by Bragg *et al.* (2011) that these truncated mutants could bind to PKR, thereby disrupting the cellular response to cytosolic/ER stress. In addition, this hypothesis could explain the disease-causing effect of a heterozygous mutation in PRKRA. The original homozygous PRKRA mutation (P222L) occurs at the border in front of domain M3, a position that is evolutionarily conserved in mammals, but it is unclear how the mutation changes structure and function of PRKRA (Camargos *et al.*, 2008).

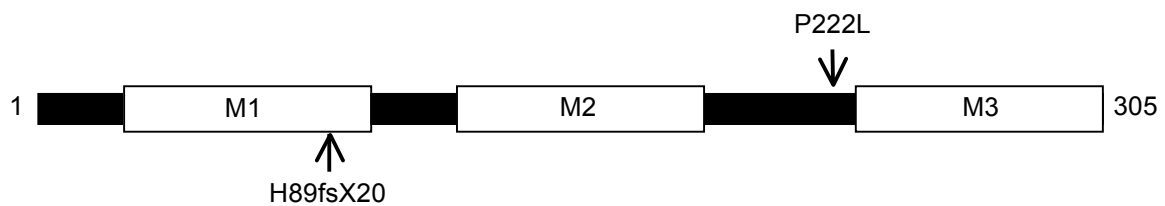


Figure 20 Schematic of *PRKRA* protein. The protein consists of 305 amino acids forming three modular domains (M1-3) that regulate protein kinase R. The two DYT16-related mutations are indicated relative to functional domains. The P222L mutation falls in the intermediate region close to M3. The H89fsX20 mutation is located in M1 leading to a truncated protein.

Bragg and colleagues (2011) further outlined some possible interacting pathways between *PRKRA* and *torsinA*. Originally, a heterozygous GAG deletion was identified in *torsinA* as the disease-causing mutation for DYT1 (Ozelius *et al.*, 1997). TorsinA belongs to the AAA⁺ superfamily of molecular chaperones, which typically function as oligomeric complexes in cellular processes, such as protein folding, membrane trafficking, and vesicle fusion (Hanson and Whiteheart, 2005). Several studies have linked torsinA with the ER/secretory pathway by demonstrating secretion defects in *torsinA*-linked dystonia patients fibroblasts and control fibroblasts that were silenced for torsinA expression (Hewlett *et al.*, 2007, 2008). The secretion defect in the patient fibroblasts was rescued by selective knockdown of mutant torsinA or upregulation of wild-type torsinA (Hewlett *et al.*, 2008). An explanation for the

impaired secretion in these fibroblasts is that it reflects a chronic, low level of ER stress, which would make a link to the ER stress-related function of PRKRA. This idea is supported by the finding that fibroblasts from patients with *torsinA* mutations are more sensitive to ER stress than control cells (Bragg *et al.*, 2011). If *torsinA* acts at some level as a chaperone in the response of ER stress, a dysfunctional mutant *torsinA* could indirectly cause an impaired clearance of misfolded proteins in the cell.

Dystonia is a neurologic disorder, thus studies in neuronal cells of the basal ganglia or animals are required to fully understand and link existing pathways. To date, it is not clear which neurotransmitter system contributes to dystonia pathogenesis. Exceptions are DYT5a and 5b (Tab. 1) with mutations in genes involved in the bipterin/DA pathway. Patients with mutations in these genes respond dramatically to levodopa substitution (Müller, 2009). Notably, some cases with *PRKRA* mutations demonstrated parkinsonian features and levodopa had a moderately positive effect on bradykinesia for a number of patients (Camargos *et al.*, 2008) suggesting a possible dysfunction in the DA pathway. To study the impact of *torsinA* mutations on neurons, several laboratories have engineered different mouse models. In one of them, the cytomegalovirus promoter drove the expression of human mutant *torsinA*. Electrophysiological recordings were performed on striatal slices derived from this mouse demonstrating that activation of postsynaptic dopamine receptor D2 (D2R) resulted in aberrant activity leading to disturbances in firing rates of neurons (Pisani *et al.*, 2006; Sciamanna *et al.*, 2009). Interestingly, these neurons exhibited a decreased surface expression of D2R (Napolitano *et al.*, 2010), which opens a potential link to *torsinA* function. D2R is processed in the ER by molecular chaperones. A previously shown direct interaction of *torsinA* and D2R (Torres *et al.*, 2004) supports the hypothesis that mutant *torsinA* might impair this process. Understanding how PRKRA function in this pathway could help to elucidate neuron-specific mechanisms in dystonia.

4.2. Human neuronal models for Parkinson disease research

The present thesis introduces a stem cell-based patient-specific neuronal cell culture model for PD research. In a first step, iPS cells were successfully derived from fibroblasts of PD patients harboring nonsense and missense *PINK1* mutations and healthy controls. In a second step, these cells were differentiated into DA neurons. Despite great efforts in the past, the mechanisms that underlie degeneration of DA neurons in PD remain unknown. One important step forward is that the theories ranging from oxidative stress and mitochondrial dysfunction to protein folding and aggregation that have been observed in various model systems are validated and further investigated in human neurons. Several human DA cell lines have been developed over the years, largely driven by the concern in generating cells

that could be grafted into the adult human brain to treat PD. But these cells may have the potential to be used for drug discovery, as well. In the following, the newly proposed model of the present study will be presented in comparison with these other neuronal PD cell models that have been reviewed recently (Schüle *et al.*, 2009). It is of interest to highlight the advantages and disadvantages, respectively. For this purpose, the cell models are divided into non-patient specific (4.2.1.) and patient-specific (4.2.2.) culture models summarized in table 4 (modified according to Schüle *et al.*, 2009).

Table 4 Human neuronal models for Parkinson disease research

Human cell source	Type	Characteristics	Exemplary references
Non-patient specific			
Cell line			
Neuroblastoma cell lines	SH-SY5Y	Differentiation with RA and TPA, expression of TH, DA receptors, DAT and VMAT2	Pahlmann <i>et al.</i> , 1995 Lopez-Carballo <i>et al.</i> , 2002
Embryonic carcinoma cell lines	NTera-2/NT2	Differentiation under co-culture with PA6, expression of most DA markers	Schwartz <i>et al.</i> , 2005
Immortalized embryonic mesencephalic cells	LUHMES ReNcell VM NSCs	Differentiation with GDNF and cAMP, expression of TH and DAT	Lotharius <i>et al.</i> , 2002 Wood-Kaczmar <i>et al.</i> , 2008
Embryonic stem cells	BG01	Differentiation under co-culture or directed neural induction, expression of most DA and midbrain markers, DA release and electrical activity in a subset of cells	Kawasaki <i>et al.</i> , 2000 Perrier <i>et al.</i> , 2004 Chambers <i>et al.</i> , 2009
Patient-specific			
Primary cells			
Mesenchymal stem cells	Idiopathic	Growth factor differentiation, expression of TH and some midbrain markers	Dezawa <i>et al.</i> , 2004 Trzaska <i>et al.</i> , 2007
Induced pluripotent stem cells	Idiopathic LRRK2-linked PINK1-linked	Differentiation under co-culture or directed neural induction, expression of most DA markers, DA release and electrical activity in a subset of cells	Soldner <i>et al.</i> , 2009 Nguyen <i>et al.</i> , 2011 Seibler <i>et al.</i> , 2011

Note: DA – dopamine, DAT – DA transporter, LRRK2 – leucine-rich repeat kinase 2, LUHMES – Lund human mesencephalic cell line, RA – retinoic acid, TPA – 12-*O*-tetradecanoyl-phorbol-13-acetate, VMAT2 – vesicular monoamine transporter, VM NSCs – ventral mesencephalic stem cells

4.2.1. Non-patient specific cell culture models

These cell cultures are derived from human adult malignant tissue as for the neuroblastoma line SH-SY5Y, human embryonic malignant tissue as for the pluripotent embryonic carcinoma cell line NTera-2/NT2, and human embryonic healthy tissue as for the Lund human mesencephalic (LUHMES) cell line and the human ES cell lines (e.g. BG01). SH-SY5Y is one of the most commonly used cell lines for investigating pathways in relation to PD that has brought great insights into the theme of neurotoxicity. These cells show measurable levels of DA beta hydroxylase activity, an enzyme that converts DA to norepinephrine. In order to reach a more DA phenotype that is combined with the expression of dopaminergic markers, cells are treated with retinoic acid (RA) and 12-*O*-tetradecanoyl-phorbol-13-acetate (TPA) (Pahlmann *et al.*, 1995). Recently, it was shown that the

differentiated cells were less susceptible to exposure to the neurotoxin 6-hydroxydopamine than undifferentiated SH-SY5Y cells, which is in contrast to the common hypothesis that DA neurons are more vulnerable to oxidative stress (Cheung *et al.*, 2009). For this reason and the fact that they lack any electric activity, more advanced models are necessary to study a neuron-specific degeneration. The NTera-2/NT2 cell line has many pluripotent characteristics and can be differentiated under co-culture with PA6 cells into DA neurons that respond to neurotransmitters, and show electric excitability (Schwartz *et al.*, 2005). Most important are the large population of TH-positive neurons and the expression of various DA markers in these cells. They have been primarily used for studies related to neuronal differentiation but could also serve as a system to model DA dysfunction and degeneration (Schüle *et al.*, 2009). However, similar to the SH-SY5Y cell line, they were derived from malignant tissue, which could contribute undefined factors to the cell culture. An alternative is the v-myc overexpressing LUHMES cell line. Tetracycline is used to down-regulate the expression of v-myc and the line can be then differentiated within 3-4 days in the presence of GDNF and cAMP into cells that express TH and dopamine transporter (DAT) (Lotharius *et al.*, 2005). A comparable cell line derived from human fetal ventral mesencephalon stem cells (ReNcell VM NSCs) has been differentiated into TH-expressing neurons and was used to study PINK1 function (Wood-Kaczmar *et al.*, 2008). Upon knockdown of PINK1, a reduced viability was observed during long-term culturing of neurons. Although these are promising data, the model needs to be validated by additional studies. The probably best characterized type of all these above mentioned differentiated DA neurons are derived from human ES cells. Several protocols are available for neural induction and some of them lead to 30-40% DA neurons that express most of the midbrain markers, are capable to release DA and exhibit electrophysiological activity (Perrier *et al.*, 2004). However, the majority of studies performed on these cells were related to neural development and cell replacement therapy (Schüle *et al.*, 2009). A challenge to the use of ES cells and the NTera-2/NT2 cell line is the longer period of differentiation (20-50 days) and the heterogeneous population of cells. Single cell analysis is needed to examine the DA neurons in these different populations consisting of mature neuronal subtypes and progenitors. Recent protocols enabled the enrichment of neuronal subtypes by using flow or magnetic cell separation techniques (Pruszek *et al.*, 2007, 2009) but these approaches are cost-intensive and need to be further optimized for disease modeling regarding the percentage of surviving cells and the goal of obtaining a pure DA population.

The non-patient-specific cell cultures have the general advantage that these are established lines that can give more consistent data in different laboratories than patient-derived primary cell cultures. However, besides the SH-SY5Y cell line, the cultures were derived from human embryonic tissue and the use of such cells stands in contrast to the ethically and legally

highly questionable “production” and utilization of human embryos. Regarding this concern, human adult multipotent or pluripotent cells open alternative possibilities for disease modeling.

4.2.2. Patient-specific cell culture models

Patient-derived cells are especially valuable for genetic disease modeling as the effect of the identified pathogenic mutations can be studied on endogenous levels in these cells. PD has been implicated with monogenetic forms and genetic susceptibility factors that may play a role in the sporadic form of the disorder. Moreover, the utilization of cells from patients allows correlating of clinical and experimental data. In the following mesenchymal stem cells (MSCs) and iPS cells from patients are presented as model systems for PD.

MSCs can be derived from bone marrow (Dezawa *et al.*, 2004). They are multipotent and have been differentiated within two weeks into TH-positive cells (12-67%) (Schüle *et al.*, 2009). One study characterized 18 MSC cultures that were derived from patients with sporadic PD and compared them to MSC cultures from controls. However, the cells did not show a phenotype and were differentiated with the same efficiency (~30%) into TH-expressing cells (Zhang *et al.*, 2008). Further studies will be needed to fully characterize these cells.

While iPS cells derived from sporadic PD patients have been differentiated into DA neurons (~5% TH/TUJ1-positive cells), no phenotype has been observed in these neurons (Soldner *et al.*, 2009). Since genetic PD has not been studied using this system, the present thesis demonstrates the first attempt by reprogramming fibroblasts from patients with *PINK1*-linked PD and genetically matched normal subjects using the four cardinal factors (OCT4, SOX2, KLF4, and cMYC). The factors were delivered via retroviral vectors that integrated into the genome of the fibroblasts. The resulting iPS cell colonies were characterized regarding their pluripotent qualities and the silencing of the factor transgenes, indicating the stable conversion of cell fate. The mutation did not affect the ability of patient fibroblasts to be induced into iPS cells. Furthermore, patient-derived iPS cells were able to differentiate into DA neurons at efficiency levels comparable to the control iPS cells within 25-30 days. However, differentiation capacity was different among the six established iPS cell colonies, though independent of the mutation status. It has been reported previously that response to differentiation signals of different iPS cell lines varies (Hu *et al.*, 2010). This observation was made also in transgene-free iPS cells, excluding the integration and residual expression of viral factors as a causal factor. Whether this effect is due to incomplete reprogramming or other abnormalities that happened during this process needs to be addressed in further studies. Hu and colleagues (2010) suggested to select for the application of iPS cells more

uniform iPS cell lines by additional criteria besides the pluripotency assays (e.g., differentiation to target cell types). In the present study, one wild-type line (iPS-WT) and one *PINK1* mutant line (iPS-PINK1) were selected based on their neural differentiation potential. Differentiation was conducted according to a published protocol that was slightly modified regarding a prolonged time period of differentiation and different coating conditions for the dishes. The subpopulation of DA neurons was slightly higher in Neuron-PINK1 ($16 \pm 1\%$) compared to Neuron-WT ($11 \pm 3\%$) as assessed by the number TH/TUJ1-positive cells (Seibler *et al.*, 2011). The higher percentage of DA neurons in this study compared to the one of sporadic PD-derived neurons could be explained by the use of a more advanced protocol for neural induction (Chambers *et al.*, 2009). Moreover, a phenotype was detected in these DA neurons that was traced back to the effect of the pathogenic *PINK1* mutation. These results are discussed in more detail in the following chapter (4.3.).

So far, there is only one additional study published on PD using patient-specific iPS cells (Nguyen *et al.*, 2011). Fibroblasts from a PD patient harboring a mutation in LRRK2 (p.G2019S) and from a healthy control individual were reprogrammed via retroviruses that delivered three factors (OCT4, SOX2 and KLF4). iPS cell identity and pluripotent potential were confirmed by using various methods. Neural induction was performed according to the same protocol used in the present study (Chambers *et al.*, 2009) but with a shorter time period of differentiation (~19 days). Up to 5% of the neurons were found to be positive for TH and the midbrain marker forkhead box A2 (FOXA2). Electrophysiological recordings demonstrated that the neurons did fire action potentials and showed spontaneous synaptic activity. Furthermore, neurons were able to release DA in response to stimulation with high potassium. These data reveal for the first time the neuronal authenticity of iPS cell-derived DA neurons. In addition, the study reports that mutant LRRK2 dopaminergic neurons were found to be more susceptible to stress agents, such as hydrogen peroxide, MG-132, and 6-hydroxydopamine, than control neurons (Nguyen *et al.*, 2011). However, these data are based on a single neurotoxicity assay that consists of immunostaining of fixed neurons with TH and activated caspase-3 antibodies.

These two studies on iPS cells (Nguyen *et al.*, 2011; Seibler *et al.*, 2011) provided the proof of principle that the new iPS technology can be adapted also to genetic PD. Moreover, differentiation into TH-positive cells was successful, thus further studies to elucidate pathways or to discover new drugs are possible. The limitation of these cultures to date is a heterogeneous population of cells, which was mentioned above in the context of ES cells (4.2.1.). To solve this problem, advanced differentiation methods and more elegant techniques for readouts of single cells are required in the future.

4.3. The effect of *PINK1* mutations on human neurons

PINK1 is a mitochondrial kinase that protects cells against mitochondrial stress (Wood-Kaczmar *et al.*, 2008), whereas loss of *PINK1* has been linked to increased levels of oxidative stress (Hoepken *et al.*, 2007) and loss of the mitochondrial membrane potential (Gegg *et al.*, 2009). Previous studies established the importance of *PINK1* in Parkin recruitment to mitochondria and in mitochondrial function but relied on *PINK1* knockdown models (Narendra *et al.*, 2010; Vives-Bauza *et al.*, 2010) and we showed by using patient fibroblast cultures harboring *PINK1* mutations that these disease-causing mutations disrupted Parkin translocation (Rakovic *et al.*, 2010). In the present study it was demonstrated that the presence of endogenous mutant *PINK1* in human DA neurons leads to diminished recruitment of Parkin to mitochondria. Two different types of human pathogenic *PINK1* mutations were studied, i.e. nonsense (c.1366C>T; p.Q456X) and missense (c.509T>G; p.V170G) mutations, and the same phenotype was observed. For this experiment, Parkin was overexpressed, since there is no Parkin antibody sensitive enough to detect endogenous Parkin by immunostaining; the only way to show this effect in DA neurons. We have previously shown by Western blotting that overexpressing wild-type Parkin in fibroblasts from *PINK1* mutation carriers led to the presence of detectable Parkin in the mitochondrial fraction (Rakovic *et al.*, 2010). However, in the present study, a lentiviral expression system was used where only very modest overexpression of Parkin was achieved compared to overexpression by transient transfection. Importantly, expression of normal *PINK1* rescued the effect of mutant *PINK1* on Parkin translocation, further validating the relevance of the *PINK1*/Parkin pathway in human neurons (Seibler *et al.*, 2011).

In addition, it was found that mtDNA levels do not decrease in depolarized mutant *PINK1* neurons as they do in wild-type neurons (Seibler *et al.*, 2011). This increase in mtDNA may reflect the impaired degradation of depolarized mitochondria due to *PINK1* deficiency as suggested previously (Narendra *et al.*, 2010). Importantly, these experiments were performed on endogenous levels of Parkin and effects in *PINK1* mutants were rescued by lentivirally expressed wild-type *PINK1*. Therefore, *PINK1* and Parkin may participate in a mitochondrial quality control pathway with a *PINK1*-mediated degradation of dysfunctional mitochondria by Parkin's ubiquitination function. Previous studies reported that full-length *PINK1* (~66kDa) is normally proteolytically processed upon entry into mitochondria to its cleaved ~55kDa form (Weihofen *et al.*, 2008). In contrast, full-length *PINK1* appeared on the mitochondria membrane of control fibroblasts when mitochondrial stressors were applied (Narendra *et al.*, 2010). The stress-dependent localization of full-length *PINK1* was confirmed in the present study in human *PINK1* mutant neurons infected with *PINK1*-V5. This observation represents an important step in the initiation of the *PINK1*-mediated translocation of Parkin. Recently, presenilin-associated rhomboid-like protein (PARL) has been identified

as the protease that cleaves PINK1 depending on mitochondrial membrane potential (Jin *et al.*, 2010). In coupled mitochondria, PINK1 is guided to mitochondria and imported into the inner mitochondrial membrane through the general mitochondrial import machinery, TOM and TIM23 complexes. There, PARL cleaves PINK1 for its subsequent degradation. Depolarization of the mitochondrial membrane potential leads then to the accumulation of full-length PINK1 on the outer mitochondrial membrane. But how PINK1 is stabilized on the outer membrane and not imported into the inner membrane remains unknown.

Interestingly, we also found upregulation of *peroxisome proliferator-activated receptor gamma, coactivator 1 alpha (PGC-1 α)* in depolarized mutant *PINK1* neurons, suggesting increased mitochondrial biogenesis in mutant cells. The transcriptional coactivator PGC-1 α regulates several metabolic processes, including mitochondrial biogenesis (Finck and Kelly, 2006) and it has been implicated in the pathogenesis of several neurodegenerative disorders (Cui *et al.*, 2006; Finck and Kelly, 2006; Weydt *et al.*, 2006; Qin *et al.*, 2009; Zheng *et al.*, 2010). Expression of PGC-1 α is inhibited in Huntington's disease (HD), an inherited neurodegenerative disease caused by a polyglutamine repeat expansion in huntingtin protein. The toxic effect of mutant huntingtin was moderated upon lentiviral-mediated delivery of PGC-1 α into the striatum of transgenic HD mice (Cui *et al.*, 2006). In brains of persons with Alzheimer disease PGC-1 α expression was decreased as a function of the progression of clinical dementia (Qin *et al.*, 2009). Its precise role in PD is still unknown. A genome-wide meta-analysis identified PGC-1 α as a potential therapeutic target for early intervention in PD. This was based on the finding that genes controlling cellular processes and expressed in response to PGC-1 α were underexpressed in PD patients (Zheng *et al.*, 2010). The increase in PGC-1 α expression in mutant *PINK1* neurons probably reflects a compensatory response to restore deficient mitochondrial function in the presence of mutant *PINK1*. Notably, a recent report described PARIS (ZNF746) as a new Parkin interacting substrate that represses the expression of PGC-1 α (Shin *et al.*, 2011). The authors demonstrated that conditional knockout of Parkin in animals led to the degeneration of DA neurons in a PARIS-dependent manner. This study suggests that low expression levels of PGC-1 α are due to Parkin deficiency leading to a pathological PD phenotype. By contrast, our model showed the ability of *PINK1* mutant neurons to increase expression of PGC-1 α . Further studies are required to examine mitochondrial function of PINK1 and Parkin in human DA neurons and to clarify the role of PGC-1 α in this context.

Why DA neurons are more susceptible to the loss of PINK1/Parkin than other neurons is unclear. It may relate to their superior dependence on functional mitochondria as DA neurons have high metabolic demands and are subject to especially high calcium fluxes that need to be buffered by mitochondria (Chan *et al.*, 2007; Guzman *et al.*, 2010).

4.4. Conclusions

***PRKRA*-linked dystonia:**

Dystonia-causing mutations in the PRKRA gene are not limited to the Brazilian population.

A number of 52 unrelated German patients with dystonia were screened for mutations in *PRKRA* and a novel frameshift mutation (c.266_267delAT) was identified in one allele of a patient presented with an early onset of generalized dystonia (3.1.2.). In addition to this mutation, two new heterozygous silent changes in *PRKRA* were found in other dystonia patients (c.126C/T and c.795C/T). While these two genetic variations are most likely not pathogenic, the heterozygous (truncating) mutation located in domain M1 of the protein is probably disease-causing (4.1.2.). So far, it is the second mutation that has been found in *PRKRA*. Investigations regarding the relevance of mutations in *PRKRA* stand at the very beginning but it seems that they are responsible for a minor subset of dystonia cases, albeit regionally not limited (Seibler *et al.*, 2008).

***PINK1*-linked PD:**

Fibroblasts from genetic PD patients can be reprogrammed into iPS cells.

To realize this, the previously reported reprogramming technique using four retroviral factors (OCT4, SOX2, cMYC and KLF4) was established in the laboratory as part of the present thesis. IPS cells were generated from skin fibroblasts taken from three PD patients with nonsense (c.1366C>T; p.Q456X) or missense (c.509T>G; p.V170G) mutations in the *PINK1* gene and from three healthy control individuals (3.2.1.). The resulting iPS cell colonies demonstrated stem cell characteristics regarding the expression of pluripotency markers, silencing of the transgenes and the differentiation potential of the cells. The mutations did not affect the ability of patient fibroblasts to be induced into iPS cells (Seibler *et al.*, 2011).

Mutant PINK1 human iPS cells can be differentiated into dopaminergic neurons.

A previously published protocol for neural induction was implemented in the laboratory and used with minor modifications. Patient-derived iPS cells were able to differentiate into DA neurons at an efficiency comparable to the control iPS cells (3.2.2.). Immunofluorescence staining revealed that approximately 60% of the total cells expressed the neuron-specific marker TUJ1. The percentage of neurons coexpressing TUJ1 and the DA marker TH was slightly higher in mutants ($16 \pm 1\%$) compared to wild-type ($11 \pm 3\%$). These neurons can be used to study the role of the endogenous *PINK1* mutations in a more relevant cell type for PD (Seibler *et al.*, 2011).

Parkin recruitment to mitochondria is impaired in mutant PINK1 dopaminergic neurons.

Two different types of human pathogenic *PINK1* mutations (nonsense and missense) were studied to examine the effect of these mutations on the PINK1/Parkin pathway. Under basal conditions, Parkin was localized in the cytosol and the neurites of DA neurons. However, treatment with the mitochondrial stressor valinomycin resulted in dramatic mitochondrial translocation of Parkin in the control but not in the *PINK1* mutant neurons. Importantly, lentiviral expression of wild-type PINK1 rescued this effect in the mutants (3.2.3.). Here it could be demonstrated for the first time in human DA neurons that the presence of endogenous mutant *PINK1* leads to diminished recruitment of Parkin to mitochondria (Seibler *et al.*, 2011).

Loss of PINK1 function leads to mitochondria-related phenotypes in human neurons.

Upon mitochondrial depolarization, reduction in mtDNA copy number was observed in controls but not in *PINK1* mutant cells. Overexpression of wild-type PINK1 in the mutant line resulted in a comparable effect of mitochondrial depolarization on mtDNA as observed in controls (3.2.4.). These results suggested that deficient translocation of Parkin to mitochondria in mutant PINK1 neurons may lead to accumulation of mitochondria due to their decreased clearance. Since the increase in mtDNA can be also due to increased mitochondrial production, the expression levels of PGC-1 α were investigated, an important inducer of mitochondrial biogenesis. Interestingly, PGC-1 α levels significantly increased in mutant *PINK1* but not in wild-type neurons upon mitochondrial depolarization, and this effect was abolished by lentiviral wild-type PINK1 expression in mutant *PINK1* cells (3.2.4.). The upregulation of PGC-1 α might reflect a compensatory response to restore deficient mitochondrial function in the presence of mutant *PINK1* (Seibler *et al.*, 2011).

5. PERSPECTIVES

So far, most of the patients examined in mutational *PRKRA* screens were diagnosed with a moderate expression of dystonia symptoms combined with a rather late onset of the disease. Therefore, additional screens are required of patients with generalized dystonia combined with an early onset of symptoms to fully define the relevance of mutations in *PRKRA*. Importantly, the new frameshift mutation was found in one allele only, whereas the original mutation was at homozygous state. Further studies are needed to explain loss-of-function and gain-of-function effects of mutations in *PRKRA*, respectively.

Except for *DYT1*, there are relatively few functional studies on dystonia pathways in neurons. A promising and moderately labor-intensive approach compared to mouse models might be the reprogramming of dystonia patient-derived fibroblasts into iPS cells and subsequent differentiation into neurons, as shown for *PINK1*-linked PD in the present study. This could reveal neuron-specific disease-causing pathways. Moreover, this approach is especially relevant for dystonia genes that are expressed predominantly in neuronal tissue.

The differentiation efficiency into DA neurons ranged between 11-16% in this study. If these cells are to be applied in drug discovery, further optimized protocols will be required that increase the effectiveness of a more selective differentiation towards a neuronal subtype. Alternately, DA precursors could be selected through generating iPS cells that express GFP driven by the TH promoter.

The impaired Parkin recruitment to mitochondria and the unchanged copy number of mitochondria show that *PINK1* mutations cause a mitochondria-related phenotype in human neurons. Extensions of these data are the analysis of mitochondrial morphology and the measurement of mitochondrial membrane potential and calcium levels. Importantly, these experiments can be performed in living cells.

The main known risk factor for PD is age and the observed neurodegeneration occurs in the adult brain. A more natural phenotype in the proposed PD model might develop during long-term culturing of mature neurons. However, to realize this, a more efficient differentiation technique is needed as precursors tend to overgrow the neurons with time. An important phenotype would be the occurrence of alpha-synuclein aggregates in TH-positive neurons.

Finally, iPS cell-derived neurons have been shown to exhibit electric activity. The natural extension of this finding is to examine *PINK1* mutant human neurons for electrophysiological abnormalities, such as impaired excitability of neurons.

6. SUMMARY

The present thesis provides novel results regarding the understanding of two monogenic forms of the movement disorders dystonia and Parkinson disease (PD). First, the dystonia-linked gene *Protein kinase interferon-inducible double-stranded RNA-dependent activator (PRKRA)* was investigated at the genomic level. Second, a human neuronal model was implemented to examine the effect of mutations in the PD-linked gene *PTEN-induced putative kinase 1 (PINK1)*.

The homozygous *PRKRA* mutation c.665C>T was found in Brazilian families associated with early-onset generalized dystonia. To further explore the role of mutations in *PRKRA* the following hypothesis was addressed: *Dystonia-causing mutations in the PRKRA gene are not limited to the Brazilian population.* On the basis of early-onset (<25 years), a positive family history, and limb involvement, 52 unrelated patients with dystonia were identified. All coding exons and flanking intronic sequences of *PRKRA* were sequenced. The known and newly detected sequence variations were tested in a further 75 patients with dystonia (>25 years) and in 189 healthy controls. A novel heterozygous mutation (c.266_267delAT; p.H89fsX20) in exon 3 of *PRKRA* was detected in one German patient. This predicted frameshift mutation, which causes premature truncation of the protein, was absent in other patients and controls. In addition, two new silent changes in *PRKRA* were found in two other patients (c.126C/T and c.795C/T). The original homozygous mutation in *PRKRA* and the GAG deletion in the *DYT1* gene were excluded in all 127 patients with dystonia. While the two silent changes are most likely not pathogenic, the heterozygous truncating mutation might have a gain-of-function effect. Additional mutational analyses and association studies are required to further elucidate the role of *PRKRA* mutations in the etiology of dystonia.

PD is a neurodegenerative disorder, characterized by loss of dopaminergic (DA) neurons in the *substantia nigra*. Recessively inherited PD can be caused by mutations in *PINK1*, a gene encoding a mitochondrial kinase implicated in the regulation of mitochondrial degradation. Recent studies have linked the E3 ubiquitin-protein ligase Parkin and *PINK1* to a common pathway. Under stress conditions, *PINK1* recruits Parkin to dysfunctional mitochondria where it ubiquitinates certain targets and thus promotes mitochondrial fission as initial step of mitophagy. While, so far, studies examined *PINK1* function in non-neuronal systems or through *PINK1* knockdown approaches, there is an imperative to examine the role of endogenous *PINK1* in appropriate human-derived and biologically relevant cell models. Recently, a new type of pluripotent cells has been introduced known as induced pluripotent stem (iPS) cells that is obtained via reprogramming of somatic cells and allows differentiation into diverse specialized cell types. Since genetic PD has not been studied yet using this system, the following hypotheses were formulated: (i) *Fibroblasts from genetic PD patients*

can be reprogrammed into iPS cells. (ii) *Mutant PINK1 human iPS cells can be differentiated into DA neurons.* Skin fibroblasts were taken from three PD patients with nonsense (c.1366C>T; p.Q456X) or missense (c.509T>G; p.V170G) mutations in the *PINK1* gene and from three healthy controls. For the production of iPS cells, the recently described reprogramming technique was implemented as part of the present thesis. Reprogramming was induced by retroviral transduction of fibroblasts with four factors: POU class 5 homeobox 1 (OCT4), SRY-box 2 (SOX2), Krüppel-like factor 4 (KLF4) and cMYC. IPS cell colonies could be isolated after four weeks of reprogramming. Expression of pluripotency markers and repression of the retroviral transgenes indicated that reprogramming of wild-type and *PINK1* mutant fibroblasts into a pluripotent state had occurred. Directed differentiation of iPS cells into DA neurons was achieved by culturing medium supplemented with various growth factors for a period of 25-30 days. Patient-derived iPS cells were able to differentiate into DA neurons at an efficiency similar as that in control iPS cells. Immunofluorescence staining revealed that approximately 60% of cells expressed the neuron-specific marker neuronal class III β -Tubulin (TUJ1). The percentage of neurons coexpressing TUJ1 and tyrosine hydroxylase (TH), the rate-limiting enzyme in the synthesis of DA, was slightly higher in mutants ($16 \pm 1\%$) compared to controls ($11 \pm 3\%$). These neurons can be used to study the role of the endogenous *PINK1* mutations in a more relevant cell type for PD.

To further explore the effect of *PINK1* mutations in this new model, the following hypotheses were addressed: (i) *Parkin recruitment to mitochondria is impaired in mutant PINK1 DA neurons.* (ii) *Loss of PINK1 function leads to mitochondria-related phenotypes in human neurons.* Immunofluorescence staining revealed that under basal conditions, Parkin was localized in the cytosol and neurites of DA neurons. However, treatment with the mitochondrial stressor valinomycin resulted in mitochondrial translocation of Parkin in the control but not in the *PINK1* mutant TH-positive neurons. Importantly, lentiviral expression of wild-type *PINK1* rescued this effect in the mutants. In addition, it was found that mitochondrial DNA (mtDNA) copy number does not decrease in depolarized *PINK1* mutant neurons as it does in wild-type neurons. At the same time levels of *peroxisome proliferator-activated receptor gamma, coactivator 1 alpha (PGC-1 α)*, an inducer of mitochondrial biogenesis, significantly increased in mutant *PINK1* but not in wild-type neurons upon mitochondrial depolarization. These alterations were corrected by lentiviral expression of wild-type *PINK1* in mutant *PINK1* neurons. The increase in mtDNA may reflect impaired degradation of depolarized mitochondria due to *PINK1* deficiency. The upregulation of *PGC-1 α* in mutant *PINK1* neurons might be explained as a compensatory response to restore deficient mitochondrial function in the presence of mutant *PINK1*. In conclusion, these studies suggest that *PINK1* mutant iPS-cell derived neurons exhibit distinct phenotypes that should be amenable to further mechanistic studies in this relevant biological context.

7. ZUSAMMENFASSUNG

Die vorliegende Arbeit liefert neue Erkenntnisse zum Verständnis von zwei monogenetischen Formen der Bewegungsstörungen Dystonie und Morbus Parkinson (MP). Zuerst wurde das Dystonie-assoziierte Gen *Protein kinase interferon-inducible double-stranded RNA-dependent activator (PRKRA)* auf genomischer Ebene untersucht. Darüber hinaus wurde ein humanes neuronales Modell eingeführt, um den Effekt von Mutationen im MP-assoziierten Gen *PTEN-induced putative kinase 1 (PINK1)* zu erforschen.

Die homozygote *PRKRA*-Mutation c.665C>T wurde in brasilianischen Familien identifiziert, bei denen eine generalisierte Dystonie mit frühem Beginn vorlag. Um die Rolle von Mutationen in *PRKRA* weiter aufzuklären, wurde folgende Hypothese formuliert: *Dystonie-verursachende Mutationen in PRKRA sind nicht auf die brasilianische Bevölkerung begrenzt.* Eine Gruppe von 52 Patienten mit Dystonie ohne Verwandtschaftsbeziehung wurde auf der Grundlage eines frühen Beginns der Erkrankung (< 25 Jahre), einer positiven Familienanamnese und dem Auftreten der Dystonie an den Extremitäten ausgewählt. Anschließend wurden alle kodierenden Exons und angrenzende Sequenzen der Introns von *PRKRA* sequenziert. Für die bereits beschriebene und alle neu detektierten Sequenzveränderungen wurden zusätzlich 75 weitere Patienten mit Dystonie (> 25 Jahre) und 189 gesunde Individuen überprüft. Eine neue heterozygote Mutation (c.266_267delAT; p.H89fsX20) in Exon 3 von *PRKRA* wurde bei einem deutschen Patienten identifiziert. Diese *frameshift*-Mutation, die einen vorzeitigen Abbruch des Proteins verursacht, wurde weder bei anderen Patienten noch bei Kontrollen detektiert. Außerdem wurden zwei neue stille Mutationen in *PRKRA* bei zwei anderen Patienten gefunden (c.126C/T und c.795C/T). Die ursprünglich beschriebene homozygote *PRKRA*-Mutation sowie die häufig vorkommende GAG-Deletion im *DYT1*-Gen konnten bei allen 127 Dystonie-Patienten ausgeschlossen werden. Während die zwei stillen Mutationen wahrscheinlich als nicht pathogen eingestuft werden können, ist für die heterozygote und zum Proteinabbruch führende Mutation der Effekt eines *gain-of-function* denkbar. Zusätzliche Mutationsanalysen und Assoziationsstudien sind erforderlich, um die Rolle von *PRKRA*-Mutationen bei der Ätiologie von Dystonien weiter aufzuklären.

MP ist eine neurodegenerative Erkrankung, die durch den Verlust dopaminerg (DA) Neurone in der *Substantia nigra* charakterisiert ist. Das rezessiv vererbte MP-Syndrom kann durch *PINK1*-Mutationen verursacht werden. *PINK1* kodiert für eine mitochondriale Kinase, die mit der Regulation des Abbaus von Mitochondrien in Zusammenhang gebracht wurde. Kürzlich veröffentlichte Studien beschreiben einen gemeinsamen Signalweg von *PINK1* und der E3-Ubiquitin-Ligase Parkin. Unter Stressbedingungen wird Parkin durch *PINK1* zu dysfunktionalen Mitochondrien rekrutiert, wo es bestimmte Zielproteine ubiquitiniert und

dadurch mitochondriale Fission als initialen Schritt der Mitophagie auslöst. Da bei bisherigen Studien die Funktion von PINK1 in nicht-neuronalen Systemen oder in Modellen mit PINK1-*knockdown* untersucht wurde, ist es notwendig, die Rolle des endogenen PINK1-Proteins in humanen und biologisch-relevanten Zellmodellen zu überprüfen. Vor kurzem wurde die Entwicklung einer neuen Art pluripotenter Stammzellen vorgestellt, sogenannte induzierte pluripotente Stammzellen (iPS-Zellen), die durch Reprogrammierung somatischer Zellen erhalten und in verschiedenen spezialisierte Zelltypen differenziert werden können. Da genetisch verursachter MP bisher noch nicht unter Verwendung dieser Zellen untersucht wurde, ergaben sich folgende Hypothesen: (i) *Fibroblasten von Patienten mit genetisch verursachtem MP können in iPS-Zellen reprogrammiert werden.* (ii) *Humane iPS-Zellen mit einer Mutation in PINK1 können in DA-Neurone differenziert werden.* Hautfibroblasten wurden von drei MP-Patienten mit *nonsense* (c.1366C>T; p.Q456X) und *missense* (c.509T>G; p.V170G) Mutationen und von drei gesunden Individuen entnommen. Für die Generierung der iPS-Zellen wurde die vor kurzem veröffentlichte Methode der Reprogrammierung im Rahmen der vorliegenden Arbeit aufgebaut. Die Reprogrammierung wurde durch retrovirale Transduktion der Fibroblasten mit vier Faktoren gestartet: *POU class 5 homeobox 1* (OCT4), *SRY-box 2* (SOX2), *Krüppel-like factor 4* (KLF4) und cMYC. Nach vier Wochen konnten Kolonien von iPS-Zellen isoliert werden. Durch die Expression von Pluripotenzgenen und die Repression retroviraler Transgene in den iPS-Zellen konnte gezeigt werden, dass die Reprogrammierung von Fibroblasten mit und ohne *PINK1*-Mutation stattgefunden hat. Die direkte Differenzierung der iPS-Zellen in DA-Neurone wurde durch das Kultivieren der Zellen für einen Zeitraum von 25 – 30 Tagen in einem Medium erreicht, dem verschiedene Wachstumsfaktoren zugeführt wurden. iPS-Zellen von Patienten differenzierten mit ähnlicher Effizienz in DA-Neurone wie die iPS-Zellen der Kontrollen. Mittels Immunfluoreszenz-Analyse wurde gezeigt, dass ca. 60 % der Zellen den Neuronenspezifischen Marker *neuronal class III β -Tubulin* (TUJ1) exprimierten. Der Anteil der Neurone, die TUJ1 und Tyrosin-Hydroxylase, das geschwindigkeitsbestimmende Enzym in der Biosynthese von DA, ko-exprimierten, war bei den Zellen mit Mutation etwas höher (16 ± 1 %) als bei den Kontrollen (11 ± 3 %). Diese Neurone können verwendet werden, um die Rolle von endogenen *PINK1*-Mutationen in einem für MP relevanten Zelltyp zu untersuchen. Um den Effekt der *PINK1*-Mutationen innerhalb dieses neuen Modells weiter zu erforschen, wurden folgende Hypothesen formuliert: (i) *Die Rekrutierung von Parkin zu den Mitochondrien ist in DA-Neuronen mit PINK1-Mutation gestört.* (ii) *Der Funktionsverlust von PINK1 führt zu einem mit Mitochondrien in Zusammenhang stehenden Phänotyp in humanen Neuronen.* Mittels Immunfluoreszenz-Färbung wurde gezeigt, dass Parkin unter basalen Bedingungen im Cytosol und den Neuriten der DA-Neurone lokalisiert ist. Nach Zugabe des mitochondrialen Stressors Valinomycin, konnte die Translokation von Parkin zu den

Mitochondrien bei den Kontrollen beobachtet werden, wohingegen die mutierten Neurone keine Reaktion zeigten. Lentivirale Expression von Wildtyp-PINK1 in diesen Neuronen konnte die Parkin-Translokation wiederherstellen. Zudem wurde gezeigt, dass die Menge an mitochondrialer DNA (mtDNA) in depolarisierten Neuronen mit *PINK1*-Mutation unverändert bleibt, während sie in den Wildtyp-Neuronen abnimmt. Darüber hinaus ist nach mitochondrialer Depolarisierung der Expressionslevel von *peroxisome proliferator-activated receptor gamma, coactivator 1 alpha* (PGC-1 α), einem Protein, das die mitochondriale Biogenese induziert, nur in mutierten Neuronen signifikant erhöht. Diese Veränderungen in den Neuronen mit *PINK1*-Mutation wurden durch lentivirale Expression von Wildtyp-PINK1 korrigiert. Die Zunahme an mtDNA könnte auf einen gestörten Abbau depolarisierter Mitochondrien als Folge des Mangels an PINK1-Protein hindeuten. Die Hochregulierung von PGC-1 α in Neuronen mit *PINK1*-Mutation könnte eine Antwort der Zelle darstellen, eine fehlerhafte mitochondriale Funktion zu kompensieren. Zusammenfassend wird anhand dieser Studien deutlich, dass aus iPS-Zellen generierte Neurone mit *PINK1*-Mutation klare Phänotypen aufweisen, die auch für weitere Prozess-orientierte Studien in diesem biologisch relevanten Kontext zugänglich sein sollten.

8. REFERENCES

- Aquilano K, Vigilanza P, Baldelli S, Pagliei B, Rotilio G, Ciriolo MR (2010) Peroxisome proliferator-activated receptor gamma co-activator 1alpha (PGC-1alpha) and sirtuin 1 (SIRT1) reside in mitochondria: possible direct function in mitochondrial biogenesis. *J Biol Chem* 285(28):21590-9.
- Bender A, Krishnan KJ, Morris CM, Taylor GA, Reeve AK, Perry RH, et al. (2006) High levels of mitochondrial DNA deletions in substantia nigra neurons in aging and Parkinson disease. *Nat. Genet* 38(5):515-7.
- Bolte S and Cordelières FP (2006) A guided tour into subcellular colocalization analysis in light microscopy. *J Microsc* 224(Pt 3):213-32.
- Bonifati V, Rizzu P, van Baren MJ, Schaap O, Breedveld GJ, Krieger E, et al. (2003) Mutations in the DJ-1 gene associated with autosomal recessive early-onset parkinsonism. *Science* 299(5604):256-9.
- Bottenstein JE (1985) *Cell Culture in the Neurosciences*. Plenum Press: New York and London.
- Bragg DC, Armata IA, Nery FC, Breakefield XO, Sharma N (2011) Molecular pathways in dystonia. *Neurobiol Dis.* 42(2):136-47.
- Brotchie JM and Obeso JA (2010) *Functional Anatomy and Physiology of the Basal Ganglia*. In: *Movement Disorders 4*. Ed: Schapira AH et al., Saunders; Philadelphia, USA.
- Burns JC, Friedmann T, Driever W, Burrascano M, Yee JK (1993) Vesicular stomatitis virus G glycoprotein pseudotyped retroviral vectors: concentration to very high titer and efficient gene transfer into mammalian and nonmammalian cells. *Proc Natl Acad Sci U S A* 90(17):8033-7.
- Butler AG, Duffey PO, Hawthorne MR, Barnes MP (2004) An epidemiologic survey of dystonia within the entire population of northeast England over the past nine years. *Adv Neurol* 94:95-9.
- Camargos S, Scholz S, Simon-Sanchez J, Paisan-Ruiz C, Lewis P, Hernandez D, et al. (2008) DYT16, a novel young-onset dystonia-parkinsonism disorder: identification of a segregating mutation in the stress-response protein PRKRA. *Lancet Neurol* 7(3):207-15.
- Chambers SM, Fasano CA, Papapetrou EP, Tomishima M, Sadelain M, Studer L (2009) Highly efficient neural conversion of human ES and iPS cells by dual inhibition of SMAD signaling. *Nat Biotechnol* 27(3):275-80.
- Chan CS, Guzman JN, Ilijic E, Mercer JN, Rick C, Tkatch T, et al. (2007) 'Rejuvenation' protects neurons in mouse models of Parkinson's disease. *Nature* 447(7148):1081-6.

- Chen X, Xu H, Yuan P, Fang F, Huss M, Vega VB, et al. (2008) Integration of external signaling pathways with the core transcriptional network in embryonic stem cells. *Cell* 133(6):1106-17.
- Cheung YT, Lau WK, Yu MS, Lai CS, Yeung SC, So KF, et al. (2009) Effects of all-trans-retinoic acid on human SH-SY5Y neuroblastoma as in vitro model in neurotoxicity research. *Neurotoxicology* 30(1):127-35.
- Chin MH, Mason MJ, Xie W, Volinia S, Singer M, Peterson C, et al. (2009) Induced pluripotent stem cells and embryonic stem cells are distinguished by gene expression signatures. *Cell Stem Cell* 5(1):111-23.
- Clark IE, Dodson MW, Jiang C, Cao JH, Huh JR, Seol JH, et al. (2006) Drosophila pink1 is required for mitochondrial function and interacts genetically with parkin. *Nature* 441(7097):1162-6.
- Cui L, Jeong H, Borovecki F, Parkhurst CN, Tanese N, Krainc D (2006) Transcriptional repression of PGC-1alpha by mutant huntingtin leads to mitochondrial dysfunction and neurodegeneration. *Cell* 127(1):59-69.
- De Carvalho Aguiar P, Sweadner KJ, Penniston JT, Zaremba J, Liu L, Caton M, et al. (2004) Mutations in the Na⁺/K⁺ -ATPase alpha3 gene ATP1A3 are associated with rapidonset dystonia parkinsonism. *Neuron* 43(2):169-75.
- Deas E, Plun-Favreau H, Wood N (2009) PINK1 function in health and disease. *EMBO Mol Med* 1(3):152-65.
- Dezawa M, Kanno H, Hoshino M, Cho H, Matsumoto N, Itokazu Y, et al. (2004) Specific induction of neuronal cells from bone marrow stromal cells and application for autologous transplantation. *J Clin Invest* 113(12):1701-10.
- Dimos JT, Rodolfa KT, Niakan KK, Weisenthal LM, Mitsumoto H, Chung W, et al. (2008) Induced pluripotent stem cells generated from patients with ALS can be differentiated into motor neurons. *Science* 321(5893):1218-21.
- Ebert AD, Yu J, Rose FF Jr, Mattis VB, Lorson CL, Thomson JA, et al. (2009) Induced pluripotent stem cells from a spinal muscular atrophy patient. *Nature* 457(7227):277-80.
- Elkabetz Y, Panagiotakos G, Al Shamy G, Socci ND, Tabar V, Studer L (2008) Human ES cell-derived neural rosettes reveal a functionally distinct early neural stem cell stage. *Genes Dev* 22(2):152-65.
- Evidente VG, Nolte D, Niemann S, Advincula J, Mayo MC, Natividad FF, et al. (2004) Phenotypic and molecular analyses of X-linked dystonia-parkinsonism ("lubag") in women. *Arch Neurol* 61(12):1956-9.
- Finck BN and Kelly DP (2006) PGC-1 coactivators: inducible regulators of energy metabolism in health and disease. *J Clin Invest* 116(3):615-22.

- Fuchs T, Gavarini S, Saunders-Pullman R, Raymond D, Ehrlich ME, Bressman SB, et al. (2009) Mutations in the THAP1 gene are responsible for DYT6 primary torsion dystonia. *Nat Genet* 41(3):286-8.
- García-Cabezas MA, Rico B, Sánchez-González MA, Cavada C (2007) Distribution of the dopamine innervation in the macaque and human thalamus. *Neuroimage* 34(3):965-984.
- García Ruiz PJ (2004) [Prehistory of Parkinson's disease]. *Neurologia* 19(10):735-7.
- Gautier CA, Kitada T, Shen J (2008) Loss of PINK1 causes mitochondrial functional defects and increased sensitivity to oxidative stress. *Proc Natl Acad Sci USA* 105(32):11364–11369.
- Gegg ME, Cooper JM, Schapira AH, Taanman JW (2009) Silencing of PINK1 expression affects mitochondrial DNA and oxidative phosphorylation in dopaminergic cells. *PLoS ONE* 4(3):e4756.
- Gibb WR and Lees AJ (1988) The relevance of the Lewy body to the pathogenesis of idiopathic Parkinson's disease. *J Neurol Neurosurg Psychiatry* 51(6):745-52.
- Grimm S (2004) The art and design of genetic screens: mammalian culture cells. *Nat Rev Genet* 5(3):179-89.
- Grünewald A, Breedveld GJ, Lohmann-Hedrich K, Rohé CF, König IR, Hagenah J, et al. (2007) Biological effects of the PINK1 c.1366C>T mutation: implications in Parkinson disease pathogenesis. *Neurogenetics* 8(2):103-9.
- Grünewald A (2008) Molecular characterisation of SGCE-associated myoclonus-dystonia and PINK1-associated Parkinson's disease. Inauguraldissertation; Universität zu Lübeck.
- Guzman JN, Sanchez-Padilla J, Wokosin D, Kondapalli J, Ilijic E, Schumacker PT, et al. (2010) Oxidant stress evoked by pacemaking in dopaminergic neurons is attenuated by DJ-1. *Nature* 468(7324):696-700.
- Hamza TH, Zabetian CP, Tenesa A, Laederach A, Montimurro J, Yearout D, et al. (2010) Common genetic variation in the HLA region is associated with late-onset sporadic Parkinson's disease. *Nat Genet* 42(9):781-5.
- Hanna J, Saha K, Pando B, van Zon J, Lengner CJ, Creighton MP, et al. (2009) Direct cell reprogramming is a stochastic process amenable to acceleration. *Nature* 462(7273):595-601.
- Hanson PI and Whiteheart SW (2005) AAA+ proteins: have engine, will work. *Nat Rev Mol Cell Biol* 6(7):519-29.
- Haque ME, Thomas KJ, D'Souza C, Callaghan S, Kitada T, Slack RS, et al. (2008) Cytoplasmic Pink1 activity protects neurons from dopaminergic neurotoxin MPTP. *Proc. Natl. Acad. Sci. U.S.A.* 105(5):1716–1721.

- Hedrich K, Eskelson C, Wilmot B, Marder K, Harris J, Garrels J, et al. (2004) Distribution, type, and origin of Parkin mutations: review and case studies. *Mov Disord* 19(10):1146-57.
- Hedrich K, Hagenah J, Djarmati A, Hiller A, Lohnau T, Lasek K, et al. (2006) Clinical spectrum of homozygous and heterozygous PINK1 mutations in a large German family with Parkinson disease: role of a single hit? *Arch Neurol* 63(6):833-8.
- Hewett JW, Tannous B, Niland BP, Nery FC, Zeng J, Li Y, et al. (2007) Mutant torsinA interferes with protein processing through the secretory pathway in DYT1 dystonia cells. *Proc Natl Acad Sci U S A* 104(17):7271-6.
- Hewett JW, Nery FC, Niland B, Ge P, Tan P, Hadwiger P, et al. (2008) siRNA knock-down of mutant torsinA restores processing through secretory pathway in DYT1 dystonia cells. *Hum Mol Genet* 17(10):1436-45.
- Hoepken HH, Gispert S, Morales B, Wingerter O, Del Turco D, Mulsch A, et al. (2007) Mitochondrial dysfunction, peroxidation damage and changes in glutathione metabolism in PARK6. *Neurobiol Dis* 25(2):401-11.
- Hu BY, Weick JP, Yu J, Ma LX, Zhang XQ, Thomson JA, et al. (2010) Neural differentiation of human induced pluripotent stem cells follows developmental principles but with variable potency. *Proc Natl Acad Sci U S A* 107(9):4335-40.
- Huang X, Hutchins B, Patel RC (2002) The C-terminal, third conserved motif of the protein activator PACT plays an essential role in the activation of double-stranded-RNA-dependent protein kinase (PKR). *Biochem J* 366(Pt 1):175-86.
- Huangfu D, Osafune K, Maehr R, Guo W, Eijkelenboom A, Chen S, et al. (2008) Induction of pluripotent stem cells from primary human fibroblasts with only Oct4 and Sox2. *Nat Biotechnol* 26(11):1269-75.
- Ichinose H, Ohye T, Takahashi E, Seki N, Hori T, Segawa M, et al. (1994) Hereditary progressive dystonia with marked diurnal fluctuation caused by mutations in the GTP cyclohydrolase I gene. *Nat Genet* 8(3):236-42.
- Jin SM, Lazarou M, Wang C, Kane LA, Narendra DP, Youle RJ (2010) Mitochondrial membrane potential regulates PINK1 import and proteolytic destabilization by PARL. *J Cell Biol*. 191(5):933-42.
- Johe KK, Hazel TG, Muller T, Dugich-Djordjevic MM, McKay RD (1996) Single factors direct the differentiation of stem cells from the fetal and adult central nervous system. *Genes Dev* 10(24):3129-40.
- Kaji K, Norrby K, Paca A, Mileikovsky M, Mohseni P, Woltjen K (2009) Virus-free induction of pluripotency and subsequent excision of reprogramming factors. *Nature* 458(7239):771-5.

- Kawasaki H, Mizuseki K, Nishikawa S, Kaneko S, Kuwana Y, Nakanishi S, et al. (2000) Induction of midbrain dopaminergic neurons from ES cells by stromal cell-derived inducing activity. *Neuron* 28(1):31-40.
- Kitada T, Asakawa S, Hattori N, Matsumine H, Yamamura Y, Minoshima S, et al. (1998) Mutations in the parkin gene cause autosomal recessive juvenile parkinsonism. *Nature* 392(6676):605-8.
- Klein C (2003) Myoclonus and myoclonus-dystonias. In: *Genetics of Movement Disorders*. San Diego, CA: Academic Press.
- Klein C (2005) Movement disorders: classifications. *J Inherit Metab Dis* 28(3):425-39.
- Klein C and Schlossmacher MG (2007) Parkinson disease, 10 years after its genetic revolution: multiple clues to a complex disorder. *Neurology* 69(22):2093-104.
- Klein C, Lohmann-Hedrich K, Rogaeva E, Schlossmacher MG, Lang AE (2007) Deciphering the role of heterozygous mutations in genes associated with parkinsonism. *Lancet Neurol* 6(7):652-62.
- Lee HY, Xu Y, Huang Y, Ahn AH, Auburger GW, Pandolfo M, et al. (2004) The gene for paroxysmal non-kinesigenic dyskinesia encodes an enzyme in a stress response pathway. *Hum Mol Genet* 13(24):3161-70.
- Lee ES, Yoon CH, Kim YS, Bae YS (2007) The double-strand RNA-dependent protein kinase PKR plays a significant role in a sustained ER stress-induced apoptosis. *FEBS Lett* 581(22):4325-32.
- Lee G, Papapetrou EP, Kim H, Chambers SM, Tomishima MJ, Fasano CA, et al. (2009) Modelling pathogenesis and treatment of familial dysautonomia using patient-specific iPSCs. *Nature* 461(7262):402-6.
- Leroy E, Boyer R, Auburger G, Leube B, Ulm G, Mezey E, et al. (1998) The ubiquitin pathway in Parkinson's disease. *Nature* 395(6701):451-2.
- Leung JC, Klein C, Friedman J, Vieregge P, Jacobs H, Doheny D, et al. (2001) Novel mutation in the TOR1A (DYT1) gene in atypical early onset dystonia and polymorphisms in dystonia and early onset parkinsonism. *Neurogenetics* 3(3):133-43.
- Li XJ, Du ZW, Zarnowska ED, Pankratz M, Hansen LO, Pearce RA, et al. (2005) Specification of motoneurons from human embryonic stem cells. *Nat Biotechnol* 23(2):215-21.
- Li R, Liang J, Ni S, Zhou T, Qing X, Li H, et al. (2010) A mesenchymal-to-epithelial transition initiates and is required for the nuclear reprogramming of mouse fibroblasts. *Cell Stem Cell* 7(1):51-63.
- Lin W and Kang UJ (2008) Characterization of PINK1 processing, stability, and sub cellular localization. *J Neurochem* 106(1):464-74.

- López-Carballo G, Moreno L, Masiá S, Pérez P, Baretino D (2002) Activation of the phosphatidylinositol 3-kinase/Akt signaling pathway by retinoic acid is required for neural differentiation of SH-SY5Y human neuroblastoma cells. *J Biol Chem* 277(28):25297-304.
- Lotharius J, Barg S, Wiekop P, Lundberg C, Raymon HK, Brundin P (2002) Effect of mutant alpha-synuclein on dopamine homeostasis in a new human mesencephalic cell line. *J Biol Chem* 277(41):38884-94.
- Lowry WE, Richter L, Yachechko R, Pyle AD, Tchieu J, Sridharan R, et al. (2008) Generation of human induced pluripotent stem cells from dermal fibroblasts. *Proc Natl Acad Sci U S A* 105(8):2883-8.
- Makino S, Kaji R, Ando S, Tomizawa M, Yasuno K, Goto S, et al. (2007) Reduced neuron-specific expression of the TAF1 gene is associated with X-linked dystonia-parkinsonism. *Am J Hum Genet* 80(3):393-406.
- Manders E, Stap J, Brakenhoff G, van Driel R, Aten J (1992) Dynamics of three-dimensional replication patterns during the Sphase, analysed by double labelling of DNA and confocal microscopy. *J. Cell Sci* 103(Pt 3):857-62.
- Marchetto MC, Yeo GW, Kainohana O, Marsala M, Gage FH, Muotri AR (2009) Transcriptional signature and memory retention of human-induced pluripotent stem cells. *PLoS One* 4(9):e7076.
- Marongiu R, Brancati F, Antonini A, Ialongo T, Ceccarini C, Scarciolla O, et al. (2007) Whole gene deletion and splicing mutations expand the PINK1 genotypic spectrum. *Hum Mutat* 28(1):98.
- Matsumoto S, Nishimura M, Shibasaki H, Kaji R (2003) Epidemiology of primary dystonias in Japan: comparison with Western countries. *Mov Disord* 18(10):1196-8.
- Moro E, Volkmann J, König IR, Winkler S, Hiller A, Hassin-Baer S, et al. (2008) Bilateral subthalamic stimulation in Parkin and PINK1 parkinsonism. *Neurology* 70(14):1186-1191.
- Müller U (2009) The monogenic primary dystonias. *Brain* 132(Pt 8):2005-25.
- Napolitano F, Pasqualetti M, Usiello A, Santini E, Pacini G, Sciamanna G, et al. (2010) Dopamine D2 receptor dysfunction is rescued by adenosine A2A receptor antagonism in a model of DYT1 dystonia. *Neurobiol Dis* 38(3):434-45.
- Narendra D, Tanaka A, Suen DF, Youle RJ (2008) Parkin is recruited selectively to impaired mitochondria and promotes their autophagy. *J Cell Biol* 183(5):795-803.
- Narendra DP, Jin SM, Tanaka A, Suen DF, Gautier CA, Shen J, et al. (2010) PINK1 is selectively stabilized on impaired mitochondria to activate Parkin. *PLoS Biol* 8(1):e1000298.

- Nguyen HN, Byers B, Cord B, Shcheglovitov A, Byrne J, Gujar P, et al. (2011) LRRK2 mutant iPSC-derived DA neurons demonstrate increased susceptibility to oxidative stress. *Cell Stem Cell* 8(3):267-80.
- Oppenheim H (1911) Über eine eigenartige Krampfkrankheit des kindlichen und jugendlichen Alters (Dysbasia lordotica progressiva, Dystonia musculorum deformans). *Neurologisches Zentralblatt* 30:1090-1107.
- Ozelius LJ, Hewett JW, Page CE, Bressman SB, Kramer PL, Shalish C, et al. (1997) The early-onset torsion dystonia gene (DYT1) encodes an ATP-binding protein. *Nat Genet* 17(1):40-8.
- Påhlman S, Hoehner JC, Nånberg E, Hedborg F, Fagerström S, Gestblom C, et al. (1995) Differentiation and survival influences of growth factors in human neuroblastoma. *Eur J Cancer* 31A(4):453-8.
- Paisan-Ruiz C, Jain S, Evans EW, Gilks WP, Simon J, van der Brug M, et al. (2004) Cloning of the gene containing mutations that cause PARK8-linked Parkinson's disease. *Neuron* 44(4):595-600.
- Paisan-Ruiz C, Bhatia KP, Li A, Hernandez D, Davis M, Wood NW, et al. (2009) Characterization of PLA2G6 as a locus for dystonia-parkinsonism. *Ann Neurol* 65(1):19-23.
- Palmer TD, Schwartz PH, Taupin P, Kaspar B, Stein SA, Gage FH (2001) Cell culture. Progenitor cells from human brain after death. *Nature* 411(6833):42–43.
- Parfait B, Rustin P, Munnich A, Rötig A (1998) Co-amplification of nuclear pseudogenes and assessment of heteroplasmy of mitochondrial DNA mutations. *Biochem Biophys Res Commun* 247(1):57-9.
- Park IH, Lerou PH, Zhao R, Huo H, Daley GQ (2008a) Generation of human-induced pluripotent stem cells. *Nat Protoc* 3(7):1180-6.
- Park IH, Arora N, Huo H, Maherali N, Ahfeldt T, Shimamura A, et al. (2008b) Disease-Specific Induced Pluripotent Stem Cells. *Cell* 134(5):877-86.
- Park IH, Zhao R, West JA, Yabuuchi A, Huo H, Ince TA, et al. (2008c) Reprogramming of human somatic cells to pluripotency with defined factors. *Nature* 451(7175):141-6.
- Patel CV, Handy I, Goldsmith T, Patel RC (2000) PACT, a stress-modulated cellular activator of interferon-induced double-stranded RNA-activated protein kinase, PKR. *J Biol Chem* (48):37993-8.
- Perrier AL, Tabar V, Barberi T, Rubio ME, Bruses J, Topf N, et al. (2004) Derivation of midbrain dopamine neurons from human embryonic stem cells. *Proc. Natl. Acad. Sci. USA* 101(34):12543-8.
- Peters GA, Hartmann R, Qin J, Sen GC (2001) Modular structure of PACT: distinct domains for binding and activating PKR. *Mol Cell Biol* 21(6):1908-20.

- Pisani A, Martella G, Tschertner A, Bonsi P, Sharma N, Bernardi G, et al. (2006) Altered responses to dopaminergic D2 receptor activation and N-type calcium currents in striatal cholinergic interneurons in a mouse model of DYT1 dystonia. *Neurobiol Dis* 24(2):318-25.
- Plath K and Lowry WE (2011) Progress in understanding reprogramming to the induced pluripotent state. *Nat Rev Genet* 12(4):253-65.
- Polymeropoulos MH, Lavedan C, Leroy E, Ide SE, Dehejia A, Dutra A, et al. (1997) Mutation in the alpha-synuclein gene identified in families with Parkinson's disease. *Science* 276(5321):2045-7.
- Pruszak J, Sonntag KC, Aung MH, Sanchez-Pernaute R, Isacson O (2007) Markers and methods for cell sorting of human embryonic stem cell-derived neural cell populations. *Stem Cells* 25(9):2257-68.
- Pruszak J, Ludwig W, Blak A, Alavian K, Isacson O (2009) CD15, CD24 and CD29 define a surface biomarker code for neural lineage differentiation of stem cells. *Stem Cells* 27(12):2928-40.
- Qin W, Haroutunian V, Katsel P, Cardozo CP, Ho L, Buxbaum JD, et al. (2009) PGC-1alpha expression decreases in the Alzheimer disease brain as a function of dementia. *Arch Neurol* 66(3):352-61.
- Rakovic A, Grünwald A, Seibler P, Ramirez A, Kock N, Orolicki S, et al. (2010) Effect of endogenous mutant and wild-type PINK1 on Parkin in fibroblasts from Parkinson disease patients. *Hum Mol Genet* 19(16):3124-37.
- Ramirez A, Heimbach A, Grundemann J, Stiller B, Hampshire D, Cid LP, et al. (2006) Hereditary parkinsonism with dementia is caused by mutations in ATP13A2, encoding a lysosomal type 5 P-type ATPase. *Nat Genet* 38(10):1184-91.
- Raven JF and Koromilas AE (2008) PERK and PKR: old kinases learn new tricks. *Cell Cycle* 7(9):1146-50.
- Reese MG, Eeckman FH, Kulp D, Haussler D (1997) Improved splice site detection in Genie. *J Comput Biol* 4(3):311-23.
- Ritz K, Groen JL, Kruisdijk JJ, Baas F, Koelman JH, Tijssen MA (2009) Screening for dystonia genes DYT1, 11 and 16 in patients with writer's cramp. *Mov Disord*. 24(9):1390-2.
- Saiki RK, Scharf S, Faloona F, Mullis KB, Horn GT, Erlich HA, et al. (1985) Enzymatic amplification of beta-globin genomic sequences and restriction site analysis for diagnosis of sickle cell anemia. *Science* 230(4732):1350-4.
- Sanger F, Nicklen S, Coulson AR (1977) DNA sequencing with chain-terminating inhibitors. *Proc Natl Acad Sci U S A* 74(12):5463-7.

- Schapira AH, Cooper JM, Dexter D, Jenner P, Clark JB, Marsden CD (1989) Mitochondrial complex I deficiency in Parkinson's disease. *Lancet* 1(8649):1269.
- Schapira AH (2008) Mitochondria in the aetiology and pathogenesis of Parkinson's disease. *Lancet Neurol* 7(1):97-109.
- Schüle B, Pera RA, Langston JW (2009) Can cellular models revolutionize drug discovery in Parkinson's disease? *Biochim Biophys Acta* 1792(11):1043-51.
- Schwartz CM, Spivak CE, Baker SC, McDaniel TK, Loring JF, Nguyen C, et al. (2005) Ntera2: a model system to study dopaminergic differentiation of human embryonic stem cells. *Stem Cells Dev* 14(5):517-34.
- Sciamanna G, Bonsi P, Tassone A, Cuomo D, Tscherter A, Viscomi MT, et al. (2009) Impaired striatal D2 receptor function leads to enhanced GABA transmission in a mouse model of DYT1 dystonia. *Neurobiol Dis* 34(1):133-45.
- Seibler P, Djarmati A, Langpap B, Hagenah J, Schmidt A, Brüggemann N, et al. (2008) A heterozygous frameshift mutation in PRKRA (DYT16) associated with generalised dystonia in a German patient. *Lancet Neurol* 7(5):380-1.
- Seibler P, Graziotto J, Jeong H, Simunovic F, Klein C, Krainc D (2011) Mitochondrial Parkin Recruitment Is Impaired in Neurons Derived from Mutant PINK1 Induced Pluripotent Stem Cells. *J Neurosci* 31(16):5970-6.
- Shimura H, Hattori N, Kubo S, Yoshikawa M, Kitada T, Matsumine H, et al. (1999) Immunohistochemical and subcellular localization of Parkin protein: absence of protein in autosomal recessive juvenile parkinsonism patients. *Ann Neurol* 45(5):668-672.
- Shin JH, Ko HS, Kang H, Lee Y, Lee YI, Pletinkova O, et al. (2011) PARIS (ZNF746) repression of PGC-1 α contributes to neurodegeneration in Parkinson's disease. *Cell* 144(5):689-702.
- Shojaee S, Sina F, Banihosseini SS, Kazemi MH, Kalhor R, Shahidi GA, et al. (2008) Genome-wide linkage analysis of a Parkinsonian-pyramidal syndrome pedigree by 500 K SNP arrays. *Am J Hum Genet* 82(6):1375-84.
- Singleton AB, Farrer M, Johnson J, Singleton A, Hague S, Kachergus J, et al. (2003) alpha-Synuclein locus triplication causes Parkinson's disease. *Science* 302(5646):841.
- Smith ZD, Nachman I, Regev A, Meissner A (2010) Dynamic single-cell imaging of direct reprogramming reveals an early specifying event. *Nat Biotechnol* 28(5):521-6.
- Soldner F, Hockemeyer D, Beard C, Gao Q, Bell GW, Cook EG, et al. (2009) Parkinson's disease patient-derived induced pluripotent stem cells free of viral reprogramming factors. *Cell*. 136(5):964-77.
- Stadtfeld M, Maherali N, Breault DT, Hochedlinger K (2008) Defining molecular cornerstones during fibroblast to iPS cell reprogramming in mouse. *Cell Stem Cell* 2(3):230-40.

- Strauss KM, Martins LM, Plun-Favreau H, Marx FP, Kautzmann S, Berg D, et al. (2005) Loss of function mutations in the gene encoding Omi/HtrA2 in Parkinson's disease. *Hum Mol Genet* 14(15):2099-111.
- Swaans RJ, Rondot P, Renier WO, Van Den Heuvel LP, Steenbergen-Spanjers GC, Wevers RA (2000) Four novel mutations in the tyrosine hydroxylase gene in patients with infantile parkinsonism. *Ann Hum Genet* 64(Pt 1):25-31.
- Takahashi K and Yamanaka S (2006) Induction of pluripotent stem cells from mouse embryonic and adult fibroblast cultures by defined factors. *Cell* 126(4):663-76.
- Takahashi K, Tanabe K, Ohnuki M, Narita M, Ichisaka T, Tomoda K, et al. (2007) Induction of pluripotent stem cells from adult human fibroblasts by defined factors. *Cell* 131(5):861-72.
- Theunissen TW, van Oosten AL, Castelo-Branco G, Hall J, Smith A, Silva JC (2011) Nanog overcomes reprogramming barriers and induces pluripotency in minimal conditions. *Curr Biol* 21(1):65-71.
- Tiscornia G, Singer O, Verma IM (2006) Production and purification of lentiviral vectors. *Nat Protoc* 1(1):241-5.
- Torres GE, Sweeney AL, Beaulieu JM, Shashidharan P, Caron MG (2004) Effect of torsinA on membrane proteins reveals a loss of function and a dominant-negative phenotype of the dystonia-associated DeltaE-torsinA mutant. *Proc Natl Acad Sci U S A* 101(44):15650-5.
- Trzaska KA, Kuzhikandathil EV, Rameshwar P (2007) Specification of a dopaminergic phenotype from adult human mesenchymal stem cells. *Stem Cells* 25(11):2797-808.
- Valente EM, Brancati F, Ferraris A, Graham EA, Davis MB, Breteler MM, et al. (2002) PARK6- linked parkinsonism occurs in several European families. *Ann Neurol* 51(1):14-8.
- Valente EM, Abou-Sleiman PM, Caputo V, Muqit MM, Harvey K, Gispert S, et al. (2004) Hereditary early-onset Parkinson's disease caused by mutations in PINK1. *Science* 304(5674):1158-60.
- Vives-Bauza C, Zhou C, Huang Y, Cui M, de Vries RL, Kim J, et al. (2010) PINK1-dependent recruitment of Parkin to mitochondria in mitophagy. *Proc Natl Acad Sci U S A* 107(1):378-83.
- Walton NM, Sutter BM, Chen HX, Chang LJ, Roper SN, Scheffler B, et al. (2006) Derivation and large-scale expansion of multipotent astroglial neural progenitors from adult human brain. *Development* 133(18):3671-81.
- Weber YG, Storch A, Wuttke TV, Brockmann K, Kempfle J, Maljevic S (2008) GLUT1 mutations are a cause of paroxysmal exertion-induced dyskinesias and induce hemolytic anemia by a cation leak. *J Clin Invest* 118(6):2157-68.

- Weihofen A, Ostaszewski B, Minami Y, Selkoe DJ (2008) Pink1 Parkinson mutations, the Cdc37/Hsp90 chaperones and Parkin all influence the maturation or subcellular distribution of Pink1. *Hum Mol Genet* 17(4):602-16.
- Weydt P, Pineda VV, Torrence AE, Libby RT, Satterfield TF, Lazarowski ER, et al. (2006) Thermoregulatory and metabolic defects in Huntington's disease transgenic mice implicate PGC-1alpha in Huntington's disease neurodegeneration. *Cell Metab* 4(5):349-62.
- Wood-Kaczmar A, Gandhi S, Yao Z, Abramov AY, Miljan EA, Keen G, et al. (2008) PINK1 is necessary for long term survival and mitochondrial function in human dopaminergic neurons. *PLoS One* 3(6):e2455.
- Wu Z, Huang X, Feng Y, Handschin C, Feng Y, Gullicksen PS, et al. (2006) Transducer of regulated CREB-binding proteins (TORCs) induce PGC-1alpha transcription and mitochondrial biogenesis in muscle cells. *Proc Natl Acad Sci U S A.* 26;103(39).
- Xu C, Inokuma MS, Denham J, Golds K, Kundu P, Gold JD, et al. (2001) Feeder-free growth of undifferentiated human embryonic stem cells. *Nat Biotechnol.* 19(10):971-4.
- Xu RH, Sampsel-Barron TL, Gu F, Root S, Peck RM, Pan G, et al. (2008) NANOG is a direct target of TGFbeta/activin-mediated SMAD signaling in human ESCs. *Cell Stem Cell* 3(2):196-206.
- Yao S, Sukonnik T, Kean T, Bharadwaj RR, Pasceri P, Ellis J (2004) Retrovirus silencing, variegation, extinction, and memory are controlled by a dynamic interplay of multiple epigenetic modifications. *Mol Ther* 10(1):27-36.
- Yu J, Vodyanik MA, Smuga-Otto K, Antosiewicz-Bourget J, Frane JL, Tian S, et al. (2007) Induced pluripotent stem cell lines derived from human somatic cells. *Science* 318(5858):1917-20.
- Yu J, Hu K, Smuga-Otto K, Tian S, Stewart R, Slukvin II, et al. (2009) Human induced pluripotent stem cells free of vector and transgene sequences. *Science* 324(5928):797-801.
- Zhang SC, Wernig M, Duncan ID, Brüstle O, Thomson JA (2001) In vitro differentiation of transplantable neural precursors from human embryonic stem cells. *Nat Biotechnol* 19(12):1129-33.
- Zhang Z, Wang X, Wang S (2008) Isolation and characterization of mesenchymal stem cells derived from bone marrow of patients with Parkinson's disease. *In Vitro Cell Dev Biol Anim* 44(5-6):169-77.
- Zheng B, Liao Z, Locascio JJ, Lesniak KA, Roderick SS, Watt ML, et al. (2010) PGC-1 α , a potential therapeutic target for early intervention in Parkinson's disease. *Sci Transl Med* 2(52):52ra73.

-
- Zimprich A, Grabowski M, Asmus F, Naumann M, Berg D, Bertram M, et al. (2001) Mutations in the gene encoding epsilon-sarcoglycan cause myoclonus-dystonia syndrome. *Nat Genet* 29(1):66-9.
- Zimprich A, Biskup S, Leitner P, Lichtner P, Farrer M, Lincoln S, et al. (2004) Mutations in LRRK2 cause autosomal-dominant parkinsonism with pleomorphic pathology. *Neuron* 44(4):601-7.

9. APPENDIX

9.1. List of abbreviations

AD	–	Autosomal dominant
AFP	–	Alpha-fetoprotein
ALS	–	Amyotrophic lateral sclerosis
AR	–	Autosomal recessive
ATP	–	Adenosine triphosphate
ATP1A3	–	ATPase alpha 3
ATP13A2	–	ATPase type 13A2
BDNF	–	Brain-derived neurotrophic factor
cAMP	–	Cyclic adenosine monophosphate
cDNA	–	Copy (complementary) DNA
CDS	–	Coding sequence
CNS	–	Central nervous system
D2R	–	Dopamine receptor D2
DA	–	Dopamine
DAPI	–	4',6-diamidino-2-phenylindole
DAT	–	Dopamine transporter
DMEM	–	Dulbeccos Modified Eagle Serum
DMSO	–	Dimethyl sulfoxide
DNA	–	Deoxyribonucleic acid
DRBM	–	Double-stranded RNA binding motif
DSC3	–	Disease-specific sequence changes
dsRNA	–	Double-stranded RNA
DYT	–	Dystonia
EB	–	Embryoid body
eIF2 α	–	Eukaryotic initiation factor 2 α
ER	–	Endoplasmic reticulum
ES (cell)	–	Embryonic stem (cell)
FACS	–	Fluorescence-activated cell sorting (Flow cytometry)
FBS	–	Fetal bovine serum
FBXO7	–	F-box protein 7
FD	–	Familial dysautonomia
FGF	–	Fibroblast growth factor
FOXA2	–	Forkhead box A2

FSC	–	Forward Scatter
GAK	–	Cyclin G associated kinase
GATA4	–	GATA binding protein 4
GCH1	–	GTP cyclohydrolase 1
GDF3	–	Growth differentiation factor 3
GDNF	–	Glial cell line-derived neurotrophic factor
GFP	–	Green fluorescence protein
GPi/e	–	Internal/external globus pallidus
HLA-DRA	–	Major histocompatibility complex, class II, DR alpha
IPS (cell)	–	Induced pluripotent stem (cell)
KLF4	–	Krüppel-like factor 4
LRRK2	–	Leucin-rich repeat kinase 2
LUHMES	–	Lund human mesencephalic
MEF	–	Mouse embryonic fibroblasts
MET	–	Mesenchymal-to-epithelial
MOI	–	Multiplicity of infection
MPTP	–	1-methyl-4-phenyl-1,2,3,6-tetrahydropyridine
MR-1	–	Myofibrillogenesis regulator 1
MRI	–	Magnetic resonance imaging
MSC	–	Mesenchymal stem cell
mRNA	–	Messenger RNA
mtDNA	–	Mitochondrial DNA
MTS	–	Mitochondrial targeting signal
NANOG	–	Nanog homeobox
NCAM	–	Neural cell adhesion molecule 1
NSE	–	Neural specific enolase
OCT4	–	POU class 5 homeobox 1
Omi/HtrA2	–	HtrA serine peptidase 2
PARL	–	Presenilin-associated rhomboid-like protein
PAX6	–	Paired box 6
PBS	–	Phosphate buffered saline
PCR	–	Polymerase chain reaction
PD	–	Parkinson disease
PE	–	Phycoerythrin
PGC-1 α	–	Peroxisome proliferator-activated receptor gamma, coactivator 1 α
PINK1	–	PTEN-induced putative kinase 1
PLA2G6	–	Phospholipase A2, group VI

PRKRA	–	Protein kinase, interferon-inducible double-stranded RNA-dependent activator
RA	–	Retinoic acid
RNA	–	Ribonucleic acid
RT-PCR	–	Reverse transcription polymerase chain reaction
RUNX1	–	Runt-related transcription factor 1
SD	–	Standard deviation
SEM	–	Standard error of the mean
SGCE	–	Epsilon-sarcoglycane
SHH	–	Sonic hedgehog
SLC2A1	–	Solute carrier family 2 facilitated glucose transporter member 1
SMA	–	Spinal muscular atrophy
SMAD	–	Mothers against decapentaplegic homolog 1 signaling
SNAI1	–	Snail homolog 1 (Drosophila)
SNc	–	Substantia nigra pars compacta
SNCA	–	Alpha-synuclein
SNP	–	Single nucleotide polymorphism
SNr	–	Substantia nigra pars reticulate
SOX2	–	SRY-box 2
SSC	–	Side Scatter
STN	–	Subthalamic nucleus
TAF1	–	TAF1 RNA polymerase II
TH	–	Tyrosine hydroxylase
TGF	–	Transforming growth factor
Ct	–	Threshold cycle
TIM23	–	Translocase of inner mitochondrial membrane 23 homolog (yeast)
TOM20	–	Translocase of outer mitochondrial membrane 20 homolog (yeast)
TPA	–	12-0-tetradecanoyl-phorbol-13-acetate
TRAP1	–	Tumor necrosis factor receptor-associated protein 1
TUJ1	–	Neuronal class III β -Tubulin
UCH-L1	–	Ubiquitin C-terminal hydrolase-L1
VMAT2	–	Vesicular monoamine transporter
VPA	–	Valproic acid
VSV-G	–	Vesicular stomatitis virus G glycoprotein
WT	–	Wild-type
XR	–	X-chromosomal recessive

9.2. Supplementary material

Table S1 Primer for PCR-amplification of genomic fragments

Gene	Forward	Reverse
<i>PRKRA</i> Ex1 ¹	CCTCGCTGGAGCAACGCAAG	GGCACGGCTTTACCCAGAATG
<i>PRKRA</i> Ex2 ¹	TCTAAAGACCTCGCTCAC	TGAGAGGTCTCAGTTTCAG
<i>PRKRA</i> Ex3 ¹	TGACTTTGTTTTGTGTATTG	AACTGTTCACTTTGTTGC
<i>PRKRA</i> Ex4 ¹	GAATGACAAGAGCAAAGAC	ATTAATTCCTTGTGTTAGCC
<i>PRKRA</i> Ex5 ¹	GAAATGGGATCAAAATTAAG	AATATTTGAAAACATTACGAC
<i>PRKRA</i> Ex6 ¹	AAACAAAGTTATCAGGTCAG	AATCACAACCTCTGAAGTAGC
<i>PRKRA</i> Ex7 ¹	AATGTTGTCTTGTTTAAATTTG	TACTATCCACAAGAATGGG
<i>PRKRA</i> Ex8 ¹	GGTGTAGTATAACCATGGAG	GAGTGTGATGGAATCTATG
<i>PINK1</i> Ex2	GCTCACGGTGCATTCTTTTC	GCTTACCGAGATGTTCCACA
<i>PINK1</i> Ex7	GAGTTCAGATTAGCCCATGG	GACCTTCACTCTGGAACGAG

Note: ¹Camargos *et al.*, 2008

Table S2 Primer for PCR-amplification of cDNA fragments

Gene	Forward	Reverse
<i>OCT4</i> endo ¹	CCTCACTTCACTGCACTGTA	CAGGTTTTCTTTCCCTAGCT
<i>OCT4</i> trans ¹		CCTTGAGGTACCAGAGATCT*
<i>SOX2</i> endo ¹	CCCAGCAGACTTCACATGT	CCTCCCATTTCCCTCGTTTT
<i>SOX2</i> trans ¹		CCTTGAGGTACCAGAGATCT*
<i>KLF4</i> endo ¹	GATGAACTGACCAGGCACTA	GTGGGTCATATCCACTGTCT
<i>KLF4</i> trans ¹		CCTTGAGGTACCAGAGATCT*
<i>cMYC</i> endo ¹	TGCCTCAAATTTGGACTTTGG	GATTGAAATTCTGTGTAACCTGC
<i>cMYC</i> trans ¹		CGCTCGAGGTTAACGAATT
<i>GATA4</i> endoderm ¹	CTAGACCGTGGGTTTTGCAT	TGGGTTAAGTGCCCTGTAG
<i>AFP</i> endoderm ¹	AGCTTGGTGGTGGATGAAAC	CCCTCTTCAGCAAAGCAGAC
<i>BRACHYURY</i> mesoderm ²	AATTGGTCCAGCCTTGGAAAT	CGTTGCTCACAGACCACA
<i>RUNX1</i> mesoderm ¹	CCCTAGGGGATGTTCCAGAT	TGAAGCTTTTCCCTCTTCCA
<i>NCAM</i> ectoderm ¹	ATGGAAACTCTATTAAAGTGAACCTG	TAGACCTCATACTCAGCATTCCAGT
<i>PAX6</i> ectoderm ²	GTCCATCTTTGCTTGGGAAA	TAGCCAGGTTGCGAAGAACT
<i>NANOG</i> ¹	TGAACCTCAGCTACAAACAG	TGGTGGTAGGAAGAGTAAAG
<i>GDF3</i> ¹	AAATGTTTTGTGTTGCGGTCA	TCTGGCACAGGTGTCTTCAG
<i>PINK1</i>	TTCCCCTTGGCCATCAAGA	ACCAGCTCCTGGCTCATTGT
<i>PGC-1α</i>	TTGCCAGATCTTCCTGAACTTG	CAAATGAGGGCAATCCGTCTTCA
<i>mtDNA</i>	AGGACAAGAGAAATAAGGCC	TAAGAAGAGGAATTGAACCTCTGAC TGTA
<i>β-actin</i>	TGAAGTGTGACGTGGACATC	GGAGGAGCAATGATCTTGAT

Note: endo – endogenous, trans – transgene, *Reverse primer specific for retroviral transgene, ¹Park *et al.*, 2008c, ²Huangfu *et al.*, 2008

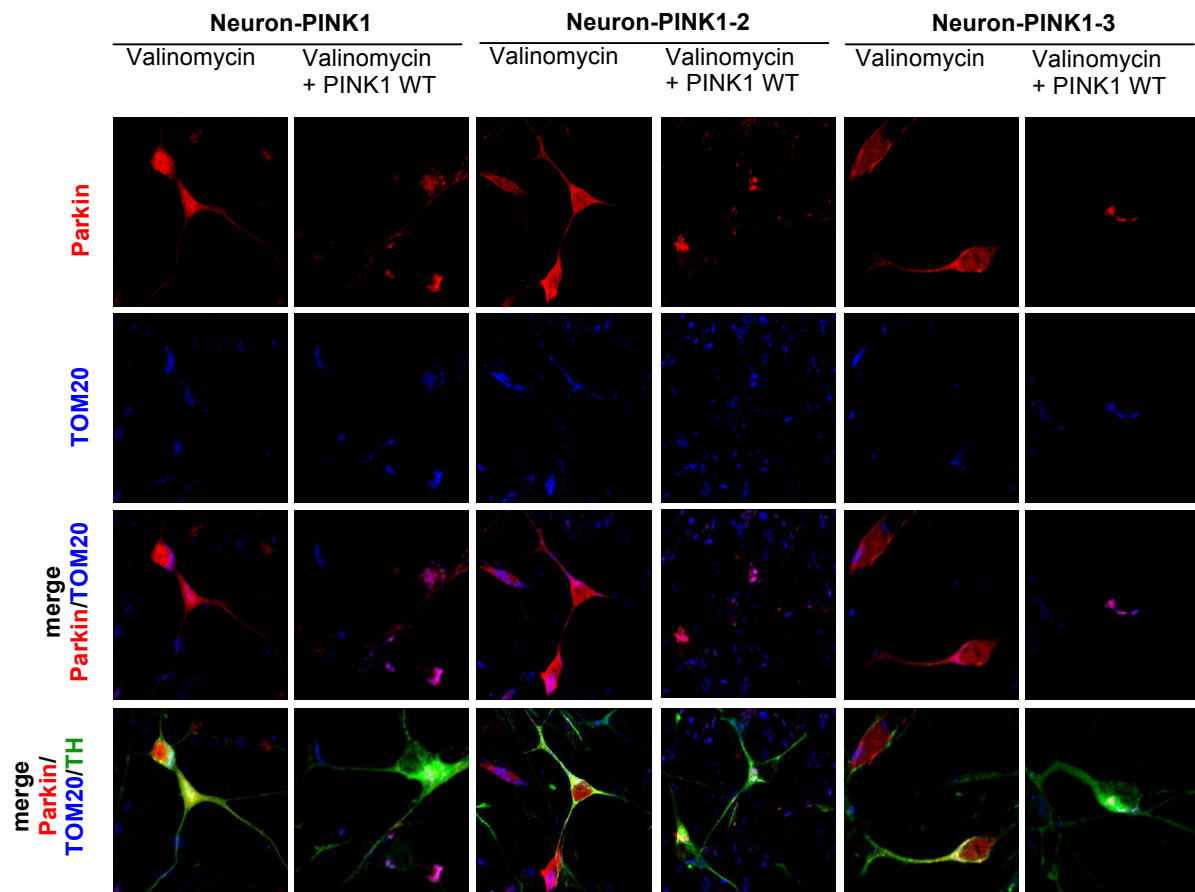


Figure S1 Stress-induced mitochondrial translocation of Parkin is impaired in all three mutant PINK1 iPS cell lines. Results are shown for the iPS cell mutant lines derived from three different patients. Neuronal cultures were infected with wild-type Parkin and treated with 1 μ M valinomycin for 12h. After treatment, cells were fixed and immunostained with antibodies against Parkin (red), the mitochondrial marker TOM20 (blue) and the DA marker TH (green). Upon valinomycin treatment, Parkin fails to colocalize with mitochondria in DA neurons. Infection of PINK1 mutant neurons with wild-type PINK1 restored Parkin translocation to the mitochondria upon valinomycin treatment.

9.3. Publications

ORIGINAL ARTICLES / LETTERS

1. Moro E, Volkmann J, König IR, Winkler S, Hiller A, Hassin-Baer S, Herzog J, Schnitzler A, Lohman K, Pinsker MO, Voges J, Djarmati A, **Seibler P**, Lozano AM, Rogaeva E, Lang AE, Deuschl G, Klein C (2008) Bilateral subthalamic stimulation in Parkin and PINK1 parkinsonism. *Neurology* 70(14):1186-1191. (IF: 7.043)
2. **Seibler P**, Djarmati A (equally contributed), Langpap B, Hagenah J, Schmidt A, Brüggemann N, Siebner H, Jabusch H-C, Altenmüller E, Münchau A, Lohmann K, Klein C (2008) A heterozygous frameshift mutation in PRKRA (DYT16) associated with generalised dystonia in a German patient. *Lancet Neurol* 7(5):380-81. (IF: 14.27)
3. Rakovic A, Grünewald A, **Seibler P**, Ramirez A, Kock N, Orolicki S, Lohmann K, Klein C (2010) Effect of endogenous mutant and wild-type PINK1 on Parkin in fibroblasts from Parkinson disease patients. *Hum Mol Genet* 19(16):3124-3137. (IF: 7.386)
4. **Seibler P**, Graziotto J, Jeong H, Simunovic F, Klein C, Krainc D (2011) Mitochondrial Parkin Recruitment Is Impaired in Neurons Derived from Mutant PINK1 Induced Pluripotent Stem Cells. *J Neurosci* 31(16):5970-5976. (IF: 7.178)

The publications have a cumulative impact factor (IF) of 35.9 and an average of 9.0.

ABSTRACTS

1. **Seibler P**, Rosenbohm A, Lohmann K, Zschiedrich K, Djarmati A, Zühlke C, Klein C, Ludolph A (2008) Autosomal dominant neurodegenerative disorder with predominantly spinocerebellar signs. *Neurology* 70(Suppl.1):A389.
2. **Seibler P**, Kock N, Orolicki S, Klein C (2008) Cellular model for monogenic parkinsonism. *DGNG*.
2. Orolicki S, Grünewald A, Rakovic A, **Seibler P**, Lohmann K, Kock N, Klein C (2009) Proapoptotic protein Bax expression and increased oxidative stress in fibroblasts from Parkin mutation carriers. *Mov Disord* 24(Suppl.1):42.
3. Orolicki S, Grünewald A, Rakovic A, **Seibler P**, Lohmann K, Kock N, Klein C (2009) Evidence for a role of the Bcl-2 family in the pathophysiology of Parkin-associated parkinsonism using a human fibroblast model. *Akt Neurol* 36(Suppl2):114.

ORAL PRESENTATIONS

1. **Seibler P.** Evidence for linkage of restless legs syndrome to chromosome 9p: are there two distinct loci? European RLSSG Meeting, Munich, December 2006.
2. **Seibler P,** Graziotto J, Heong H, Simunovic F, Klein C, Kranic D. Mitochondrial Parkin Recruitment Is Impaired in Neurons Derived from Mutant PINK1 Induced Pluripotent Stem Cells. NGFN-Plus and DGNG Meeting: Highlights of Posters Session. Tübingen, November 2010.
3. **Seibler P.** Human neuronal model of Parkinson disease: iPS approach. Scientific colloquium at the Department of Physiology, University of Kiel, May 2011.

9.4. Acknowledgements

At this point I would like to thank everyone who supported me during the practical work and the completion of this thesis.

In particular I thank my supervisor Professor Christine Klein. Her constant support, motivation and fruitful suggestions helped me throughout my time of research from the Bachelor to this PhD thesis! Moreover, I would like to thank her for the unique chance to gain international academic experience in Boston.

Professor Dimitri Krainc I would like to thank for being my supervisor in Boston. I am very thankful for his helpful scientific advice and the critical review of our publication. Furthermore, I would like to thank him for the warm welcome in his group.

I would like to give my special thanks to my colleagues from the Neurogenetics Group in Lübeck and the MIND Department in Boston, not only for helpful discussions and experimental advice but also for their patience and continuous interest.

My parents and my sister encouraged me and stayed with me during the entire time. I give thanks to you, especially for your waiting and hoping with me for the “Nervis” to grow.

I thank my friends from the SMD Lübeck and the RPC in Cambridge for all the moments we have shared. My roommate and beer-brewing partner David McKinney made my stay in Cambridge most memorable.

Finally, I give thanks to my Lord Jesus Christ for being faithful and so gracious to me. I say with the psalmist: “Your steadfast love, O Lord, extends to the heavens, your faithfulness to the clouds.” (Psalm 36.5, The Bible)

9.5. Declaration

Ich versichere, dass ich die Dissertation ohne fremde Hilfe angefertigt und keine anderen als die angegebenen Hilfsmittel verwendet habe.

Weder vor noch gleichzeitig habe ich andernorts einen Zulassungsantrag gestellt oder diese Dissertation vorgelegt.

Ich habe mich bisher noch keinem Promotionsverfahren unterzogen.

Philip Seibler

Lübeck, den 21.06.2011